CUMULONIMBUS CONVECTION AND PARAMETERIZATION

by

Hok Yau Tam

Atmospheric Physics Group
Physics Department
Imperial College of Science and Technology
London

A Thesis submitted for
the Degree of Doctor of Philosophy
in the University of London

1979

CUMULONIMBUS CONVECTION AND PARAMETERIZATION

Hok Yau Tam

ABSTRACT

Cumulonimbus convection is necessarily three-dimensional. Its mathematical representation is considerably simplified when it is approximated as being made up of two orthogonal two-dimensional circulations. This approximation is valid if the time scale of the flow is much less than that of the vertical component of vorticity. This is found to be the case in numerical simulations of organised cumulonimbus convection. The two components of the three-dimensional circulation are a "mid-latitude" circulation along the direction of maximum mean shear, and a "tropical" circulation along a perpendicular direction. The propagation velocity of a cumulonimbus is the vector sum of these two components. Predicted values compared favourably with the observed values.

The characteristic of deviatory propagation of a cell is due to the preferred propagating direction of the tropical circulation, it depends on the velocity profile on that plane. One of the results is that when the hodograph turns clockwise with height, a right moving cell is favoured, and visa versa. It agrees with numberical results of Klemp and Wilhelmson (1978).

The velocity of a storm mass is due to two factors -- the velocity of its constituent cells, and a discrete propagation. The latter is an apparent motion due to the process of regeneration of cells. It is a result of the interaction of the downdraught outflow with the low level flow. A downdraught is a dynamically dominant circulation, thus it tends to propagate with a different velocity from that of the updraught. If the downdraught tends to propagate towards the left of the cell, a leftward discrete propagation would result, and visa versa. Realistic storm velocities were predicted.

Experiments with the two two-dimensional circulations in different velocity profiles showed that the position of low level jets has little effect on their propagation speeds. The steering level in the mid-latitude circulation is not affected by a realistic size of the jet, while the propagation speed of the tropical circulation varies linearly with the size of the jet.

A simple 3-layer model for parameterization is proposed, based on the above model, with the downdraught originating from the mid-level. The transfer produces a warming and a cooling to the top and bottom layer respectively, and shear is enhanced. The mid-layer is modified through large scale subsidence.

CONTENT

CHAPTER ONE: INTRODUCTION

CHAPTER TWO: STUDIES OF 2-DIMENSIONAL CIRCULATIONS

CHAPTER ONE : INTRODUCTION

1.1 INTRODUCTION

Convection is the motion arising from the conversion of available potential energy into kinetic energy, involving the exchanges of entropy, moisture and momentum. It is a process in which the imbalance set up by the uneven distribution of radiation or differential advection is partially restored. Different scales of convection interact with one another, thus a better understanding of a particular type or scale of convection serves to give a better understanding of convective processes as a whole. In recent years using observational, theoretical and numerical modelling, the concept of organised flow within storms has become very important in explaining its transfer and its propagation, and needs further study. The momentum transfer, for instance, is not downgradient, the flow must be organised to give good positive and negative correlation between u (the horizontal veocity) and w (the vertical velocity). Another aspect of the organization is manifestated in the propagation of cumulonimbus. It travels with a different velocity to that of the wind at all levels, and often travels along a straight path for hundreds of kilometres. Radar studies suggests that the circulation is in a quasi-steady state (Browning(1962)). The convection model in this thesis is quasi-steady. The deviatory motion of the storm is a result of two factors -- the motion of the cell and the process of regeneration of new cells. They are subjects of chapter 3 and 4 respectively.

Cumulonimbus convection lies within the mesoscale which is not resolved in global numerical weather prediction models or climate models. The importance of transfers from cumulonimbus is shown in

Palmen and Newton (1959) who found that cumulonimbus contributed 37 percent of the vertical flux of angular momentum required to balance the torque for the latitude belt from 30 to 50 degree north during the summer and about 7 percent during the winter. Houze (1973) found that the momentum flux transferred by the cumulonimbus is of the same magnitude as the large scale vertical momentum flux at Boston during at least one season. Thus sub-grid scale motion is vital for a better global circulation model.

It is the aim of this thesis to tackle these problems with a simple three-dimensional analytic model.

1.2 Types of Cumulonimbus

It is enlightening to trace through the development in the understanding of deep convection. The discussion is separated into four main groups, each centres around a particular model of cumulonimbus. Their development in observational, analytical and numerical models is discussed. In the latter half of this chapter, the theories on deviatory motions, and the distinction between storm and cells are discussed.

1.3 (i) Isolated Heatstorms

They are characterised by a short life time, typically under one hour, in which the whole life cycle evolves: it can be divided into two main phases: growth and decay, both are dominated by small scale mixing.

1.3.1 Growing Phase

The cumulonimbus consists of a single growing updraught, formed from a local heat source. The moisture condenses in the updraught,

giving the bubbly appearance of the cloud. The turbulent appearance at the top and around the updraught suggests that the updraught is constantly being mixed with air originating from the environment at that level --- this process is referred to as entrainment, it is a dominant mechanism by which heat and moisture are transfered.

1.3.2 Decaying Stage

When enough moisture is accumulated in the cloud to allow water droplets to coalescese at a large enough rate, the heavy droplets fall out as rain. This sets off the decaying stage. The rain droplets have the effect of slowing down the updraught current through drag (the net drag force exerted on a parcel of air is approximately equal to the total weight of the condensed water assuming they are falling at terminal velocities), and the effect of evaporative cooling in the boundary layer. This results in the weakening and the eventual depletion of the updraught which is thus replaced by a downdraught, at least in the lowermost level.

1.4 (ii) Mid-latitude Storm

The mid-latitude storm is long lasting. It is distinguishable in three phases through its life cycle -- the growing, mature, and the decaying phases. During the mature phase, updraught and downdraught co-exist; the updraught is taken from air laden with moisture at low levels. Latent heat is released in the updraught as the moisture condenses. The condensed droplets fall out of the updraught region into the relatively dry surrounding air. The process of evaporative cooling, and to a lesser extent drag, create a downdraught. At the surface, the downdraught outflow spreads out and creates a cold front, which can cause convergence and lift more air into the updraught.

This co-operation between updraught and downdraguht leads to a long mature phase. This is found to be the case for long lasting storms.

Severe storms are observed in regions of strong vertical shear, and in some instances upper level jets were present, as noted in Ramaswamy (1956) and Miller (1959). Fawbush et.al.(1951) pointed out that vertical shear is a necessary condition for deep convection to take place. In Browning and Ludlam (1962), a dynamical model based on radar observations of a severe storm which occured over south-east England was proposed. The model was further simplified to two-dimensions. A circulation based on this simplified two-dimensional model is referred to as the mid-latitude storm, or mid-latitude circulation. This concept paved the way to subsequent active research work into the dynamics and numerical simulations of mid-latitude storms.

The model proposed by Browning and Ludlam (1962) is of a quasi-steady circulation. The updraught was assumed to lean over the downdraught. Thus it allows condensed water droplets to fall out of the updraught region into the downdraught; a steady circultion can be maintained.

The updraught leaves the storm towards the same direction at which the storm travels. Thus the anvil travels in front of the storm -- a feature that is commonly observed in mid-latitude storms. Analytical and numerical models seek to quantify and understand the dynamics of these convective phenomena

1.4.1 Analytic Modelling.

The problem of modelling a mid-latitude type storm can be viewed from two standpoints :

(1) a finite amplitude approach which considers the actual circulation, and imposes the necessary boundary conditions on the equations of motion. This involves solving non-linear equations which are complicated.

(2) a small amplitude approach though is not as realistic, often results in linear boundary value problem, and considerable progress has been made.

The linearized theory of instability is appropriate in the initial growing stage of a cumulonimbus; any large amplitude non-linear instabilities find their origins in a small amplitude unstable wave. The two approaches can complement each other to provide a better model as is done in this thesis.

The finite amplitude approach is more appropriate to cumulonimbus convection modelling. The resultant equations are non-linear, thus making a certain degree of numerical work necessary. The first such work in which the concept of Richardson number was introduced was presented in Green and Pearce (1962). A two-dimensional inviscid flow was considered. The paper was presented in two parts. Green, in the first part, found that for an incompressible atmosphere, the steering level is an eigenvalue of an eigenvalue problem, determined by the extreme outflow height and the value of a non-dimensional number which resembles a Richardson number. When the condition of continuity of pressure is applied at the flow boundary between updraught and downdraught, the updraught should lie underneath the downdraught. In the second part, Pearce assumed that the updraught was overlying the downdraught. From the vorticity distribution, by integration, the distribution of $(\theta'-\theta'_o)$ was calculated (where θ' is the deviation of potential temperature from the undisturbed state, and

θ'_o is the value of θ' at the updraught-downdraught interface), yielding the distribution of heat source and heat sink necessary for the maintainance of the flow. The two individual parts of the paper gave conflicting results for the slope of the interface.

Moncrieff and Green (1972) derived two conservative quantities from a set of Boussinesq equations. One is a vorticity constraint which is applicable for a strictly two-dimensional circulation, the second conservative quantity is in the form of a Bernoulli energy integral for a Boussinesq fluid. The former was used in the analytical studies. A non-dimensional number R was defined as the ratio of the convective available potential energy to the kinetic energy of the inflow air relative to the undisturbed air at the extreme outflow height. A steering level was defined in terms of R, the vertical extent of the convective system and the density scale height, the propagation speed of a storm can be predicted, when the direction with which the storm travelled was given, the model was able to predict, realistically, the speed of the storm when the value of R is small and less than unity. The transfer of heat and momentum was expressed in terms of large scale parameters. It was concluded that these could not be represented by a Fickian-type diffusion.

The successful maintainance of a steady mid-latitude circulation lies in the orientation of the updraught: an upshear orientated updraught is essential. In Moncrieff and Green (1972), the thermodynamic term in the updraught and downdraught are independent of updraught orientation, the mathematical model may represent a physically impossible quasi-steady circulation.

The feasibility of a two-dimensional mid-latitude circulation was investigated in Moncrieff (1978) using the lateral boundary conditions

as given by the solutions of Moncrieff and Green (1972) --- the asymptotic solution for the steering level and remote flow in an ambient flow with constant shear. The momentum and thermodynamic equations were solved to determine the internal streamline structure. The updraught-downdraught interface was treated as a free boundary. The orientation of the interface confirms the results of Green (1962) for all values of R between -1/4 and 1. This result was unaffacted by the effect of compressibility, or by the details of the vorticity generation at the interfacial boundary. When different values of R were given to the updraught and downdraught branch, the same basic result was obtained. An upshear orientation was successfully induced by providing a thermodynamic forcing not consistent with the wet adiabatic process, the flow obtained was, however, transient.

1.4.2 Numerical Modelling

The introduction of electronic computers meant that complicated equations can be solved numerically in a relatively short time. This marks the new approach of modelling of convection by numerical techniques. Complicated microphysical processes can be included in a crude way. The complexity of the representation of these processes in these numerical models depends on the speed and the size of computers available. During the early period of computerization, two-dimensional numerical experiments were carried out with different degrees of sophistication in the representation of the microphysics, such as water droplet size distribution, and the effect of mixing.

The problem was approached in two different ways : axial symmetry and slab symmetry.

Axisymmetrical models are pseudo-two-dimensional, such as Ogura

(1963), Murray (1970), Murray and Koenig (1972) and Soong and Ogura (1973). They suffer from two disadvanages :

(1) There is a difficulty in the verification of results-- Wiggert (1972).

(2) It is impossible to include the effects of basic wind flow including the effects of vertical shear of the horizontal wind.

An axisymmetric approach is applicable to small scale shallow cumuli and isolated heatstorms.

Slab symmetrical models allow free movement in two directions, basic wind profiles can be included in a simplified way. Orville (1965,1968), Takeda (1965,1966,1971), Liu and Orville (1969) , Orville and Sloan (1970a), Schlesinger (1973), Hill (1974), and Hane (1973) adapted this approach to simulate deep convection.

Orville (1965,1968), Liu and Orville (1969) and Orville and Sloane (1970b) performed a series of numerical experiments on the life cycle of a cumulonimbus originating from flow over a heated orographic barrier. Shallow Boussinesq approximated equations of motion in vorticity form were used in Orville and Sloane (1970b), the numerical integrations were carried out over a domain of 10 kilometres with a 100 metre grid length. The Reynold stress term and scalar eddy fluxes are represented with a constant eddy viscosity closure scheme --- the magnitude of the eddy viscosity was taken large enough to prevent non-linear computational instability from developing. The storm simulated passed throught the three phases from growth to decay, with a mature stage with strong updraught and downdraught coexisting. During the decaying phase, a strong downdraught developed, even to the extent of creating clear spaces inside the cloud. The downdraught

eventually weakened and no futher convection took place.

Liu and Orville (1969) included the effect of cloud shadow on the temperature of a hill, and found that the shadow encouraged the formation of multiple convective cells. The results presented were claimed to agree with past observations --- it resembled a mid-latitude circulation.

In experiments of Takeda (1971), it was found that in a strongly sheared environment, the updraught was inclined downshear and the simulated convection was short lived. He concluded that the formation of a long lasting cloud required the existence of a jet in the lower layer. The height at which the jet centred was found to be an important factor in influencing the lifetime of the convection.

Schlesinger (1973) modelled deep convection in a rectilinear region. He found two basic relationships between storm duration: moisture supply, and vertical shear.

(1) The existence of a strongly sheared environment prohibits a long lasting storm, if the moisture supply is limited. When the moisture supply is large enough, the updraught life is somewhat prolonged.

(2) Increasing moisture tends to shorten the life of the updraughts at small and moderate shear, and prolong the life of an updraught at high shear.

Hane (1973) presents a numerical simulation of a squall line, building on the earlier attempts of Sasaki (1959) and Ogura and Charney (1960). The grid resolution is increased to 400 metres in both horizontal and vertical. Hane (1973) used a moisture perturbation in an environmental sounding characteristic of observed

soundings prior to the squall line passage. He experimented it with environments of different vertical shear. He concluded that a stronger sheared environment supports a longer lasting, more intense and a broader circulation than in the case of a weakly or moderate shear in the environment.

An opinion expressing the importance of three-dimensional modelling was given by all above authors.

1.5 (iii) Tropical Squall Lines

Cumulonimbus in the tropics behave fundamentally in a different manner from those in the mid-latitude (Ludlam(1962)). Tropical squall lines are also known for their longevity and they very often travel for hundreds of miles. They spend the bulk of their lives in the mature stage.

The main feature observed is that its lateral dimension is many times bigger than its width, of the order of hundreds of kilometres. The major difference from the mid-latitude cumulonimbus is its propagation, it travels faster than the wind along the direction of propagation in the layer in which it is embedded. Therefore, the inflow approaches the squall line from one direction. This configuration of circulation produces an anvil which trails behind the squall line.

The environment in which squall lines develop is different, notably in the absence of wind shear. There are two school of thought for the mechanism responsible for the organization. It can be organised through its own dynamics, or be organised by large scale wave forcing--- the easterly wave.

1.5.1 Analytical Modelling

Moncrieff and Miller (1976) considered the dynamics of the circulation through a squall line to be an important factor in governing its behaviour. The flow field was idealised to a pseudo-three-dimensional form. The inflow into the squall line was treated as two-dimensional, as was the outflow behind the squall line. The flow inside, however, was three-dimensional. This idealised convective system is referred to as the tropical or propagating circulation.

The downdraught, for the sake of mathematical simplification was taken to originate at the top of the convective system. This assumption although unrealsitic, provided reasonable dynamical conclusions. A relationship between the propagation speed and the convective available potential energy was derived. The outflow from the squall line was found to produce a jet of positive momentum at the mid-level, and two negative outflow jets at the extreme top and bottom.

Raymond (1976) considered the organization of convection to be the consequence of the regions of convergence and divergence generated by the forced inertial-gravity waves. Convection was regarded as the provisor of energy, and the waves the organisor. The concept behind the model is similar to the wave CISK model of Lindzen (1974) proposed to explain cloud clusters in the tropics. The velocity of the convective system was determined by the velocity of the most unstable gravity wave.

1.5.2 Numerical Modelling

In the second part of Moncrieff and Miller (1976), a numerical simulation of a tropical squall line observed in VIMHEX was presented. The simulation produced a squall line that travels faster than the wind at all levels.

They suggested a cold density current may be the mechanism which forced the squall line to propagate. The cold density current is a result of the cold downdraught spreading out at the ground. When the current is travelling at the same speed as the cloud, the result is a net convergence zone beneath the updraught.

Miller and Betts (1977) pursued the mechanism of density current further, and found that there was a reasonable agreement between the atmospheric data and the laboratory observations of density current. They concluded that the propagation speed of the squall line was related to that of the density current. The simulation produced a system and a cell downdraught which modified the environment in different ways.

1.5.3 Observations

In Betts, Grover and Moncrieff (1976), the analytical model presented in Moncrieff and Miller (1976) was compared with the characteristics of squall lines observed in VIMHEX II experiments. The averaged propagation speed of all the squall lines was in agreement with the predicted value. The outflow velocity profile resembles that predicted in the numerical simulation.

The observations on the modification after the passage of the squall line presented in Miller and Betts (1977) are in general agreement with Betts, Grover and Moncrieff (1976). The modification in the lower part of the troposphere was attributed to two factors:

cell and system downdraughts. The cell downdraught was forced down through evaporative cooling, thus it is cooler. The system downdraught is a result of dynamical forcing, it lies just above the cell downdraught. The result was a net warming of the lower troposphere above the cell downdraught. A warming was of the order of one degree Kelvin.

Among early papers on experiments carried out during GATE, Mansfield (1978) presented a study of four squall lines using radars and radiosondes on board Oceanographer. A composite picture on the modification of the thermodynamic quantities on the environment is similar to the results of the previous two papers. The velocity profile modification was somewhat different.

1.6 (iv) Three-dimensional Severe Storm

It is recognised that the circulation through a severe storm is necessarily three-dimensional. The simplified two-dimensional model in the form of a mid-latitude circulation proposed by Browning and Ludlam (1962) was conceived to provide the beginings of a mathematically tractable model.

1.6.1 Observational Model

A third dimension is necessary to explain that severe storms, particularly those developed in the mid-west of the United States, travel at very different directions to those of mean winds, the deviations are between 20 to 40 degrees to the right and occasionally to the left. The deviation of storms developed over England is less so, around 10 to 20 degrees. The concept of deviatory motion is contrary to the concept of steering, it also invokes inflows into the storm from different directions.

Browning (1964) presented an interlocking circulation model of a severe right moving storm. It is an improved version of the circulation model based on the studies of the Wokingham storm. Subsequent observers, such as Chisholm (1973) produced similar circulation in their models. These are further discussed later.

1.6.2 Numerical Model

The removal of the restriction of two-dimensionality for deep convection modelling was first reported in Wilhelmson (1974). The moist, precipitating anelastic set of equaions were integrated on a staggered, finite difference 600 metre mesh. The results were compared with a two-dimensional simulation using the same technique presented in the paper. The conclusion is that a three-dimensional cloud grew deeper, with the calculated value of the maximum vertical velocity being twice that of the two-dimensional case.

Schlesinger (1975) presented a three-dimensional primitive equation model in height co-ordinates. The preliminary results agreed with those of Wilhelmson (1974), and Newton and Newton (1959): the updr ght core acted as an obstacle to the environmental flow, a double vortex ring in the lee of the updraught was observed. Schlesinger (1975) evaluated the pressure forces at various points, and found that when the wind vector veered with height, a pressure gradient was effected to force the updraught towards the right.

Miller and Pearce (1974) presented a three-dimensional primitive equation model. The distinct feature of this model was in its use of pressure as the vertical co-ordinate, and that it was non-hydrostatic. A series of experiments based on this model were presented in Moncrieff and Miller (1976), Miller (1978) and Thorpe and Miller

(1978). Moncrieff and Miller (1976) was directed towards the simulation of tropical squall line. Miller (1978) described the result of the simulaion of the Hampstead storm. Thorpe and Miller (1978) carried out two simulations; a right moving storm and a splitting storm. These results are futher discussed.

Klemp and Wilhelmson (1978) included sound waves in their model, the sound wave was treated separately by a splitting procedure which saved on computer time. A splitting storm pair was produced. When the wind hodograph turns clockwise with height, a single right moving storm evolved from the splitting process. Conversely, an anticlockwise turning of the horizontal hodograph eventually produced a left moving storm.

1.6.3 Analytical Model

The analytical study of a three-dimensional severe storm from a set of primitive momentum equation is a formidable task. Haman (1978) attempted to produce a method to predict the propagation velocity of a severe storm, based on the two-dimensional mid-latitude work of Moncrieff and Green (1972). He assumed that the storm was steered by the mean wind, it was given an orthorgonal velocity component by the downdraught. It is not obvious that the downdraught should travel at a right angle to the updraught. The mechanism of linking the two velocities together is not clear and was not given. One major assumption made was that the severe storm was not to produce any velocity change in the environment. This means that no work is done by the pressure field. This is an unreasonable assumption; it contradicts the observed enhancement of shear after the passage of a severe storm, and the belief that cumulonimbus is one of the mechanisms in maintaining the high level jet. No case study was

carried out to validate the theory.

This thesis presents a three-dimensional analytical model based on the approximation that a three-dimensional flow can be represented by two orthorgonal, two-dimensional flows in regions where the development of vertical vorticity is small, an assumption substantiated by Johnson (1978). It models the dynamical behaviour of the circulation, it is based on the results of both observational and numerical models.

1.7 Translational Motion Of Severe Storms

The movement of severe storms has received much attention, due in part to the desire to predict the path of a severe storm in the field of forecasting.

In his "Physics of the Air ", Humphrey (1928) postulated that the velocity of a cloud is usually that of the wind in the layer in which it is embedded. Later studies partly confirmed his postulate. Brook (1946) made a statistical study of rainstorms, and concluded that small rainstorms moved with the lower tropospheric wind; the early radar studies of Lidga and Mayhew (1954), who studied the movements of precipitating echoes reached similar conclusion.

The first comprehensive study using aircraft and radar technique was during the Thunderstorm Project described in Byers and Braham (1949). They found that in general, storms moved with the direction of the mean wind from the ground to a height of 7 kilometres; the type of storms investigated was mostly small single cell storms, thus the work is in effect a verification of Brook's studies.

1.7.1 Concept Of Deviatory Motion Due To New Cloud Growth

The first deviatory motion of storms were presented in Newton and Katz (1958). They used over 2000 rain gauges stationed throughout the mid-west in the United States. From the available hourly precipitation records, they were able to track large convective rain areas, and correlated their motion with the mean wind between 850 to 500 mb. Their results showed that rainstorms moved with a systematic deviation of 25 degrees to the right of mean wind directions. They explained that the storm cells were travelling with mean winds, the rightward deviative motion was due to a generation of new cells on the right flank, with concurrent dissipation of cells on the opposite side. The process of dissipation and generation of cells were observed in studies by Browning (1962) and Hammond (1967). However, the rate of this process is not sufficiently high to account for the deviatory motion in many cases. Deviatory motion is also observed when the process of generation- dissipation of cells did not occur (Browning(1962)).

1.7.2 Concept Of Deviatory Motion Due To A Rotating Updraught

When a rotating solid body is introduced as an obstacle to a moving fluid, in addition to the resisting force along the direction of the moving fluid, there is a sideway thrust ; this is known as the Magnus force.

If the updraught can be regarded as a solid rotating body, the Magnus lift force may be the mechanism of deviatory motion. Byers (1942) explained a rightward moving thunderstorm using a "rotor" principle. The first comprehensive study was by Fujita and Grandoso (1968), using numerical calculations of aerodynamic drags with observations of a storm which splits into a left moving and a right moving storm. They were able to obtain very good agreement by giving

a cyclonic rotation to the left moving storm updraught and an anticyclonic rotation to the right moving updraught. The maximum deviatory motion occured when a tangential rotating speed of a few metres per second was imposed on it. A splitting pair would necessarily be made up of two counter rotating updraughts.

There is serious doubt as to whether it is appropriate to apply a theory based on rotating solid body to a dynamical system such as the updraught. The drag forces acting on the material which momentarily constituted the updraught cannot be equated to the storm as a whole. The former presumably responds to aerodynamic and drag forces. However, the velocity of the material and the propagation velocity of the storm are different. A stationary storm, such as the Hampstead storm serves to illustrate the point; while the cloud mass remains stationary, the material velocity clearly is near that of the ambient wind.

1.7.3 Deviatory Motion Due To Dynamical Forcing

A cumulonimbus travels at the mean wind velocity when it is developing. Browning (1964,1965) observed that the storm changed its direction of propagation when it developed into a supercell. A deviatory motion cannot be a simple regeneration process as proposed by Newton and Katz (1958), since the same cell was involved. The likely explanation is that the storm cell acquires a different dynamical circulation --- a quasi-steady circulation. The answer of the deviatory motion must, therefore, lie in the dynamics of the storm cell as a whole.

The idea of any disturbance in the atmosphere being "steered" by the mean wind is deeply entrenched in the two conceptual explanations

of deviatory motion. It may have its origin in the studies of instabilities in fluids; unstable waves always travel with the velocity of the flow. When a cumulonimbus reaches a severe storm stage, with a well organised updraught and downdraught, it occupies the whole depth of the troposphere. This situation cannot be compared with unstable waves of small amplitude in a medium with an effectively infinite vertical extent.

1.8 Further Classification Of Storm

Within the cumulonimbus type (iv), three classified subgroups can be identified according to the behaviour of cells within the storm as indicated by radar studies.

(a) Supercell

A supercell is a storm which comprises a single large convective cell. Marwitz (1972) and Chishom (1973) in their studies of hailstorms over Alberta observed that they travelled to the right of mean winds. In their classification, the supercell was to move to the right of the mean wind. Left moving supercells, however, have been observed, e.g. The Union City Storm. Left moving supercells are included in this subgroup.

In a region of high shear ($0.01\ s^{-1}$) Chisholm (1973) defined a new type of storm : the severely sheared supercell. The models derived from wind data were the same as those from a supercell, even the radar echoes were similar. The difference lies in the way such a system evolved. The dynamics of the two types of supercell in Chisholm (1973) were similar, and therefore, fall into the same classification.

(b) Multicell

A storm is more often made up of a number of cells arranged laterally. The cells within a storm usually travel at different velocities to that of the storm, but at similar velocities to one another. There is a discrete sideways movement either to the right or to the left, as observed in the Wokingham storm (Browning (1962)). This sideward movement is evidently due to the generation of new cells on one side and dissipation of older mature cells on the opposite flank. Thus a storm, as a whole can move in a deviatory fashion or with the mean wind.

(c) Squall Lines

A squall line is, in many ways, similar to a multicell system. It consists of cells arranged laterally. The cells do not seem to interfere disruptively with one another, and persist as a group for a long time very often for as long as the lifespan of the entire squall line. They move at the same velocity, and not necessarily towards the direction perpendicular to the squall line.

1.9 Discussion Of The Dynamics Of A Storm And A Cell

A cumulonimbus constitutes a very complicated flow, involving all scales of motion up to the vertical extent of the troposphere. The aim of a severe storm model is to present the most important, and hence the most dominant feature of the system capable of explaining the various functions the severe storm performs. This involves the isolation of many secondary effects, for example, the small orographic effect and sub-cloud scale mixing processes are usually ignored. The degreee of simplification also depends on the method used. In numerical modelling, where a vast amount of data can be handled in a relatively short period of time, the simplification on the physical

processes involved is limited to how well they are understood, and the ability of the computer to process them in a reasonable length of time.

In the making of a dynamical model from observations, the approach has been to reduce the complexity of the different motion inside a storm to a single convective unit. Thus various features, such as convective cells, are ignored. The method adopted by Browning (1964) and others in describing the circulation through a storm is to subtract the velocity vector of the storm from the wind velocity profile of the environment. With the knowledge that the updraught originates near ground level, and flows out at a thermodynamic equilibrium level, and the assumption that the downdraught enters the storm somewhere in the mid level, a model for the flow through the storm is, in principle, obtained. This treatment presumes that the dynamical effects of numerous convective cells with their own updraughts and downdraughts are equivalent to one single updraught and downdraguht as deduced by the method described.

This much simplified storm model can lead to misleading results. The Rimbey storm (Marwitz (1972)) was observed to move along with the mean wind. The inflow into the updraught approached the storm from the right when the storm assumed the role of the basic dynamical convective unit. The downdraught, in this case, had near zero inflow speed. The movement of the storm can be accounted for by two different mechanisms acting together. It was found to be made up of a number of convective cells aligned laterally, they travelled with a different velocity from that of the storm; to the left of the mean wind. The second contribution to the storm velocity lay in the rate at which new cells were being generated on the extreme right flank,

and the rate at which older cells were dissipated on the opposite flank. To an observer, who plotted the movement of a storm through tracing out the path of the centre of radar echoes, the net effect of the second factor led to a velocity vector, which when added to the velocity of the cell gave the velocity of the storm observed.

The observed deviatory motion of the cell showed that they are not unorganized plumes which would travel with the mean wind, but a steady dynamical structure which forced the sideways movement; it is this interpretation which is used in the analytical treatment here.

The method adopted by Browning in deducing air flow through storm system has been widely exploited. Hammond (1967) deduced an airflow model of a severe left moving storm, though the cells and the storm travelled with different velocities, they both deviated to the left. Chisholm (1973) applied the same principle to a variety of storm types, though only updraught branches were considered.

In the first generation of numerical simulations of convection using two-dimensional models, there was no need to distinguish storms and cells; only one cell was simulated at any one time. With the introduction of sophisticated three-dimensional model multicell storms were simulated. The interpretation of results was not as clear cut as one would have thought, since there is not the physical existence of a cloud to obscure the issue.

Thorpe and Miller (1978) presented the results of the simulation of two storms -- the Haml1 storm and the Wokingham storm (modified soundings obtained at Crawley before the outbreaks of Hampstead and Wokingham storms were used. Haml1 signifies the particular numerical run, the simulation of the actual Hampstead storm is Ham7, in Miller

(1978)). New cells were found to grow on the right flank of the Hamll storm. This produced a rightward moving storm in much the same way as Newton and Katz (1958) postulated. The emphasis was on the flow relative to the convective cells, and the direction of preferred growth was explained in terms of the interaction of the cell downdraughts with the low level flow. The distinction between a cell and a storm, in this case, is clear.

In the simulation of the Wokingham storm, a convective cell which developed during the first 45 minutes subsequently evolved into two cells. They lasted the rest of the simulation time and migrated out of the simulated region. The difference between this and the Hamll storm was that in the latter case, no two cells co-existed for a significant period of time. The evolution of a single cell into two persistent convective cells was interpreted as splitting, thus each individual cell was interpreted as a storm. The results obtained was compared with observations of splitting storms and the theory of splitting.

The two co-existant convective cells were travelling with the same velocity as that of the parent cell. The simulation did not show a normal splitting in which there is usually a large difference in speed and direction with which the splitted pair propagates. Though the pair of cells started to drift apart as they were passing through the boundary, this is probably boundary effects. The point at which a cell became a storm is not obvious from this paper. The results, however, if interpreted in an alternative way, showed the process of evolution of a single cell into a multicell storm and the mechanism required for such a process to occur.

The two-dimensional analytical models of Moncrieff and Green

(1972) and Moncrieff and Miller (1976) used the concept of a storm being the simpliest convective unit. This is reflected in applications of their models, thus a mid-latitude squall line was simplified to a line of convection. The difficulties involving the application of a two-dimensional model in a real storm situation are numerous, as it is often difficult to decide which direction to choose for the y axis (along y, d/dy=0), particularly when the storm velocity is not known.

Haman (1978) suggested a multicell storm could be averaged out through some "suitable" process, and therefore could be regarded as a supercell storm. The "suitable" process was not mentioned.

In this thesis, the dynamics of updraught and downdraught are considered analytically. They are treated separately, since they are dynamically independent from each other. They interact through thermodynamic and pressure forcing, both of which are implicit in the appropriate boundary conditions. The model so obtained is that of a convective cell. An alternative model is proposed (in chapter 4) to predict the motion of a storm.

CHAPTER TWO: STUDIES OF 2-DIMENSIONAL CIRCULATIONS.

2.1 INTRODUCTION

It is suggested in Chapter 3 that a 3-dimensional cumulonimbus cir lation can be approximated as being made up of two two-dimensional circulations: the mid-latitude and the tropical circulation. Before discussing the three-dimensional model, it is informative to study the two circulations in a more general context than those carried out in Moncrieff and Green (1972) and Moncrieff and Miller (1976), (hereafter MG and MM respectively), and in environments likely to be encountered when applied in the three-dimensional model.

2.2 A General Mathematical Formulation Of 2-dimensional Circulation.

In the region in and around the cumulonimbus, the variabilities in the density, pressure and temperature are small compare with the horizontal mean of the same physical parameters. The equations of motion can be simplified into the Boussinesq form:

$$\frac{D}{Dt}(\underset{\sim}{v}) + \text{grad}\frac{\delta p}{\rho} - g\delta\phi\,\underset{\sim}{k} = 0 \qquad (2.1)$$

with the following assumptions :

(1) the flow is inviscid.

(2) the Rossby number is large: of order ten, the term involving Coriolis force is ignored.

(3) the deviation of any variables is small compare with their mean values, thus:

$$\left|\frac{\delta p}{P}\right| << 1$$

$$\left|\frac{\delta\phi}{\phi}\right| << 1 \qquad (2.2)$$

$$\left|\frac{\delta\rho}{\rho}\right| << 1$$

Where $\phi = \frac{1}{\gamma}\ln(p) - \ln(\rho)$ = log potential temperature

The symbols have their usual meaning.

$$\begin{aligned} \text{And } p(x,y,z,t) &= P_o(z) + \delta p(x,y,z,t) \\ \rho(x,y,z,t) &= \rho_o(z) + \delta\rho(x,y,z,t) \\ \phi(x,y,z,t) &= \phi_o(z) + \delta\phi(x,y,z,t) \end{aligned} \qquad (2.3)$$

The continuity and energy equations are simplified to

$$\text{div}(\rho v) = 0 \qquad (2.4)$$

$$D/Dt\ (\delta\phi) + wB = Q \qquad (2.5)$$

where B is the static stability of the environment and the mean troposphere is in a hydrostatic balance. As a consequence of the approximation, the set of equations is anelastic; the effects of density fluctuation are neglected in so far as they affect the inertia of the fluid motion while only buoyancy effects in the fluids are accounted for.

2.2.1 Conservation Of Energy

In considering steady flow (D/Dt = V.grad), a Bernuolli type equation is obtained by mulitplying equation (2.1) with the velocity vector ($\underline{MG}$) .

$$\frac{D}{Dt}\left[\frac{1}{2}\underset{\sim}{V}^2 + \frac{\delta p}{\rho} - g\int \delta\phi_p\, dz\right] = 0 \qquad (2.6)$$

where $\delta\phi_p = \phi_p - \phi_o$ where ϕ_p is the log potential temperature of the parcel of air and ϕ_o is that of the undisturbed environment.

In two dimensions the conservative quantity becomes:

$$\left[\frac{1}{2}u^2 + \frac{\delta p}{\rho} - \frac{1}{2}g\int \delta\phi\, dz\right]_{1_{xz}}^{3} = 0 \qquad (2.7)$$

where subscript xz denotes the plane in which the two dimensional circulation is to take place. The subcript 3 and 1 denote the

evaluation of the expression inside the bracket in region 3 and 1 respectively (figure (2.1)). They represent regions of outflow and inflow where the motion is assumed to be horizontal and in hydrostatic equilibrium. The factor of a half is from the equipartitioning of convective available potential energy between these two degrees of freedom : along x and y (see chapter 3).

By definition, inflow at infinity is the mean environment, thus in hydrostatic balance. The function ϕ can be written as $\int(\Gamma - B)\,dz$ where Γ is the parcel's lapse rate. It is, in practice a very complicated function. For the sake of simplicity in the analytic treatment that follows, let it be a constant.

$$\Gamma = \gamma = \text{constant}$$

thus
$$\delta\phi_2 = \int_1^2 (\gamma - B)\,dz = (\gamma - B)(z_2 - z_1) \qquad (2.8)$$

The pressure term δp in the outflow is due to two factors: a dynamical pressure generated across the system which can be regarded as uniform across the outflow, and a pressure analomy generated by the effect of heating or cooling.

$$\frac{\delta p}{\rho} = \Delta P - \frac{1}{2} g \int \delta\phi_3\, dz \qquad (2.9)$$

where $\delta\phi_3$ is the deviation of log potential temperature in region 3 and ΔP is the pressure gradient across the system, and is taken to be at a height Z_* where the inflow height equals the outflow height; this marks the upper boundary of the updraught inflow.

Substitute equation (2.9) and (2.8) into (2.7) and divide through by $u_1^2/2$, putting $\delta\phi_3 = (\gamma - B)(z_3 - z_1)$ and $\delta\phi_2 = (\gamma - B)(z_2 - z_1)$ and from the continuity equation (considering motion along x axis)

$$\rho u_1 dz_1 = -\rho u_3 dz_3 \qquad (2.10)$$

(2.7) becomes

$$\left(\frac{\rho dz_1}{\rho dz_3}\right)^2 = 1 - \frac{2}{u_1^2}\left(\Delta P + \frac{1}{2}g(\gamma-\beta)\int_{z_*}^{z_3}(z_3 - z_1)\,dz_1\right) \qquad (2.11)$$

the equation is non-dimensionalised ,

$z = H\lambda$

$u = Uu(\lambda)$

$E = \frac{\Delta P}{\frac{1}{2}U^2}$

H = height of the convective system.

$$\left(\frac{d\lambda_1}{d\lambda_3}\right)^2 = \left(\frac{\rho_3}{\rho_1}\right)^2\left[1 - \frac{1}{u_1^2}\left(E + R\int_0^{\lambda}(\lambda_3 - \lambda_1)\,d\lambda_1\right)\right] \qquad (2.12)$$

where $R = g(\gamma - \beta)\, H^2 / U^2$

which is the ratio of the convective available potential energy to the square of the maximum velocity difference between the top and bottom boundaries.

And E is a non-dimensional number; a ratio of pressure energy to the maximum kinetic energy.

The position of $\lambda = 0$ is defined to be at the z_* level, thus λ_1 is negative and λ_3 is positive; both are necessarily less than unity, and the maximum magnitude of λ_1 is λ_*.

Equation (2.12) forms the basic equation from which the mid-latitude and the tropical circulations are derived, and is analagous to that of MM .

In the following section, solutions are obtained which are more general than those of MG or MM , and comparisons with their solutions are made.

2.3 The Mid-latitude Circulation

This type of circulation takes place along the plane where the wind shear is large. The level = 0 is referred to as the steering level, the inflow and outflow velocities there are zero and also at that point the air parcel is stationary relative to the circulation.

Thus the various parameters in (2.12) are :

$$E = 0$$

$$\left(\frac{d\lambda_1}{d\lambda_3}\right)^2 = \left(\frac{\rho_2}{\rho_1}\right)^2 \left[1 - \frac{R_m}{u_1^2} \int_0^{\lambda_1} (\lambda_3 - \lambda_1)\, d\lambda_1 \right] \qquad (2.13)$$

Where $R_m = g(\gamma - B)\, H / (\Delta U)^2$, it is the value of R for the mid-latitude circulation.

ΔU = velocity difference between top and bottom boundaries.

2.3.1 Boundary Conditions

The overturning process is assumed to take place between two rigid boundaries --- the ground and the top of the system, the top is defined by the thermodynamic equilibrium level of parcel originated at ground level, figure(2.3.1).

Thus when $\lambda_1 = -\lambda_*$ (2.14)

$$\lambda_3 = (1 - \lambda_*)$$

and at the steering level (z_*)

$$\lambda_1 = 0 \quad ; \quad \lambda_3 = 0 \qquad (2.15)$$

2.3.2 The Incompressible Solution

Constant Vertical Shear

The simpliest possible case was treated by MG , for constant vertical shear in an incompressible atmosphere so that

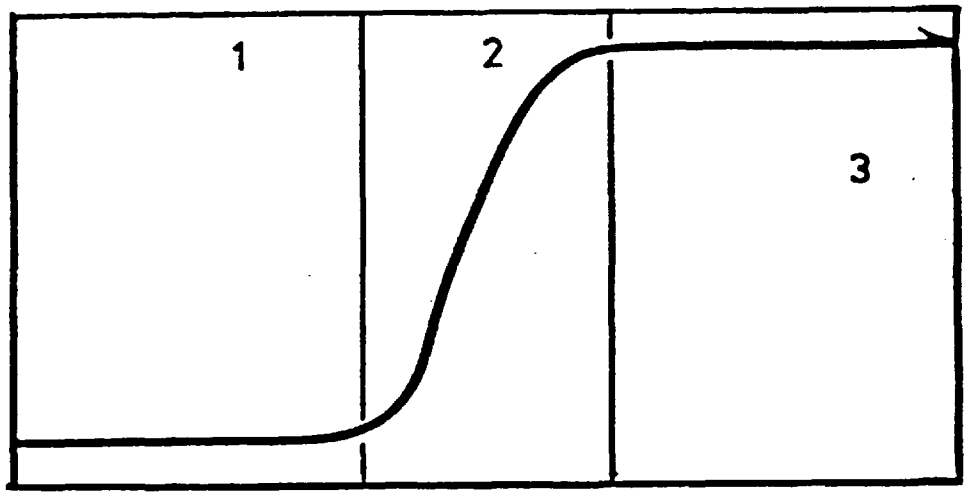

Figure 2.1 The three regions along the trajectory of an air parcel. Region (1) and (3) are inflow and outflow respectively.

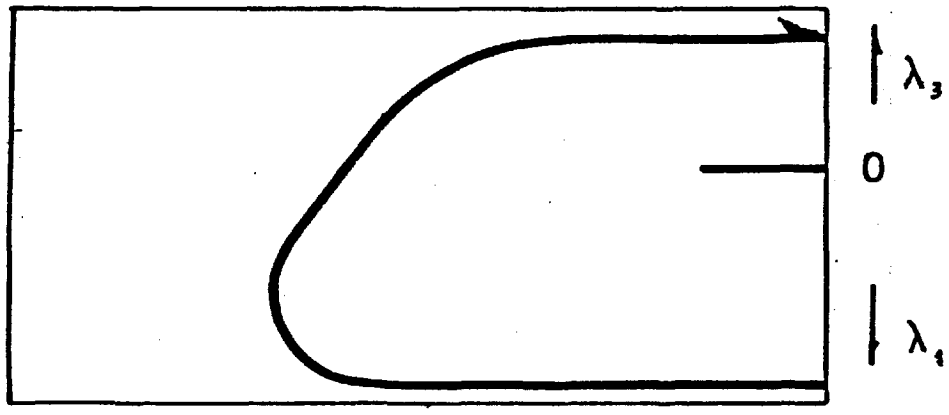

Figure 2.3.1 Schematic diagram of a mid-latitude circulation.

and
$$\rho_1 = \rho_3 \qquad (2.16)$$
$$u_1 = \lambda_1$$

equation (2.12) becomes

$$\left(\frac{d\lambda_1}{d\lambda_3}\right)^2 = \left[1 - \frac{R_m}{\lambda_1^2}\int_0^{\lambda_1}(\lambda_3 - \lambda_1)\,d\lambda_1\right] \qquad (2.17)$$

R_m is the eigenvalue of this eigenvalue equation. Analytic solutions exist if $\frac{d\lambda_1}{d\lambda_3}$ equals to a constant equals $-\beta$. (MG)

giving $$R_m = 2\beta(\beta - 1) \qquad (2.18)$$

applying the boundary conditions gives

$$\lambda_* = \frac{\beta}{1+\beta} \qquad (2.19)$$

the corresponding steering level in height scale is

$$z_* = \frac{\beta}{1+\beta} H \qquad (2.20)$$

The steering level is necessarily higher than the mid-level; this is because R_m is always positive, β is bigger than one --- convection occurs to reduce the overall potential energy, which is always finite and positive. One of the results is that the outflow shear is constant, and is increased by a factor of β^2 .

$$u_3 = \beta^2 \lambda_3 \qquad (2.21)$$

The circulation is completely defined by the non-dimensional number R_m.

2.3.3 Non-constant Shear Profile of Horizontal Velocity

In this section, more general solutions are obtained for non-constant shear since a strictly linear velocity profile is idealised. It is important, therefore, to investigate the effect of such a profile on the general behaviour of the model.

Let $$u_1(\lambda_1) = \lambda_1 + a(\lambda_1) \qquad (2.22)$$

where $a(\lambda_1)$ is an arbitrary function of λ_1 , and normalised with respect

to ΔU. Differentiate (2.17) with respect to λ_3 and rearrange. Notice that $\frac{d\lambda_1}{d\lambda_3} \neq 0$ except at the steering level.

$$\frac{d^2\lambda_1}{d\lambda_3^2} = \frac{R_m}{2}\left[\frac{\lambda_1 - \lambda_2}{u_1^2}\right] + \frac{1}{u_1}\frac{du_1}{d\lambda_1}\left(1 - \left(\frac{d\lambda_1}{d\lambda_3}\right)^2\right) \qquad (2.23)$$

except at $z = z_*$.

2.3.4 Local Analytical Solution In The Region Of $\lambda_1 \to 0$

Solutions to the equation requires values of λ_1 or λ_3 and its derivative to be specified at two boundaries. The boundary condition at $\lambda_1 = 0$ presents problems, since equation (2.23) becomes singular. This boundary condition can be replaced by

$$\lambda_1 = h \qquad (2.24)$$

where h is small.

Substitute into (2.23) and assuming $\frac{d\lambda_1}{d\lambda_3}$ changes very little in the range $0 < \lambda_1 < h$. It is accurately represented in

$$\left(\frac{d\lambda_1}{d\lambda_3}\right)^3 = \frac{d\lambda_1}{d\lambda_3} - \frac{R_m}{2u_1^2} h^2 \left(\frac{d\lambda_1}{d\lambda_3} - 1\right) \qquad (2.25)$$

$$\left.\frac{d\lambda_1}{d\lambda_3}\right|_h = -\frac{1}{2}\left[1 \pm \sqrt{\left(1 + \frac{2h^2}{u_1^2} R_m\right)}\right] \qquad (2.26)$$

since $\frac{d\lambda_1}{d\lambda_3}$ is always negative, the positive sign is chosen. In the limit that $u \to h$,

$$\frac{d\lambda_1}{d\lambda_3} = -\frac{1}{2}\left[1 + \sqrt{(1 + 2R_m)}\right] \qquad (2.27)$$

Thus locally, the solution is analagous to that obtained globally for the constant shear problem considered previously, which gives $\frac{d\lambda_1}{d\lambda_3}$ a constant value, it depends only on the value of R_m. Thus at $\lambda_1 = h$, the value of $\frac{d\lambda_1}{d\lambda_3}$ is known. olution is obtained from a shooting method technique. The equation is integrated from $\lambda_1 = h$ towards the other boundary and the solution there is made to match the condition $|\lambda_1| + \lambda_3 = 1$, using an iterative method. (further details in Hall and

Watts (1976)).

2.3.5 General Velocity Profiles

Any profile can be described by a sum of a series of sines and cosines terms.

$$a(\lambda_1) = \sum_{n=0}^{\infty} a_n \cos k_n \lambda_1 + b_n \sin k_n \lambda_1 \qquad (2.28)$$

For ease of computation and to act as an illustration, only one k value is considered to represent a velocity profile which resembles some of those encountered in the atmosphere, such as a small curvature and a local large deviation from the contant shear profile at low level, commonly referred to as the low level jet.

2.3.6 Special Case : $R_m = 0$

A unique solution occurs when $R_m = 0$, from (2.23) , it can be seen that $\frac{d\lambda_1}{d\lambda_3} = -1$ and is independent of the profile described by $a(\lambda_1)$. Though $R_m = 0$ is an unrealistic case since no convection occurs at zero potential energy, the implication is that when R_m is very small, due to a very high directional shear in the environment, the value of z_* will not be influenced by the non-linear part of the velocity profile $a(\lambda_1)$, but on the overall shear, and the density stratification which is expanded upon later.

2.3.7 Small Curvature

For $a(\lambda_1) = a(\cos(k\lambda_1) - 1)$.

where $k = \frac{2\pi}{8\lambda_*}$

For small curvature the profile obtained is a small deviation from the linear case. The deviation is of the same sign and thus does not interfere with overall shear throughout the depth. Figure (2.3.2)

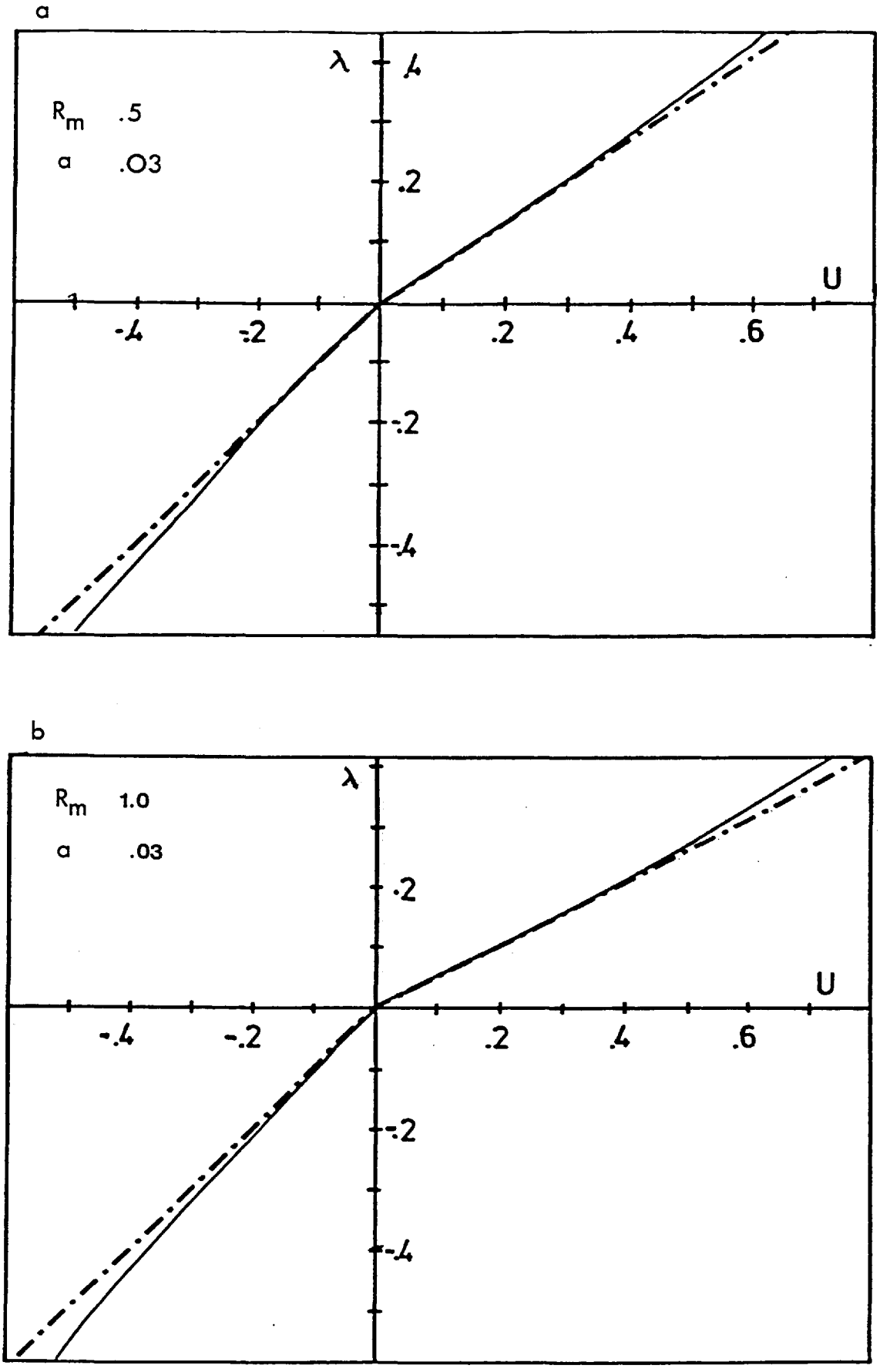

Figure 2.3.2 Velcoity profiles of inflow and outflow for a constant shear inflow profile (dashed lines) and a small positive deviation from it (continuous lines)

shows the inflow and outflow profiles when 'a' is positive (the dashed line represents the constant shear case, and the continuous line indicated the profile with non-constant shear) .

In the outflow, the deviation from the constant shear profile is suppressed. As R_m increases, the outflow tends to the constant shear outflow profile. The deviation of velocity at the top extreme outflow is 0.06 at $R_m = 0.5$. This is reduced to 0.05 at $R_m = 1.0$, despite a larger deviation at the inflow.

When a is negative, the deviation from the constant shear profile at the inflow is translated into a bigger deviation in the outflow, see figure (2.3.3) .

A small deviation at the inflow produces a deviation of the opposite sign at the outflow. The circulation reduces the size of the deviation at the outflow when there is a positive deviation at the inflow. The positive deviation at the outflow is amplified when there is a negative deviation at the inflow.

The effect of $a(\lambda_1)$, however, is negligible on the height of the steering level; it does not change by more than one percent for a varying from -0.2 to 0.2.

2.3.8 Low Level Jet Profile

A local velocity maximum can be set up by putting

$$a(\lambda_1) = a(1 - \cos(\frac{2\pi}{\lambda_*}\lambda_1)) \qquad (2.29)$$

in which case maximum deviation from the mean constant sheared profile is situated at $\lambda_1 = \lambda_*/2$. a positive produces a jet pointing towards the direction of the shear, and in the opposite direction for a negative value of a. These directions are referred to as forward and backward pointing jet, or a positive and a negative jet respectively.

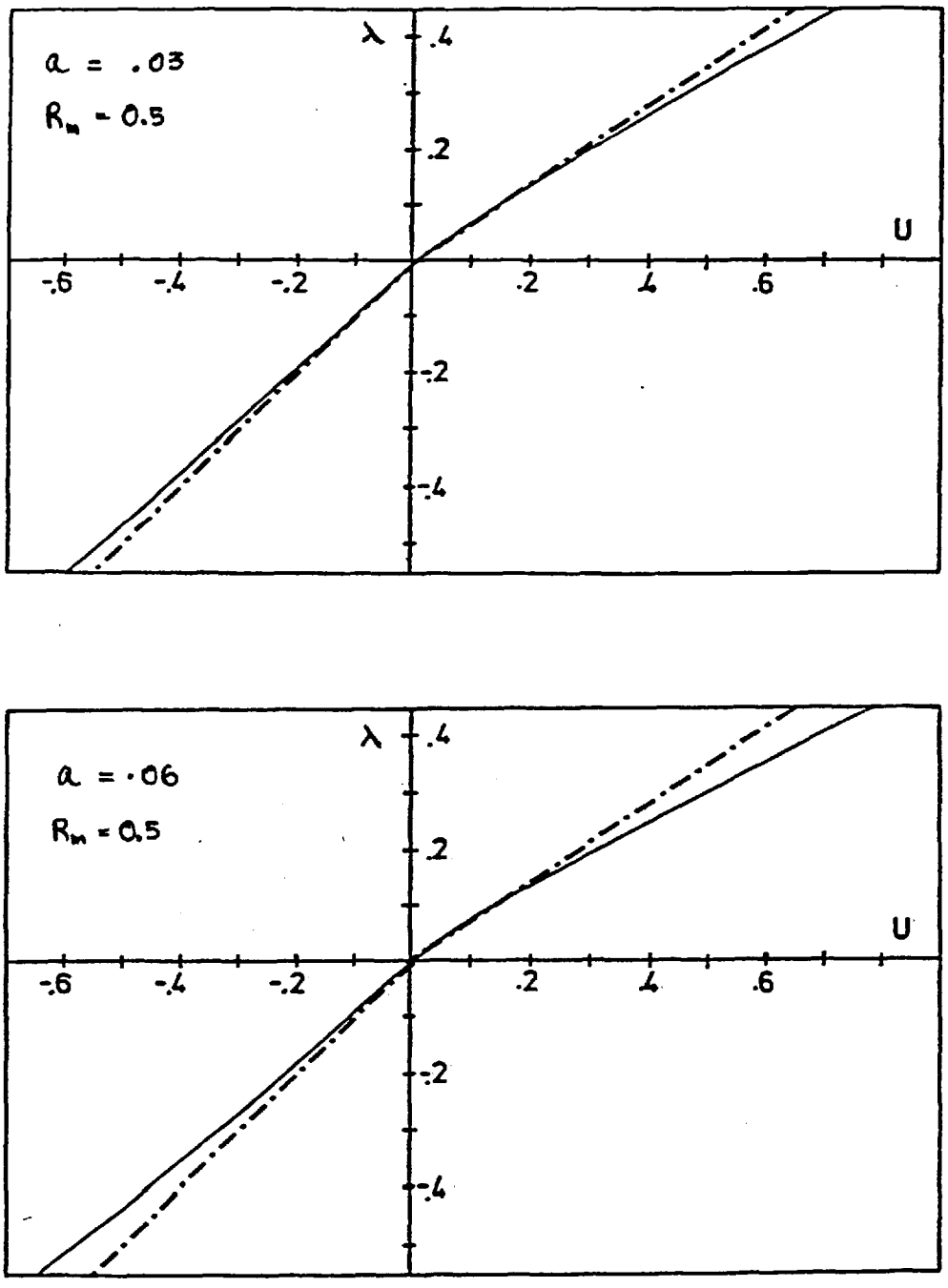

Figure 2.3.3 Velocity profiles of inflow and outflow for a constant shear inflow profile (dashed line) and a gentle negative deviation from it (continuous line).

The terminology is far from satisfactory, but it serves to distinguish the two types of jets. The deviation amplitude is to be interpreted as the size of the jet. A jet at the inflow produces a jet which points towards the opposite direction at the outflow. This result is consistent with those obtained earlier. Relative to the moving circulation, a forward jet at the inflow means a smaller inflow speed at that point. The corresponding outflow speed is expected to be smaller than the case when the forward jet is absent.

2.3.8.1 Backward Pointing Jet (a Negative)

Figure (2.3.4) shows two profiles at a = -0.02 and a = -0.06. There is a significant increase in the maximum deviation from the linear profile at the outflow; for instance, in the lower profile when a = - 0.06, a jet of size 0.12 at the inflow produces a jet at the outflow of size 0.26.

2.3.8.2 Forward Pointing Jet (a Positive)

The converse of the above is true in the case when a is postive. This is illustrated in fig (2.3.5). In the lower figure, an inflow jet of size 0.2 is reduced to 0.15 in the outflow.

Though only two examples are presented in each case of positive and negative jets, the same trend is exhibited in calculations with different values of R_m and a .

The effect of a low level jet on the dynamics is reflected in the change of λ_* at constant values of R_m with different values of 'a'. The effect of a negative and a positive low level jet is similar, there is a non-linear increase of λ_* with 'a', figure (2.3.6)

2.3.8.3 Position of a Low Level Jet

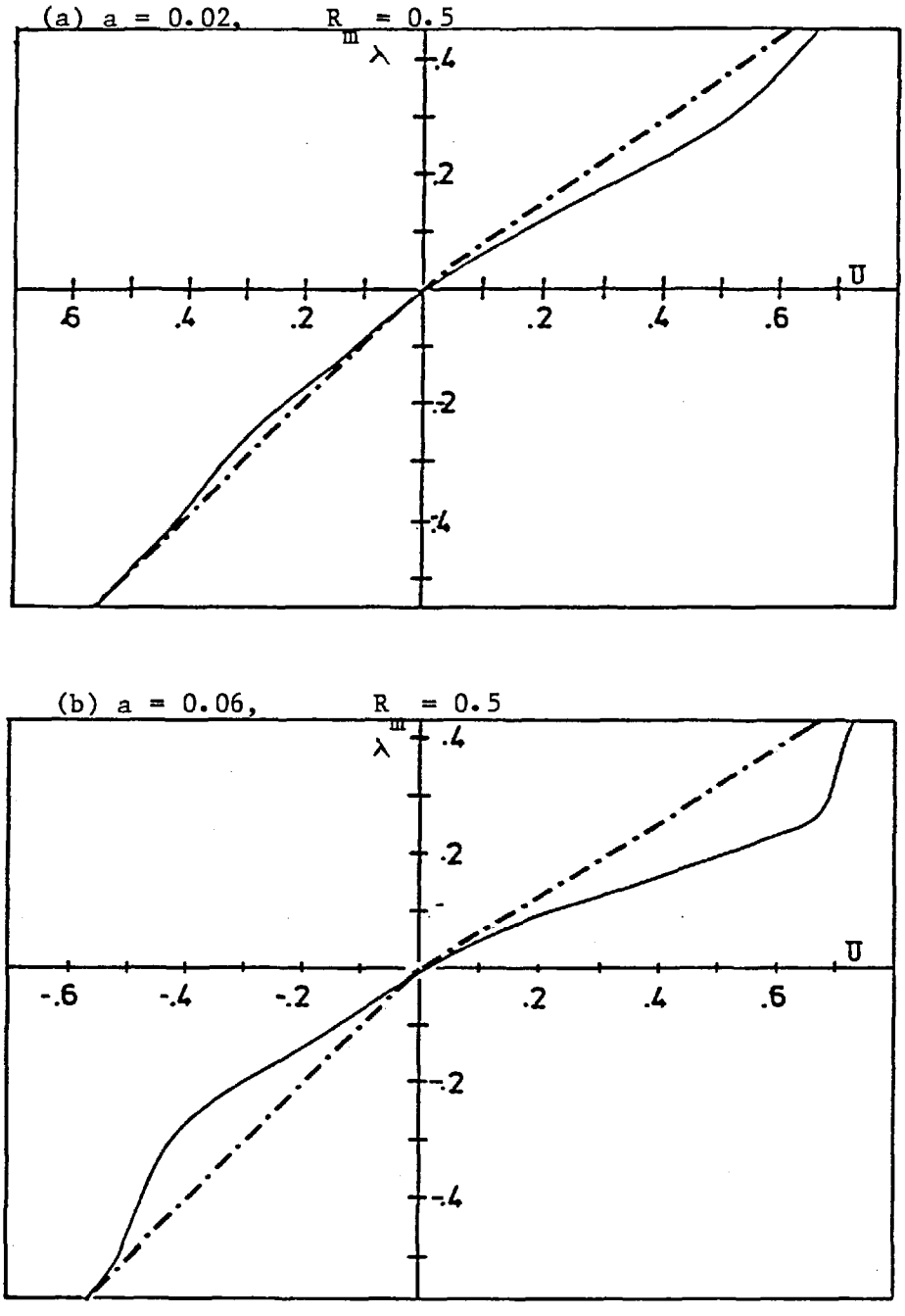

Figure 2.3.4 Velocity profiles of inflow and outflow for a constant shear inflow profile (dashed line) and a negative low level jet (continuous line).

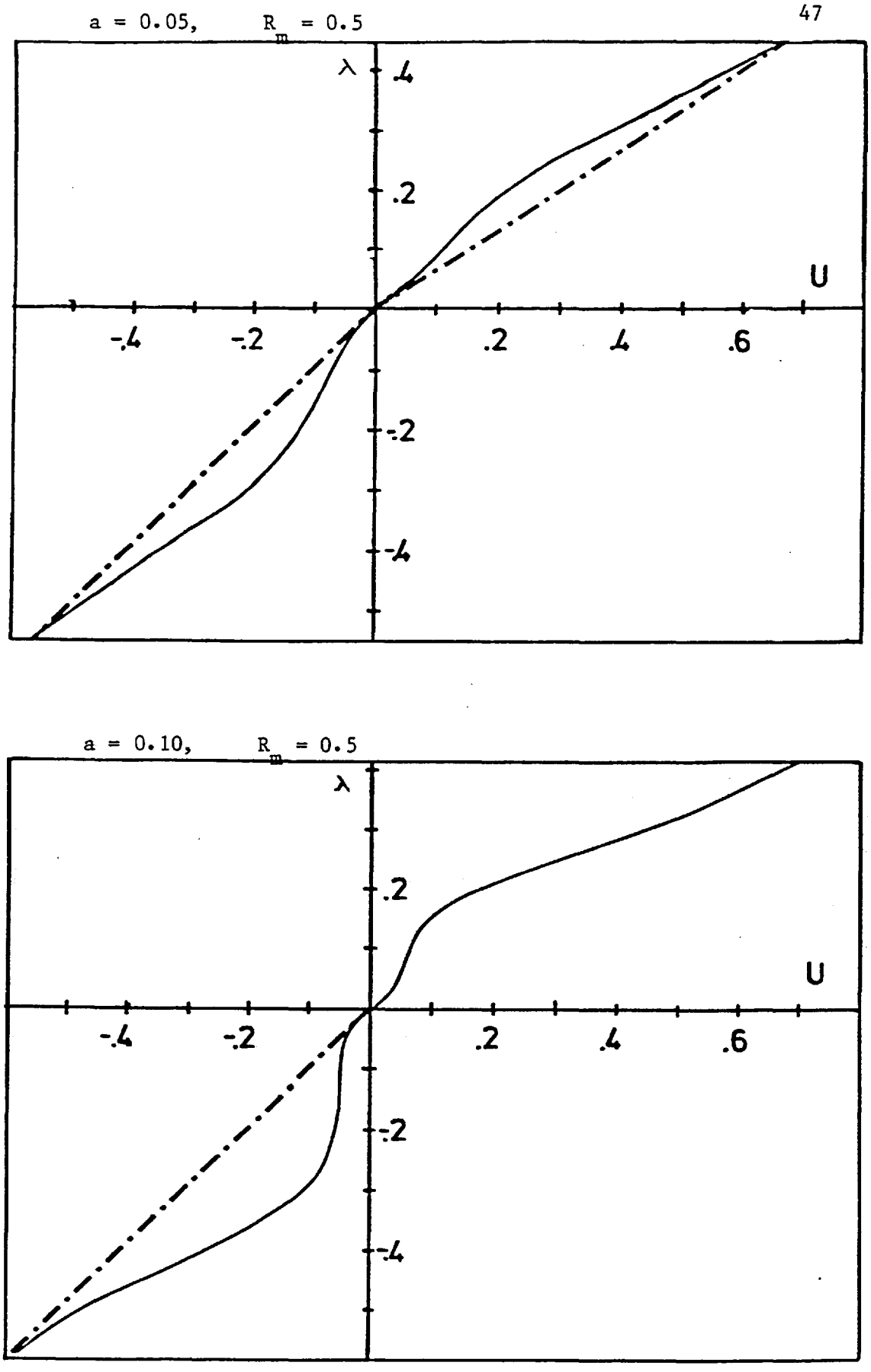

Figure 2.3.5 Velocity profiles of inflow and outflow for a constant shear inflow profile (dashed line) and a positive low level jet (continuous line).

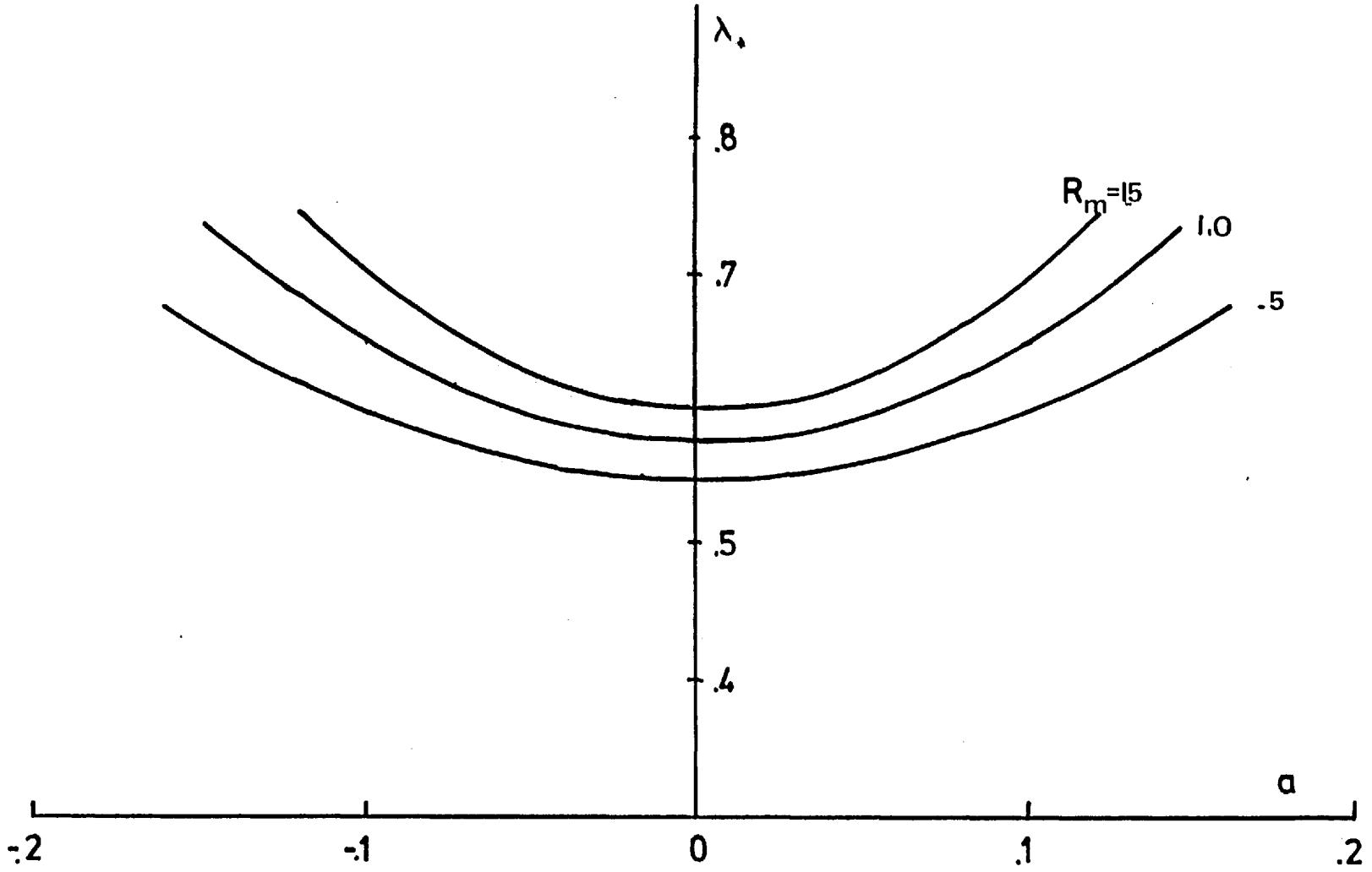

Figure 2.3.6 Variation of the steering level λ_* with the amplitude of the low level jet, a.

By putting

$$a(\lambda_1) = a(1 - \cos(\frac{\pi}{\lambda_*}\lambda_1)) \qquad (2.30)$$

the maximum deviation occurs at $\lambda_1 = -\lambda_*$, this can be thought of as a crude way to represent a low level jet situated very near the ground. A positive jet at the inflow produces a smaller negative at the outflow, and visa versa for a negative jet. This is illustrated in fig (2.3.7) and fig (2.3.8). They are in agreement with the above observations.

The variation of λ_* with 'a', is shown in figure (2.3.9). It shows that λ_* increases with |a|, though at a lesser rate than is the case when the jet is at a higher level (see figure 2.3.6), indicating that the position of the jet may affect the steering level and its dynamics, when its magnitude is large.

The general result is that a deviation at the inflow is translated into a deviation of the opposite sign at the outflow. When the deviation at the inflow is positive, the deviation at the outflow is lesser, and visa versa.

It is worth noting that when a = -0.1, the size of the jet is 0.2 times the velocity difference between the top of the troposphere to the ground. In the cases studied, the average is of the order 50 ms^{-1} a 10 ms^{-1} jet does not very often occur; the likely range of 'a' is below 0.05. This range lies in the flatest part of the curves, thus in the cases observed here at least, 'a' plays a minor role.

2.3.9 Compressible Solution

The incompressible solution gives an insight to the dynamics of the circulation, however, for the purpose of comparing it with the atmosphere, the density variation has to be taken into account. From

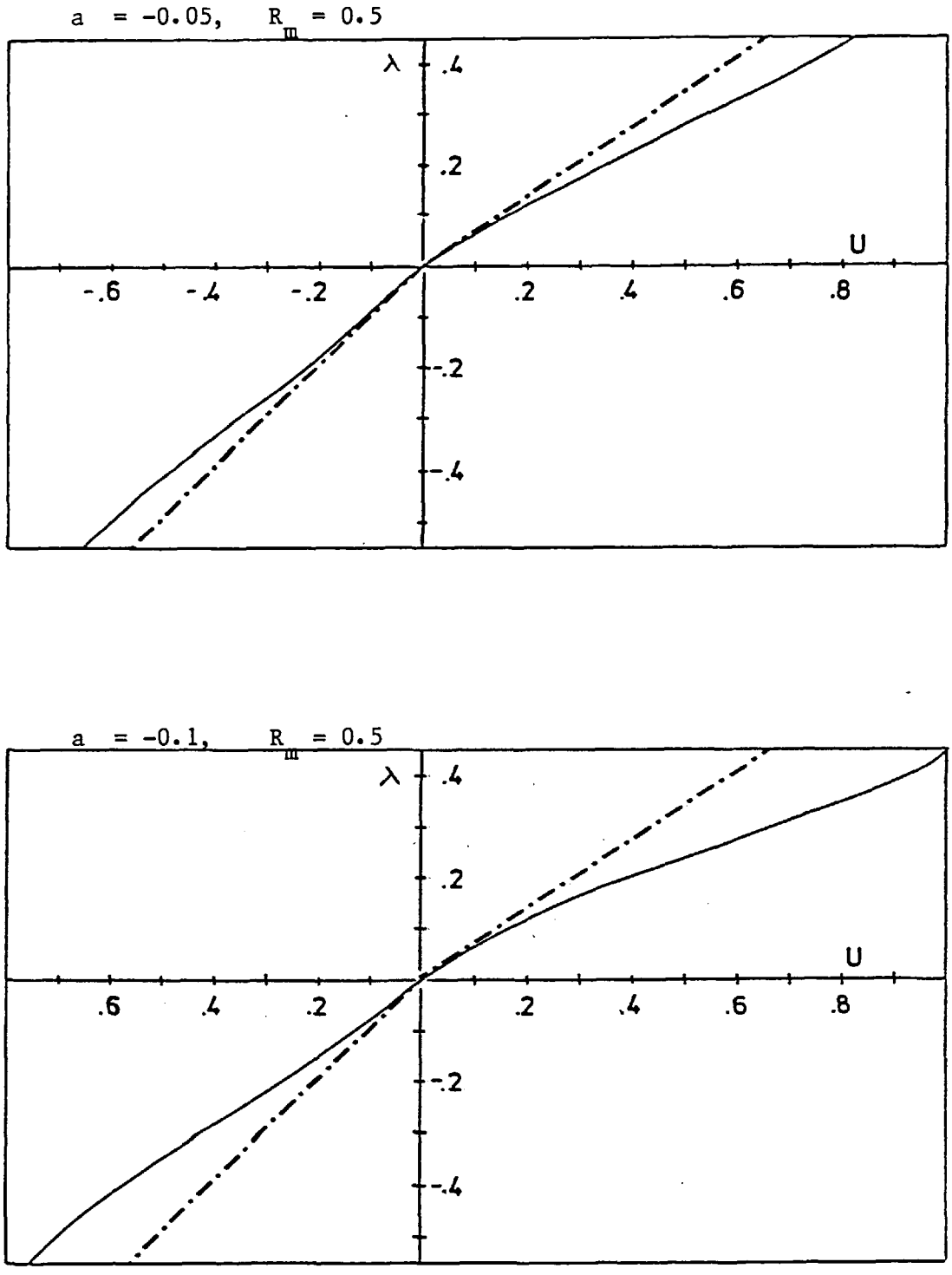

Figure 2.3.7 Velocity profiles of inflow and outflow for a constant shear inflow profile (dashed lines) and a negative low level jet profile (continuous lines).

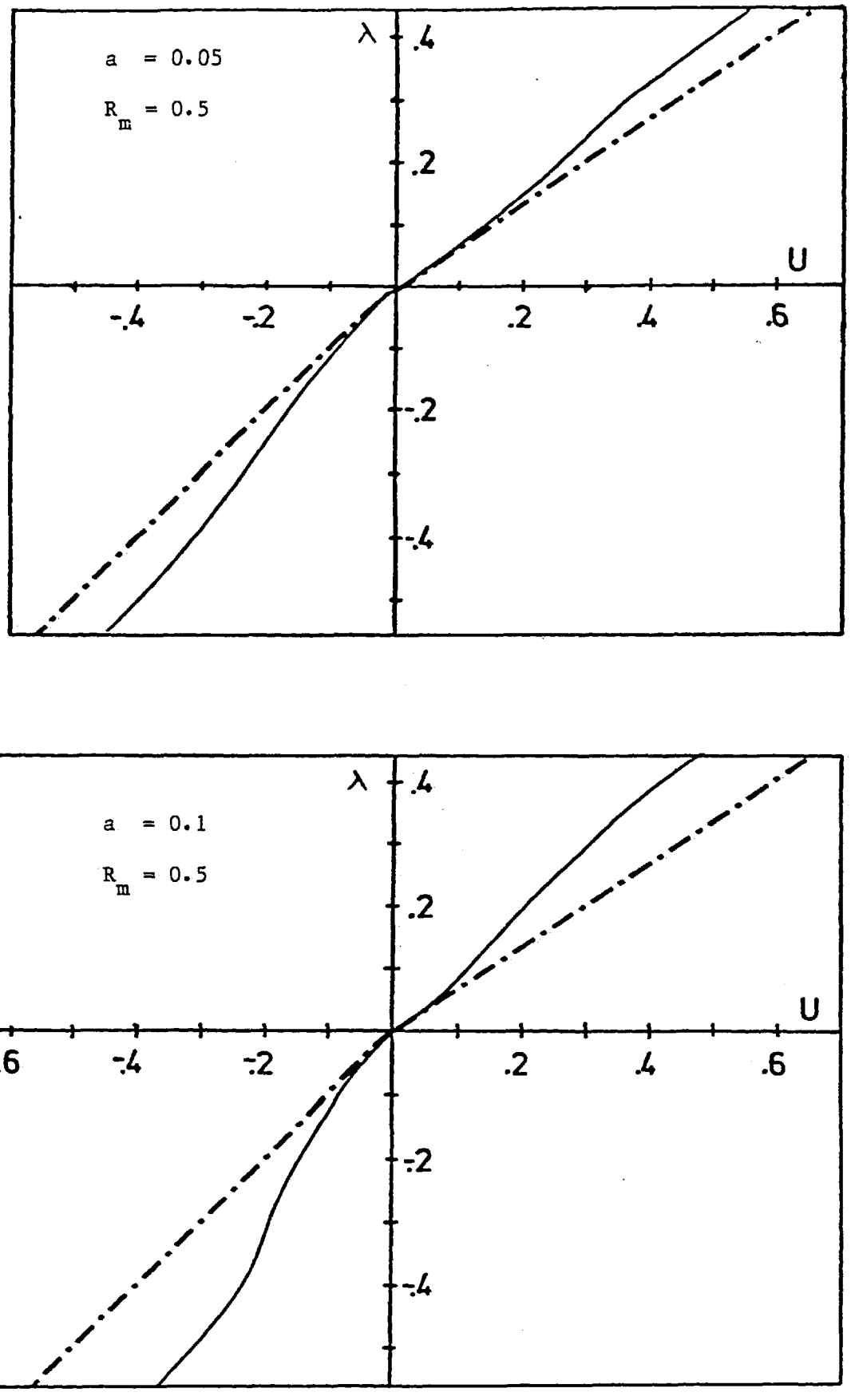

Figure 2.3.8 Velocity profiles of inflow and outflow for a low level jet situated at ground level (continuous lines) and in constant shear, (dashed lines)

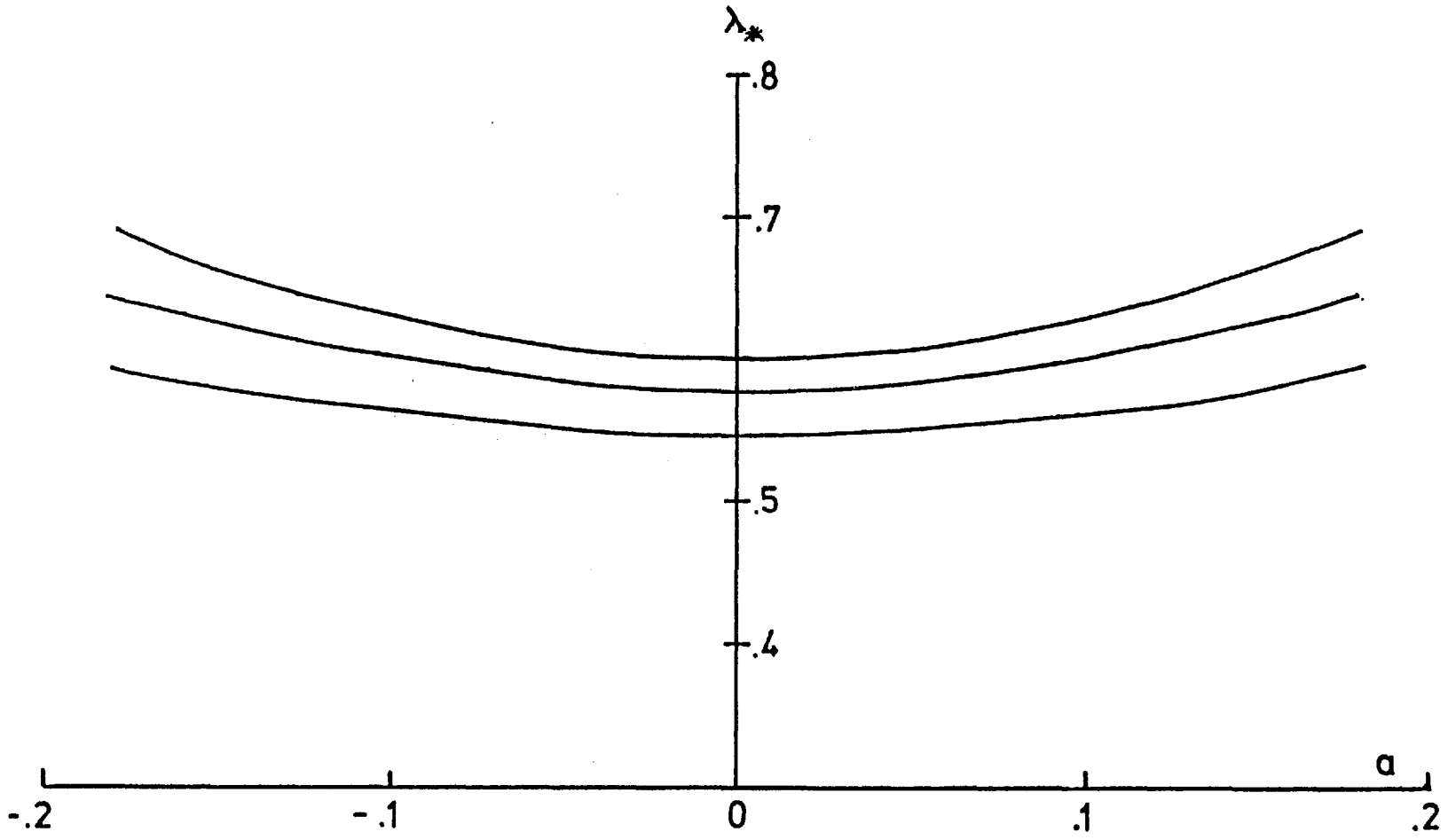

Figure 2.3.9 Variation of the steering level λ_* with the amplitude of the low level jet, a .

equation (2.13) , differentiate with respect of λ_3 and rearrange, for the case of constant shear

$$\frac{d\lambda_1}{d\lambda_3^2} = \left(\frac{d\lambda_1}{d\lambda_3} - 1\right)\frac{d\lambda_1}{d\lambda_3} D + e^{-2(\lambda_3-\lambda_1)D}\left(\frac{1}{\lambda_1} - \frac{R_m}{2\lambda_1^2}(\lambda_3-\lambda_1)\right) - \frac{1}{\lambda_1}\left(\frac{d\lambda_1}{d\lambda_3}\right)^2 \quad (2.31)$$

The solution is presented in figure (2.3.10) as a graph of λ_* varies with D for various values of R_m. Within the range of D calculated, λ_* varies linearly with D .It can be described by

$$\frac{d\lambda_*}{dD} = -.11 \quad (2.32)$$

This linear relationship holds for D < 1.5 to a very good approximation. It can be extended to D = 2.0 with a consequent error of less than 6 percent.

This linear relationship is valid for D being negative. D negative is the case when the density stratification is in the reverse sense. In considering the dynamics of the downdraught, air parcels descend from a high level to a lower level, such circulation see a negative value of D (a full discusion is in chapter 4). Thus for the updraught λ_* decreases with a stronger density stratification, the equivalent steering level in the downdraught circulation increases with D.

Figure (2.3.11) shows two velocity outflow and inflow profiles for two values of D at $R_m = 1$. The outflow velocity is reduced as a result of density stratification. This is in direct contrast with the amplitude of a disturbance such as gravity wave, the specific kinetic energy of which is constant, thus the velocity increases as density decreases. However, cumulonimbus is a bigger scale of motion expanding the whole depth of the troposphere, the analysis of a small disturbance in an atmosphere which is in effect an infinite medium does not apply.

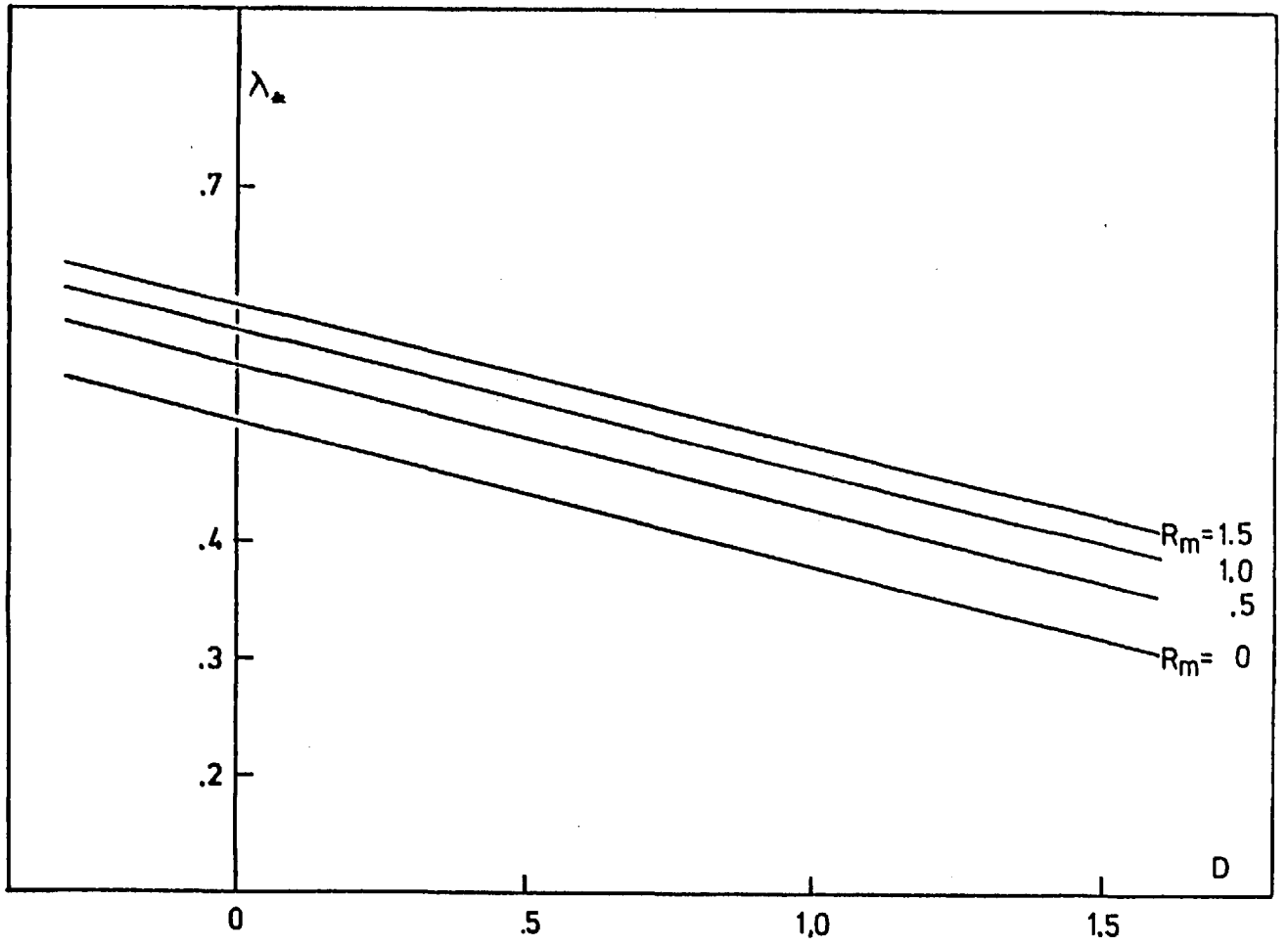

Figure 2.3.10 Steering level λ_* as a function of density stratification D, at discrete values of R_m.

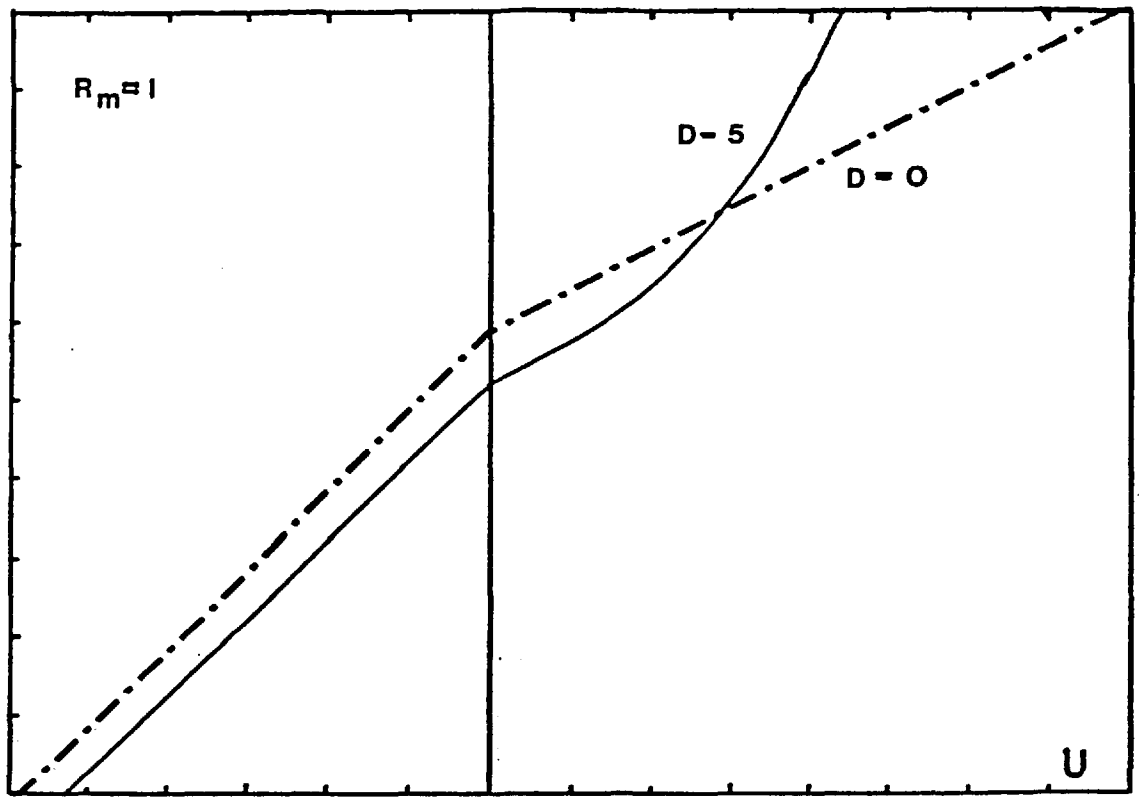

Figure 2.3.11 Velocity profiles of inflow and outflow at two different values of D.

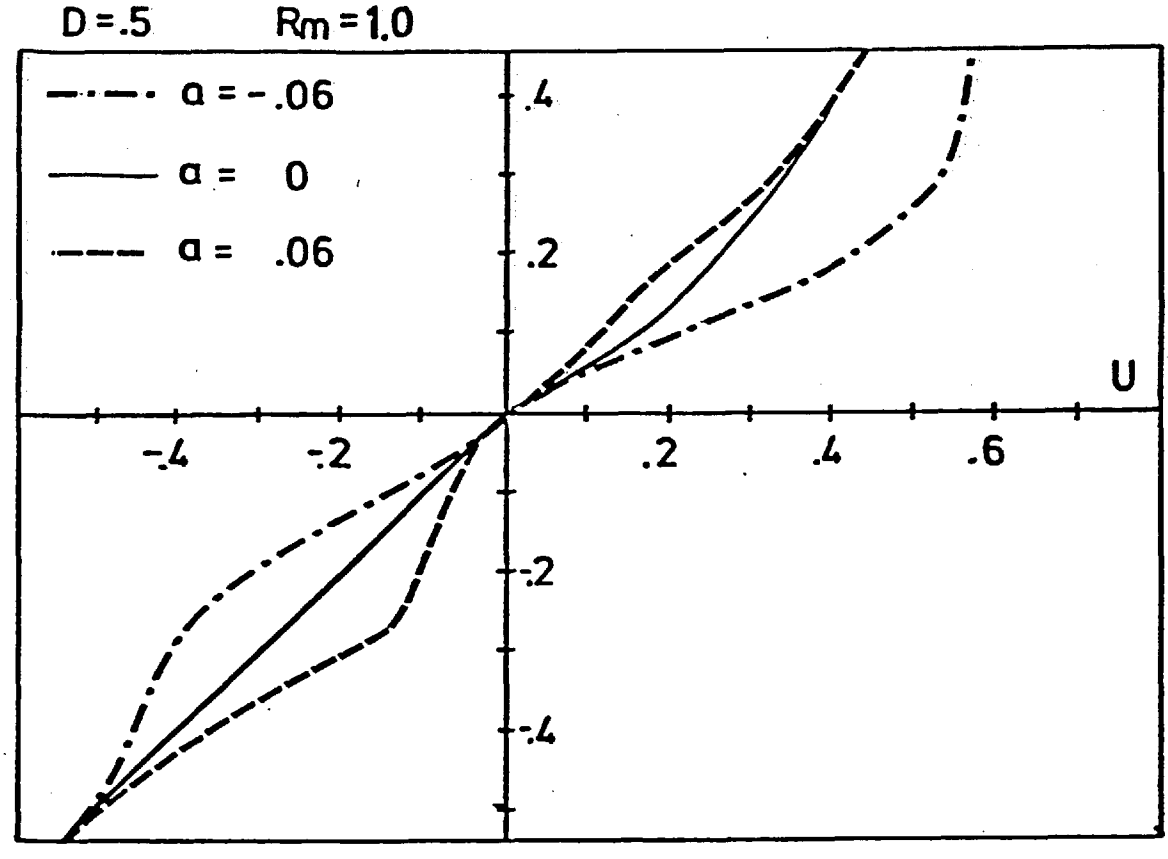

Figure 2.3.12 Velocity profiles of inflow and outflow for a positive and a negative low level jet in the presence of density stratification.

The effect of a negative low level jet exhibits similar amplification at the outflow as in cases when D = 0 similar reduction with a positive jet can be observed in figure (2.3.12).

2.4 Tropical Circulation

The effects of more complicated dynamics than those considered by MM are discussed in this section. In MM only solution with zero inflow and constant inflow shear were considered and it is possible that there may be some overestimation.

In this circulation the inflow approaches the system at all levels; there is no steering level as in the case of the mid-latitude circulation, that is the flow is in the same sense at all levels of inflow (and outflow)

Equation (2.12) becomes

$$\left(\frac{d\lambda_1}{d\lambda_3}\right)^2 = \left(\frac{\rho_3}{\rho_1}\right)^2 \left[1 - \frac{1}{V_1^2}\left(E + R_t \int_0^{\lambda_1} (\lambda_3 - \lambda_1)\, d\lambda_1 \right] \right. \qquad (2.33)$$

where

$$R_t = \frac{g(\gamma - \beta)H^2}{C^2} \qquad (2.34)$$

where C = propagation velocity of the tropical circulation. Let

$$\left(\frac{\rho_3}{\rho_1}\right)^2 = \exp(-2(\lambda_3 - \lambda_1)D) \qquad (2.35)$$

ignoring the solution $\frac{d\lambda_1}{d\lambda_3} = 0$ everywhere.

2.4.1. Boundary Conditions

The inflow at the bottom exit at the top, figure(2.4.1) ,thus

$$\lambda_1 = \alpha - 1 \quad ; \quad \lambda_3 = \alpha \qquad (2.36)$$

moreover, since the middle streamline is assumed not to be displaced

$$\lambda_1 = 0 \quad ; \quad \lambda_3 = 0 \qquad (2.37)$$

the thickness of inflow varies according to the dynamics.

2.4.2 Incompressible Solutions

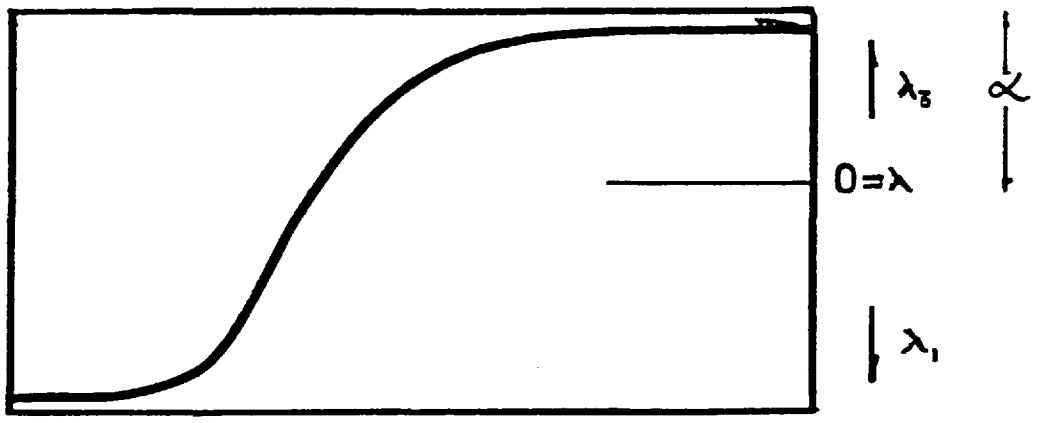

Figure 2.4.1 Schematic diagram of a tropical circulation

For $V_1 = 1$, there is no wind shear, an analytic solution exist to the incompressible problem. (in MM, $\alpha = 1/2$ was presented.)

$$\lambda_1 = \lambda_3 - \sqrt{\left(\frac{R_t}{2}\right)}\left[1 \pm \sqrt{(1-E)}\right] \sinh\left(\sqrt{\frac{R_t}{2}}\,\lambda_3\right) \qquad (2.38)$$

application of the boundary condition yields :

$$\alpha = \sqrt{\frac{2}{R_t}} \sinh^{-1}\left[\sqrt{\frac{R_t}{2}}\left(1 + \sqrt{(1-E)}\right)\right] \qquad (2.39)$$

It has been shown in MM that for a system consistent with the assumption that all inflows approach the system from one direction; and for maximum conversion of available potential energy into mean flow kinetic energy, E = 1. For the remaining part of the analysis on tropical circulation, E is given the value of 1.

The parameter R_t determines the profile of the outflow, as well as the propagation speed of the tropical circulation relative to the level at $\lambda = 0$, figure (2.4.2) gives the relationship between C and α.

The velocity outflow is determined from equation (2.38)

$$V_3 = C\left(1 - \cosh\frac{\lambda_3}{C}\right) \qquad (2.40)$$

relative to the moving tropical circulation, and non-dimensionalised with respect to CAPE.

The outflow profiles for various value of α are shown in figure (2.4.3), the direction of propagation is defined as the positive direction. The profiles are those of hyperbolic cosines. As α decreases, the propagation speed reduces, so does the positive velocity at the mid-level. The negative velocity at higher level however, increases.

2.4.3 Non Constant Velocity Profile

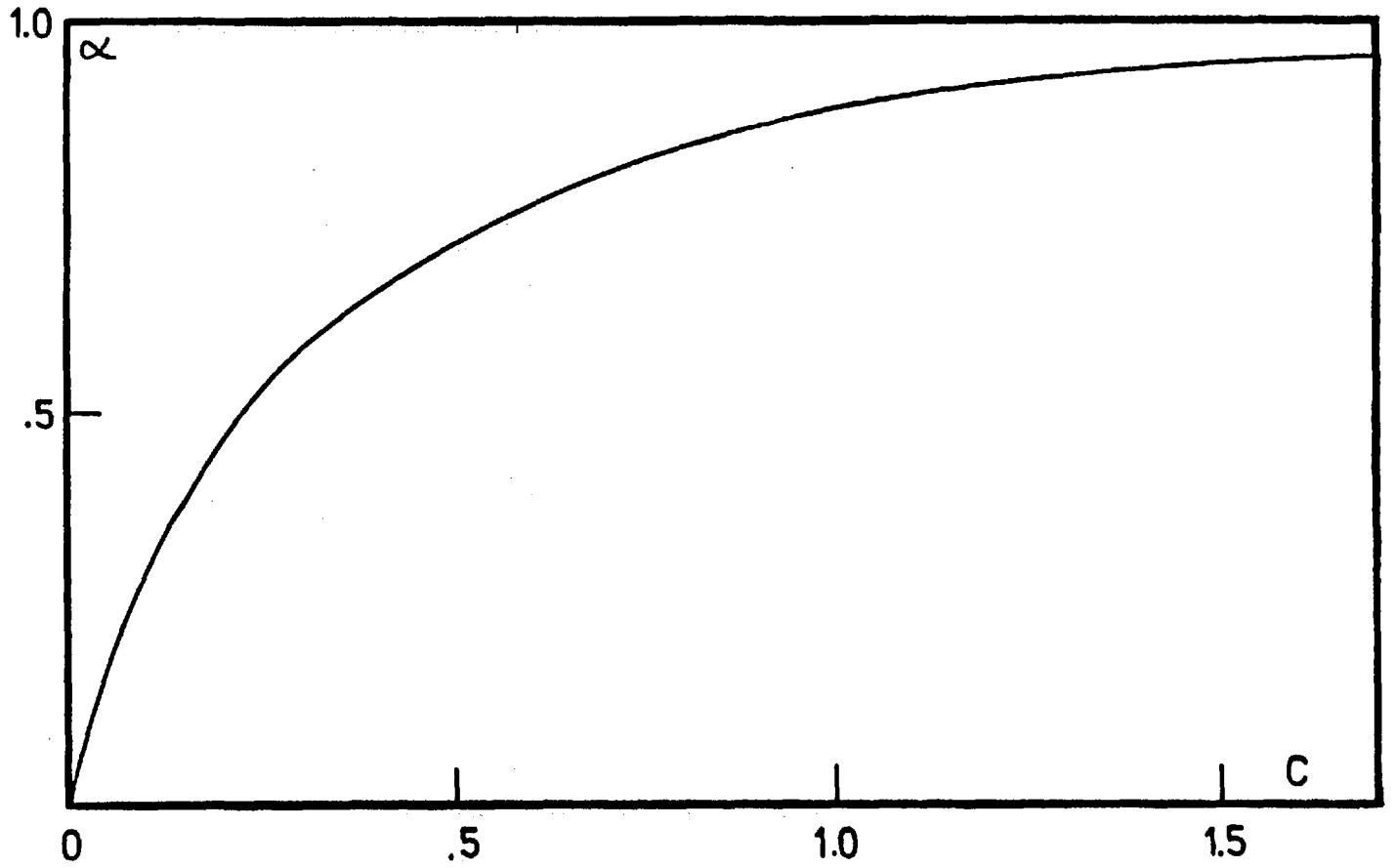

Figure 2.4.2 Variation of the maximum outflow height α with the propagation speed C.

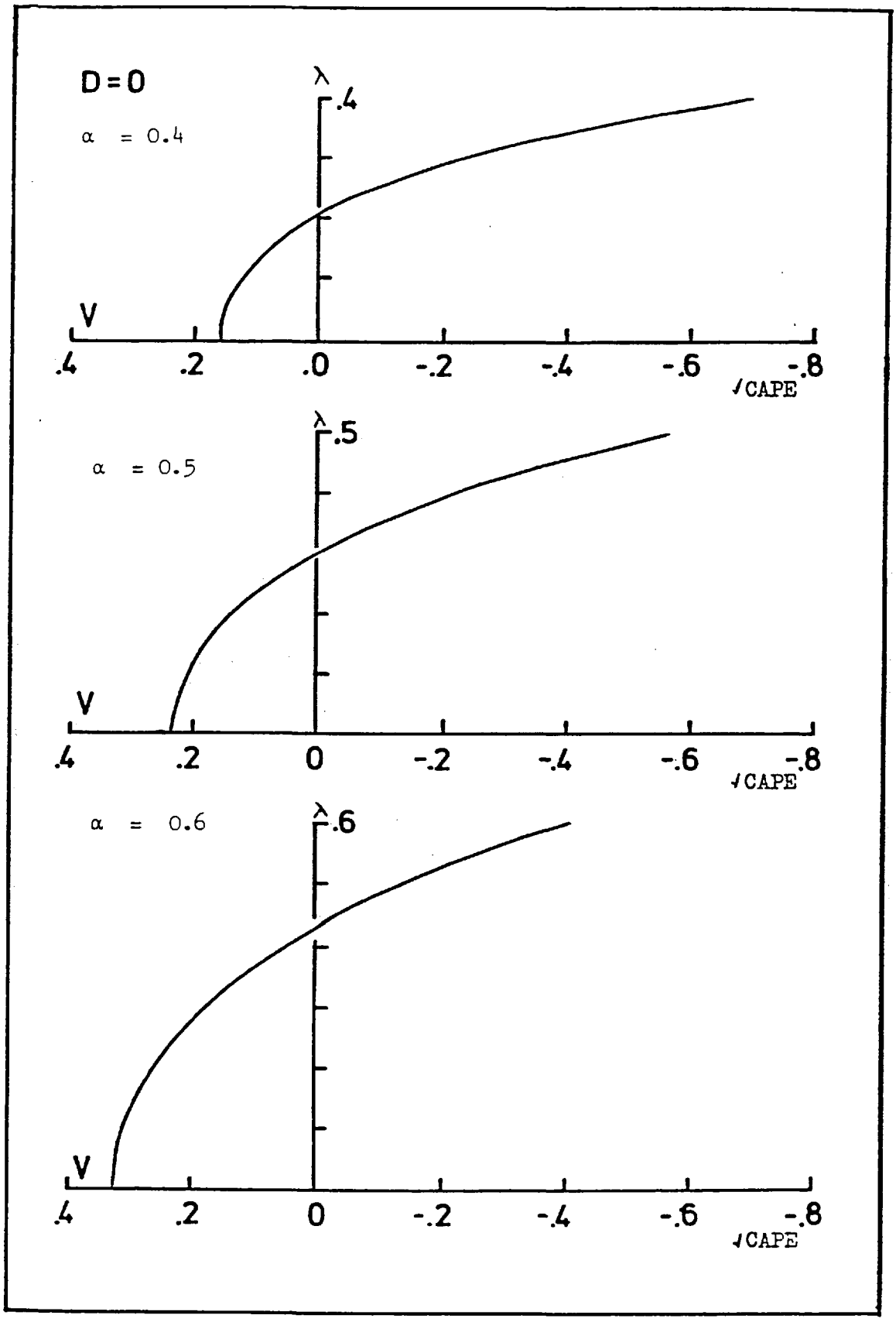

Figure 2.4.3 Velocity profiles of outflow at three discrete value of α .

The departure of a uniform constant velocity profile was investigated using several simple functions to represent certain characteristic velocity profiles that are observed.

If $$V_1 = 1 + v_1(\lambda_1)$$

where $v_1(\lambda_1)$ represents the departure from the uniform constant profile, and is normalised with respect to $\sqrt{CAPE}$. Differentiating equation (2.33) and rearranging gives :

$$\frac{d^2\lambda_1}{d\lambda_3^2} = -\frac{R_t(\lambda_3-\lambda_1)}{2(1+v_1)^2} + \frac{1}{(1+v_1)}\frac{dv_1}{d\lambda_1}\left(1+\left(\frac{d\lambda_1}{d\lambda_3}\right)^2\right) \qquad (2.41)$$

R_t is an eigenvalue to be determined from this two boundary value problem. It was solved numerically using an iteratively shooting methods technique (as in section 2.3.4).

2.4.4 Parabolic Profile.

$$v_1(\lambda_1) = a\lambda_1^2 \qquad (2.42)$$

The outflow velocity profiles for $\alpha = 0.4$ is shown in figure (2.4.4) for various value of 'a' which is normalised with respect to $\sqrt{CAPE}$. The outflow profiles are similar to the hyperbolic cosine profile obtained earlier when a = 0. Figure (2.4.5) tells the same story, for the case when $\alpha = 0.5$. The numerical solutions showed that $\frac{d\lambda_1}{d\lambda_3}$ changes in the opposite sense as the inflow velocity. Thus at $\lambda_1 = (\alpha - 1)$, where the inflow velocity is smallest, $\left|\frac{d\lambda_1}{d\lambda_3}\right|$ is largest. For example,for $\alpha = 0.5$ and $\lambda_1 = -0.5$, when a = 0, $\frac{d\lambda_1}{d\lambda_3} = -3.47$; it decreases to -13.3 when 'a' is increased to 0.2. The net effect is to maintain a similar velocity outflow profile, despite changes at the inflow.

R_t is a non-linear function of 'a', it is generally a large number, bigger than 10. However, there is a near linear relationship

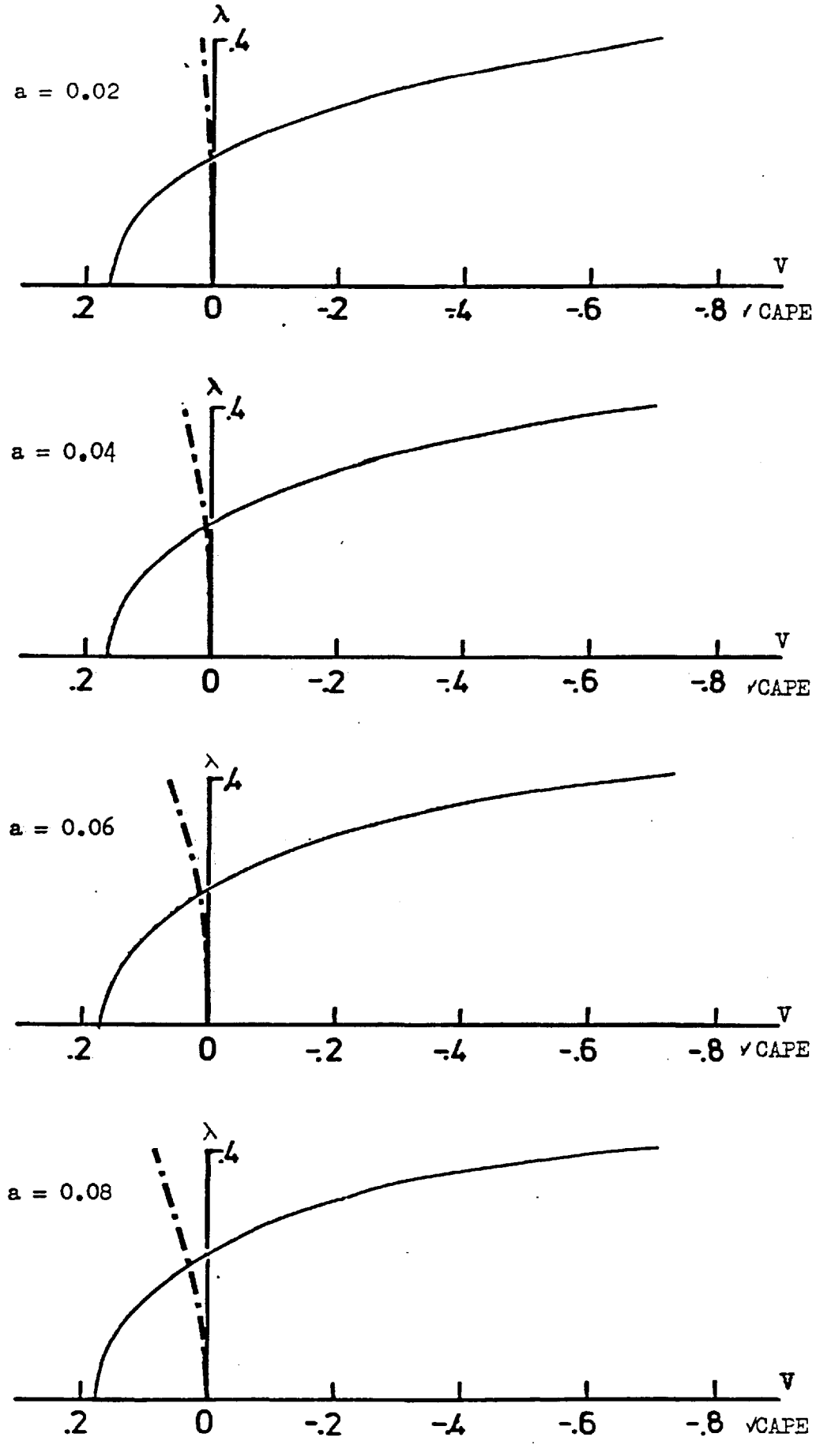

Figure 2.4.4 Velocity profiles of outflow (continuous lines) for a parabolic inflow profile (dashed lines).

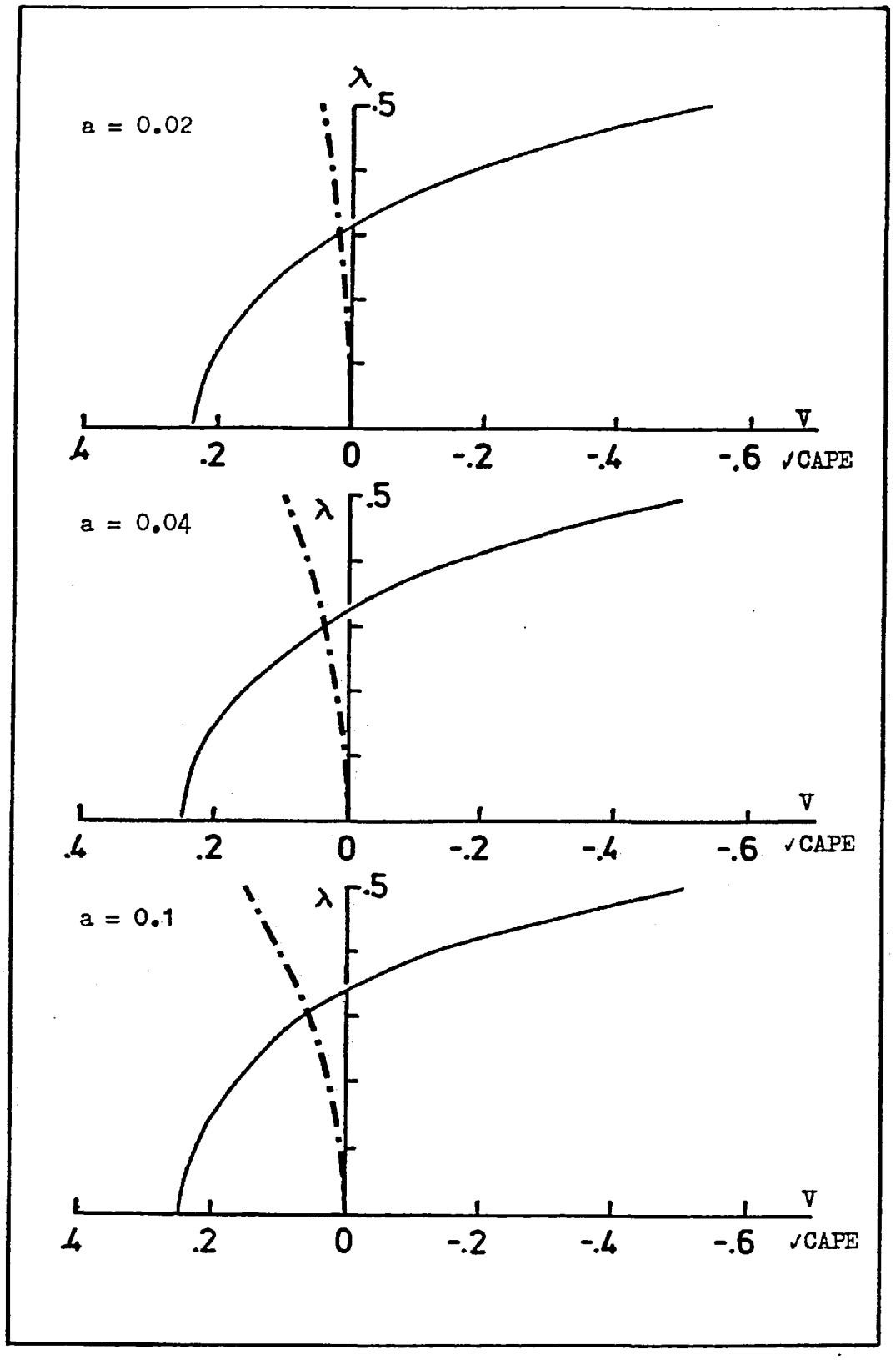

Figure 2.4.5 Velocity profiles of outflow (continuous lines) for parabolic inflow profiles (dashed lines), at α = 0.5.

between C and 'a'. It can be described by

$$C = .23 + .14a \qquad (2.43)$$

the value of $\frac{dC}{da}$ increases as α decreases. This variation, too, is approximately linear and can be described by equation (2.44) to an error of less than one percent within the range $0.3 < \alpha < 0.7$. Thus

$$C = (.55 - .8\alpha)\, a + f(\alpha) \qquad (2.44)$$

where $f(\alpha)$ is a function as described in figure (2.4.2)

2.4.5 Low Level Jet Profile

On occasions when a severe storm occurs, a low level velocity maximum is sometimes observed. Such a velocity profile in the lower half of the troposphere emcompassing the low level jet is a complicated function of height, such as the profile in figure (2.4.6) (taken from the wind sounding of Wokingham storm). A simpler profile resembling that of a low level jet is the cosine profile

$$V_1(\lambda_1) = a\left[\cos\left(\frac{2\pi}{(1-\alpha)}\lambda_1\right) - 1\right] \qquad (2.45)$$

It gives a velocity maximum at $\lambda_1 = -0.5(1-\alpha)$. The problem defined by substituting (2.45) into (2.41) was solved by the same numerical technique as before.

A jet is described as positive if it points towards the direction of propagation. It is negative if it points to the opposite direction. The size of the jet is given by the magnitude of a.

2.4.5.1 Negative Low Level Jet (a Is Negative)

The existence of a low level jet at the inflow alters the outflow

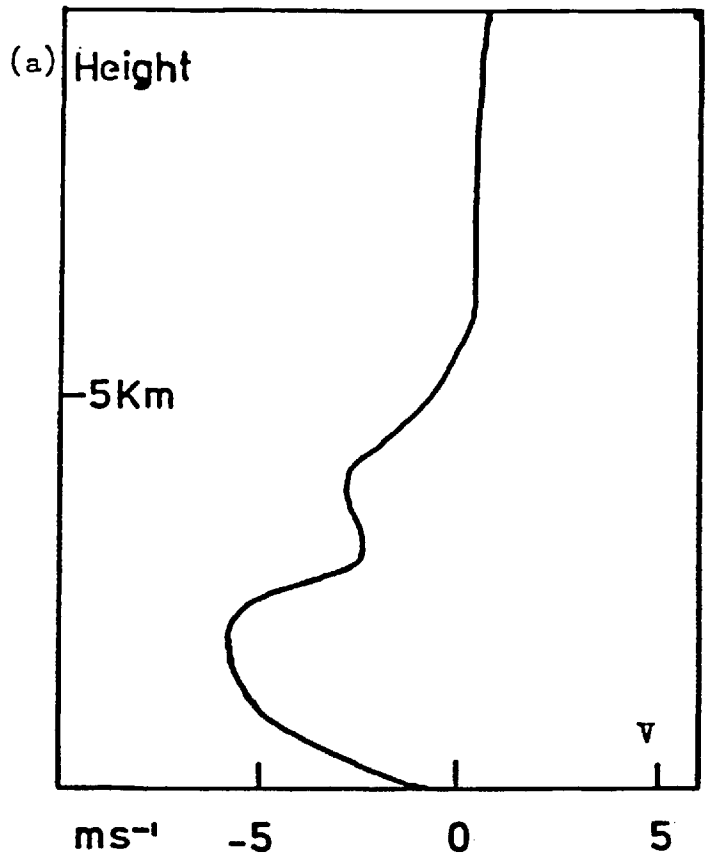

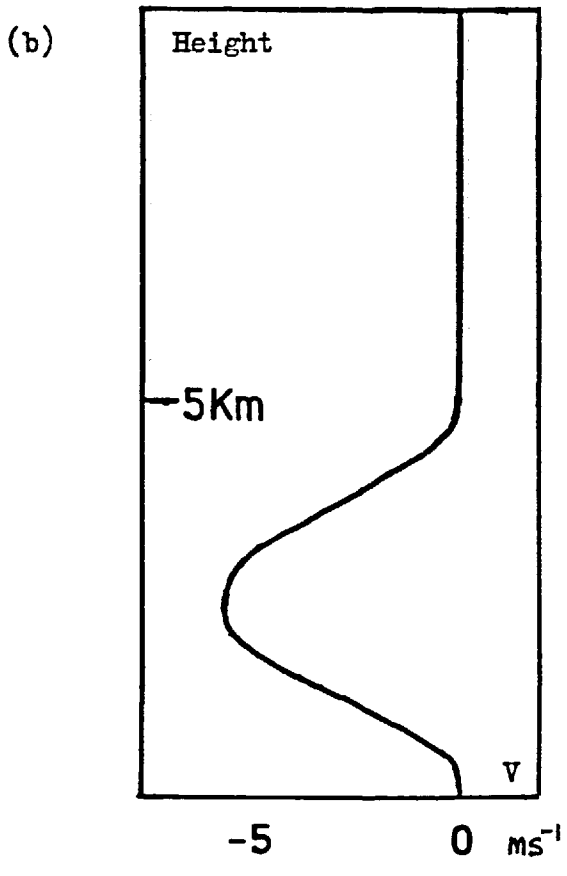

Figure 2.4.6 (a) Velocity profile showing a low level jet (taken from the sounding of the Wokingham Storm).
(b) A low level jet profile approximated to a cosine profile.

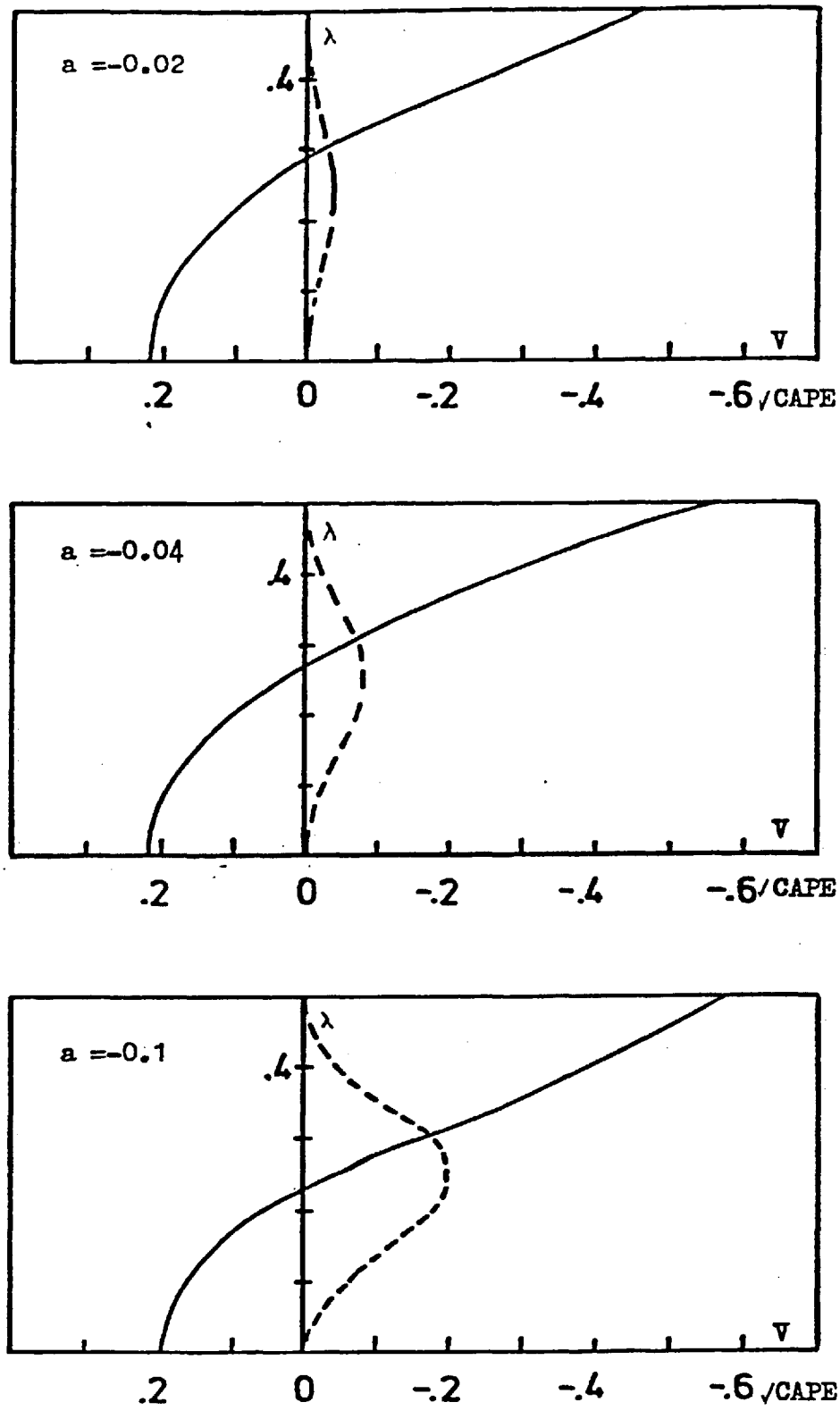

Figure 2.4.7 Velocity profiles of outflow (continuous lines) in the presence of a negative low level jet at the inflow (dashed lines), $\alpha = 0.5$.

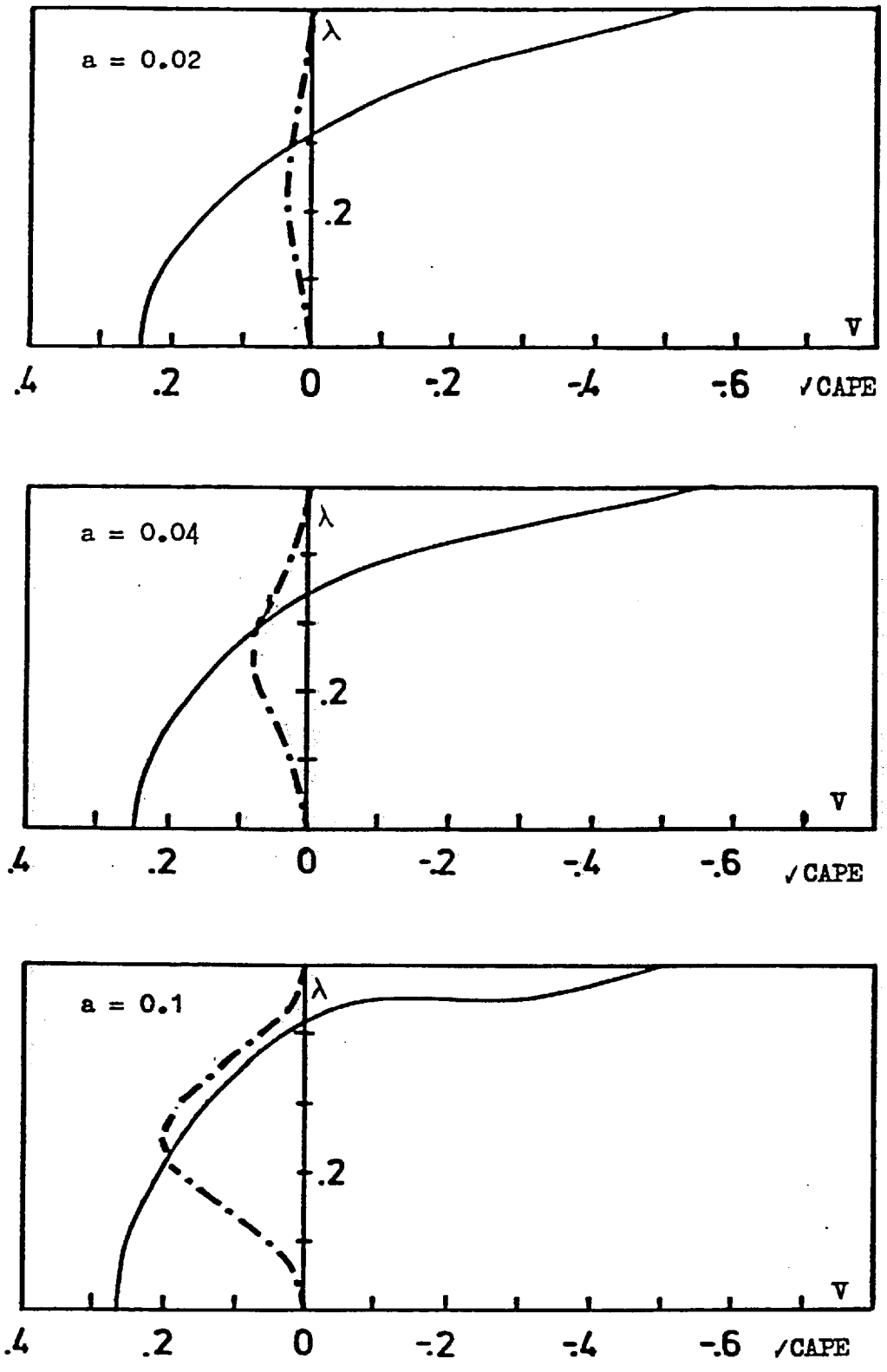

Figure 2.4.8 Velocity profiles of outflow (continuous lines) in the presence of a positive low level jet at the inflow (dahsed lines), α = 0.5.

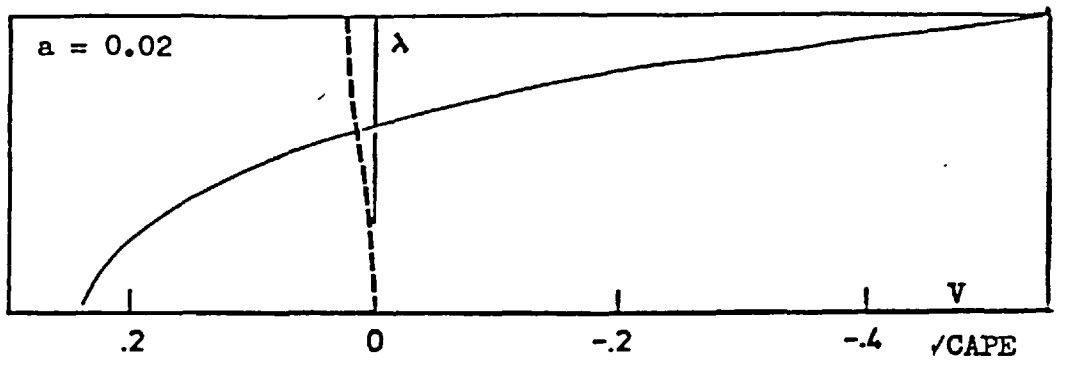

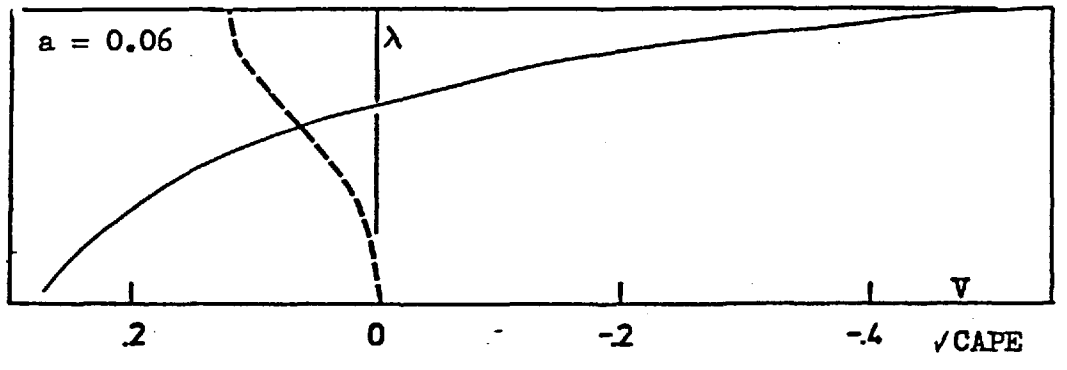

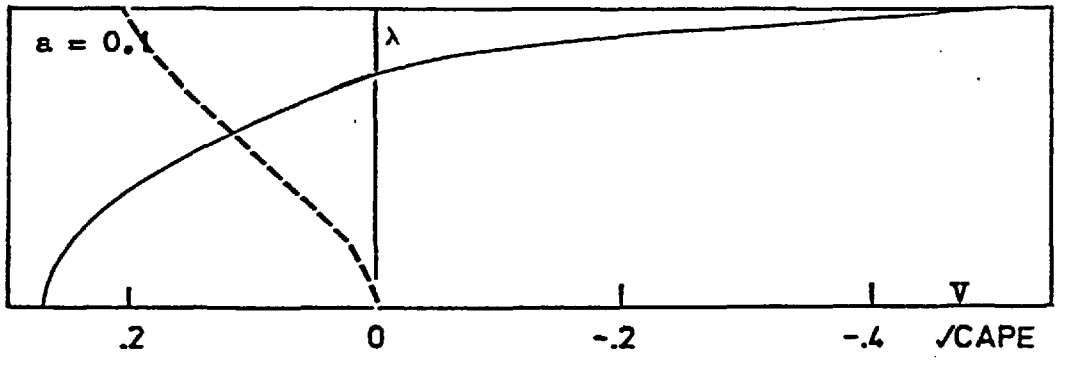

Figure 2.4.9 Velocity profiles of outflow (continuous lines) in the presence of a positive low level jet situated at ground level (dashed lined), $\alpha = 0.5$.

profile. It is illustrated in figure (2.4.7). In the case when a = 0, there is a negative jet with a maximum outflow velocity at the top boundary. The magnitude of this jet increases with |a|, while the depth occupied by this jet also increases.

The size of the positive outflow jet below the negative outflow jet reduces as |a| increases, and it occupies a smaller depth, at a = 0.02, the depth occupied by the positive jet is .29H, and it is reduced to .23H at a = 0.1.

2.4.5.2 Positive Low Level Jet (a Is Positive)

The circulation reacts differently to a positive low level jet. The negative jet at the top boundary becomes stronger and shallower as a increases. At a = 0.02, it occupies a depth of about 0.2H. At a = 0.1, its depth is reduced to 0.08H.

The propagation velocity of the tropical circulation can be expressed in terms of a linear relationship with a.

For $\alpha = 0.5$

$$C = 0.4a + f(\alpha) \qquad (2.46)$$

2.4.5.3 Low Level Jet At Ground Level

When $$V_1(\lambda_1) = \alpha\left[\cos\left(\frac{\pi}{(1-\alpha)}\lambda_1\right) - 1\right]$$

there is a maximum deviation at $\lambda_1 = -(1-\alpha)$. This is the case of a jet situated at ground level. It can be seen from figure (2.4.9) that the outflow profiles resemble those in figure (2.4.5) where parabolic inflow profiles were considered. It was found that the value of $\frac{d\lambda_1}{d\lambda_3}$ varies with 'a' in such a way that a similar outflow profile was obtained for various value of 'a'.

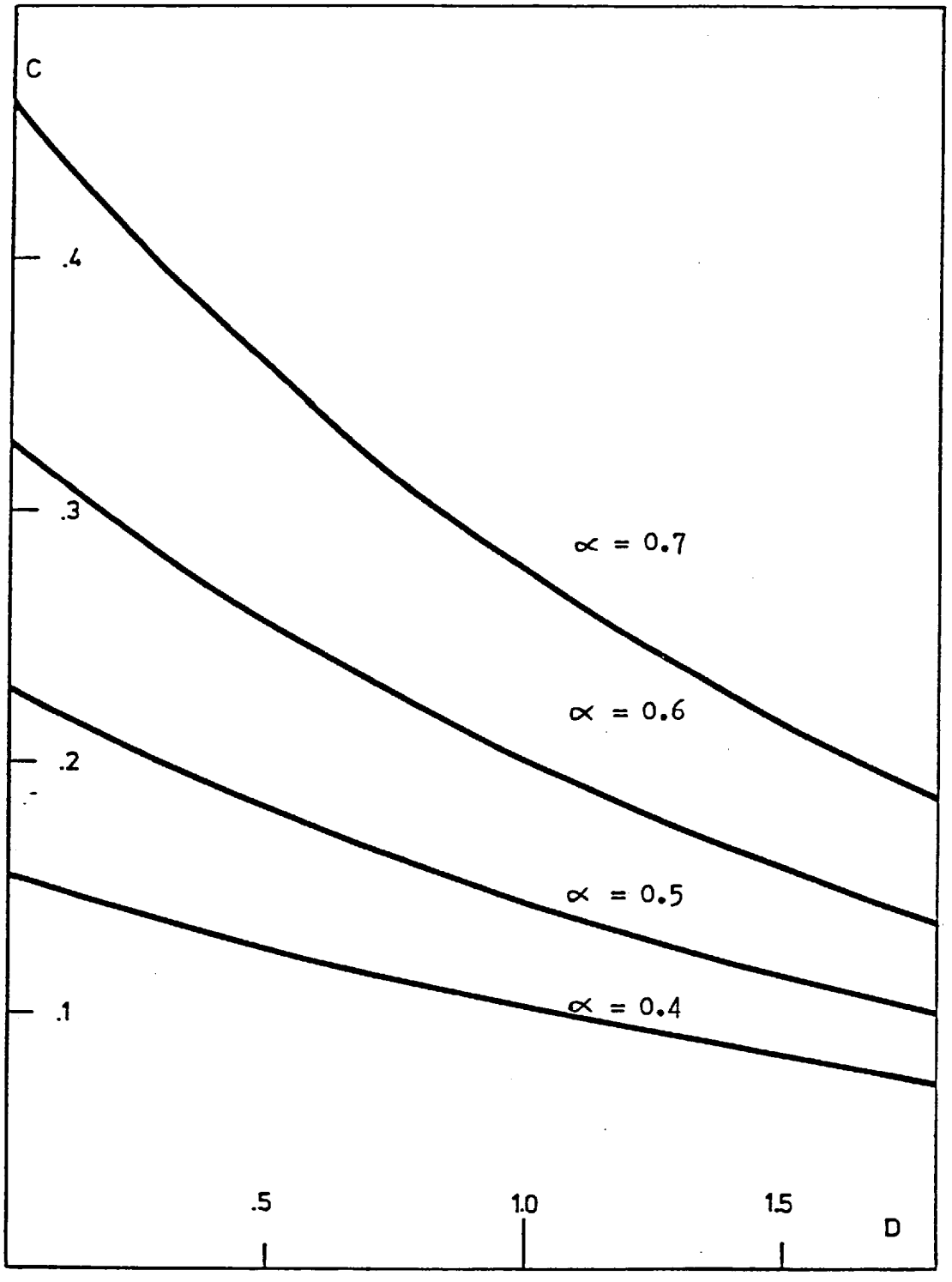

Figure 2.4.10 Propagation speed C as a function of density stratification D at discrete values of $\propto$.

The propagation velocity C can be expressed as:

$$C = .38a + f(\alpha) \qquad (2.47)$$

It is worth noting that the actual size of the inflow jet is 2a. Thus, when a = 0.1, the magnitude of the jet is $0.2\sqrt{CAPE}$. Take a typical value of CAPE of 1000 JKg^{-1}, when a = 0.1, the amplitude of the jet is 6.4 ms^{-1}. The likely range of 'a' is of order or below 0.1. Equations (2.47) and (2.46) show that the position of the low level jet plays a minor role in determining the propagation speed. Bolton (1979) using a linearized model, found that the propagatin speed of a squall line was almost independent of the position of the low level jet.

2.5.6 Compressible Solution

Since the variation in density within the depth of the storm is fairly large, solutions will not be complete without compressibility. Putting V = 1 in equation (2.33) after some manipulations

$$\frac{d^2\lambda_1}{d\lambda_3^2} = \left(\frac{d\lambda_1}{d\lambda_3} - 1\right)\frac{d\lambda_1}{d\lambda_3} D - \frac{R_t}{2}(\lambda_3 - \lambda_1)\, e^{-2(\lambda_3-\lambda_1)D} \qquad (2.48)$$

The eigenvalue R_t is found to increase with D in a non-linear manner. This implies a decrease of C with D, as in figure (2.4.10) . The relationship can be summarized to a very good accuracy as:

$$C = f(\alpha)\ (30\alpha)^{-.17D} \qquad (2.49)$$

The outflow profiles show an increase in outflow speed is enhanced as D increases, the specific momentum involved, however, is reduced.

2.5 Summary

The mid-latitude circulation is possible for an environment with

non-constant shear. If the constant shear inflow profile and the outflow profile resulted from this inflow profile are regarded as the zero reference. A positive deviation at the inflow produces a negative deviation at the outflow. The deviation at the outflow is smaller than that at the inflow and visa versa. The steering level of the system is found to be raised for a finite deviation from the constant shear profile. If a realistic magnitude of deviation is considered, the effect on the steering level is small. Thus in calculating the steering level of the mid-latitude circulation, this effect can be safely ignored.

The tropical circulation requires inflow at all level. The circulation adjusts its dynamics to accomodate changes from the constant velocity profile. The propagation speed is not sensitive to the position of the low level jet, however, it increases if the jet is pointing forward, and decreases when the jet is pointing the opposite direction. The variation is linear with the magnitude of the jet which is typically less than $0.1\sqrt{CAPE}$. Since the most likely value of α is between 0.5 and 0.6, the relationship can be approximately represented by

$$C = f(\alpha) + 0.4a \qquad (2.50)$$

At the outflow, a positive jet is produce at the top part of the outflow, and a deeper and less intense positive jet is situated below it.

CHAPTER THREE : A SIMPLE THREE DIMENSIONAL MODEL.

3.1 INTRODUCTION

An air parcel is constrained by dynamical considerations, hence in order to describe its movement and behaviour fully, a full set of three-dimensional equations should ideally be used. However, under certain conditions, to understand dynamical principles, its motion can be approximated as two-dimensional; (for example, in the analysis of barotropic instabilities (Rossby waves), and the cloud street problem). In large scale dynamics, this approximation is valid because the vertical extent of the phenomenon is much smaller than its horizontal scale.

The horizontal and vertical length scales of a cumulonimbus are, however, of the same order. Thus strictly it should be treated as a three-dimensional problem. There are several approaches: the linearized theory of Raymond (1976) treated the storm as a collection of plumes organised by small amplitude gravity waves, and found the direction in which the most unstable mode should grow. The two-dimensional approximation of MG modelled storms occured predominantly in mid-latitudes; and MM presented a pseudo-three-dimensional model of a tropical squall-line, the latter two models are non-linear.

These approaches have certain details in common; to include essential details and physics , and to avoid the use of direct numerical simulation in order to extract as much information on the effects due to few physical processes included.

This chapter is devoted to the representation of a three dimensional problem in terms of two two-dimensional systems. Like all

attempts before it, it tries to explain a complicated system through a much simplified mathematically tractable model.

A 3-dimensional circulation is too complicated to be tackled through analytical methods. However, if it can be thought of as being made up of two 2-dimensional circulations, the problem is considerably simplified. Here, it is shown the conditions under which this representation is a good approximation, and later in the chapter, observed evidence is presented.

3.2 Relevance of Two-dimensional Circulations in Three Dimensional Flow-- A Mathematical Approach.

Consider the horizontal scalar product Boussinesq equation in steady state with $\underset{\sim}{V}_h = U\underset{\sim}{i} + V\underset{\sim}{j}$

$$\frac{D}{Dt}\frac{1}{2}u^2 + u\frac{\partial}{\partial x}\frac{\delta p}{\rho} = 0 \qquad (3.1)$$

$$\frac{D}{Dt}\frac{1}{2}v^2 + v\frac{\partial}{\partial y}\frac{\delta p}{\rho} = 0 \qquad (3.2)$$

where the fluid is assumed inviscid, and in a steady state.

$$\frac{D}{Dt} = u\frac{\partial}{\partial x} + v\frac{\partial}{\partial y} + w\frac{\partial}{\partial z} \qquad (3.3)$$

subtracting (3.1) from (3.2)

$$\left[\frac{D}{Dt_{xz}}\frac{1}{2}u^2 + u\frac{\partial}{\partial x}\frac{\delta p}{\rho}\right] - \left[\frac{D}{Dt_{yz}}\frac{1}{2}v^2 + v\frac{\partial}{\partial y}\frac{\delta p}{\rho}\right] = uv\zeta \qquad (3.4)$$

where $u\frac{\partial}{\partial x}\frac{1}{2}v^2 - v\frac{\partial}{\partial y}\frac{1}{2}u^2 = uv\zeta$

and

$$\frac{D}{Dt_{xz}} = u\frac{\partial}{\partial x} + w\frac{\partial}{\partial z}$$

$$\frac{D}{Dt_{yz}} = v\frac{\partial}{\partial y} + w\frac{\partial}{\partial z} \qquad (3.5)$$

and ζ is the vertical component of the vorticity.

$\frac{D}{Dt_{xz}}$ and $\frac{D}{Dt_{yz}}$ are two-dimensional operators and denote flows in the x-z and y-z plane respectively. It is worth noting that in

equation (3.4), the right hand side is in the form of two-dimensional energy equations in the x-z and y-z plane. Though energy is a scalar quantity, it is convenient in this context, to be seen as being made up of two contributions, arising from motion along the x direction and along the y direction. Thus, for example, the first term in equation (3.4) is referred to as the change of the x-component of energy in the x-z plane. The term "component" is usually associated with vector quantities, here it is used to distinguish contributions to the total energy from motions along a particular direction. Equation (3.4) shows that the x-component of energy in the x-z plane and the y component of energy in the y-z plane are coupled together by the vertical vorticity. The significance of the coupling term is discussed.

3.2.1 The Generation Of The Vertical Component Of Vorticity

In an inviscid fluid, vertical vorticity can be generated through the process of tilting and stretching. Baroclinic effects, which are important in cumulonimbus, introduce predominantly horizontal components of vorticity, which can then be twisted into the vertical by the storm circulation. The calculation of Johnson (1978) showed that the dominant terms in the generation of vertical vorticity are tilting and stretching, which agrees with the observations of Heymsfield (1978).

If there is no vertical component of vorticity in the undisturbed environment, a vortex tube approaching a cumulonimbus lies horizontally. It can be tilted upward as it enters the storm; and made to lie near horizontal again on outflow. Thus although the local component of vertical vorticity may be high in magnitude compared with the mean values, the net generation of vertical component of vorticity

is small.

The simple picture of the life history of a vortex tube through a cumulonimbus is supported by Heymsfield (1978) who analysed the kinematics and the dynamics of a storm occured on 8th June 1974, using dual doppler radar. He found that there was a positive generation of vertical vorticity in the lower half of the updraught with a maximum of $40 \times 10^{-5} s^{-1}$ at about 3 kilometres high. A negative production was observed at higher level with similar magnitude.

A more precise quantitative calculation of the generation of the vertical vorticity following a parcel through the cumulonimbus from inflow to outflow was carried out by Johnson (1978). The value of D/Dt at the three points labelled A, B and C (figure(3.2.1)) are 44,115,and -163 x $10^{-7} s^{-1}$ respectively, thus the change introduced by tilting over the entire path of the parcel trajectory is much smaller than locally high values.

3.2.2 Distribution Of The Vertical Component Of Vorticity.

The small production of vertical vorticity by the cumulonimbus is reflected in the low averaged value of ζ over the entire grid area of 400 Km in which the storm is enclosed (from the model of Johnson (1978)). The average value of ζ over the model area is of the order $10^{-6} s^{-1}$.

To access the importance of each term in (3.4), it is instructive to compare D/Dt(ζ) with $UV\zeta$, taking U of the order of V; the comparison is between the two time scales: the parcel traverse time through the convective system, and that given by the vertical component of vorticity. Let

$$R = \frac{\frac{D}{Dt}}{\zeta} \qquad (3.6)$$

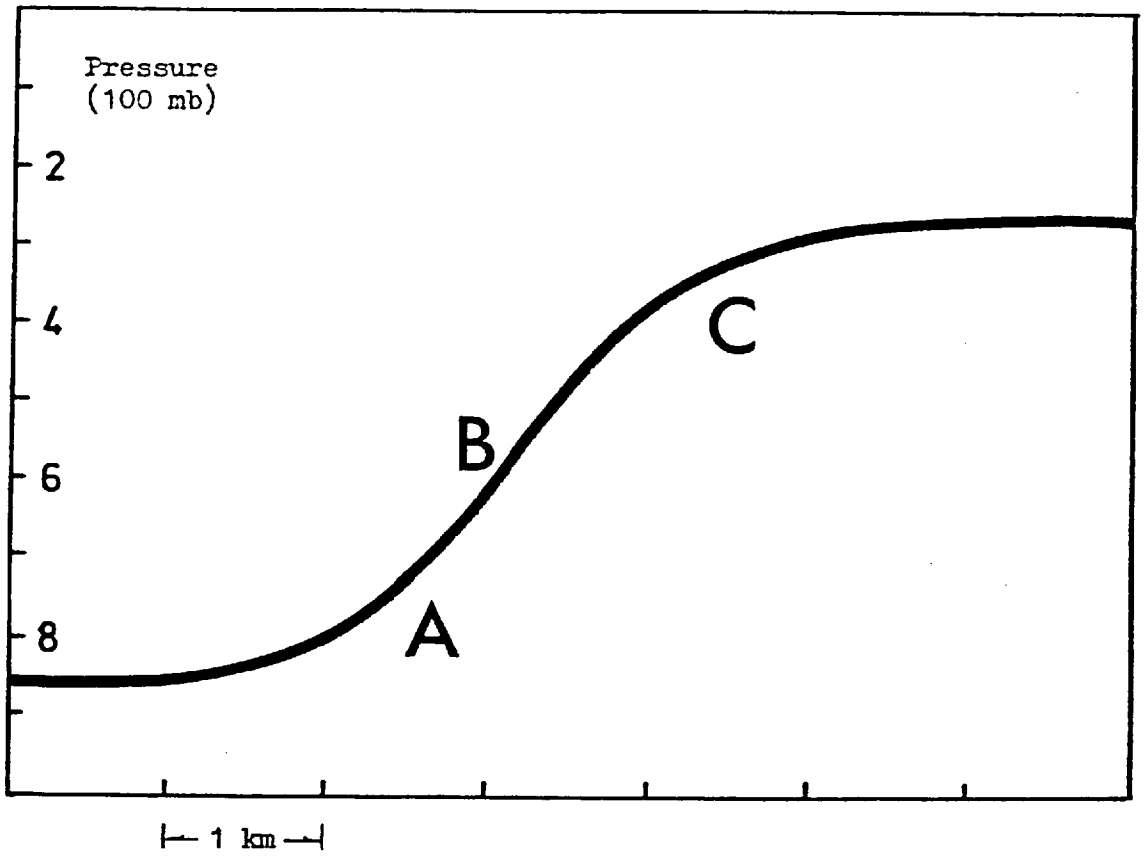

Figure 3.2.1 Schematic diagram showing the position of A, B and C along the trajectory of a parcel.

$\mathcal{R}$ is then a non dimensional number in the form of a Rossby number. If a parcel takes, say, 20 minutes to pass through the system, then using the above values of ζ gives $\mathcal{R} \sim 10^3$.

The term $\mathcal{R}$ averaged over the model area can be calculated from the model of Johnson (1978), the results for the Hampstead storm (Miller(1978)) and the Wokingham storm are given in fig(3.2.2). They show a consistently large value of $\mathcal{R}$. It is inflated owing to the constraint of the model, namely the overall balance of vertical vorticity over the entire model volume which is over twice as large as that used by Johnson (1978). However, the large value of $\mathcal{R}$ is indicative of the size of the term. Thus (3.4) can be written to a very good approximation as

$$\frac{D}{Dt_{xz}}\left(\frac{1}{2}u^2 + \frac{\delta p}{\rho}\right) = \frac{D}{Dt_{yz}}\left(\frac{1}{2}v^2 + \frac{\delta p}{\rho}\right) \qquad (3.7)$$

In regions where the magnitude of the vertical component of vorticity is high, there is a large value of vertical velocity. Ray (1978) found that a strong positive vorticity is located just inside the updraught, where the vertical velocity is large. The results of Heymsfield (1978) and Johnson (1978) are similar.

In region of small vertical motion, it is expected that the horizontal advection term in equation (3.6) becomes important. In regions of high vertical vorticity, where W is also large, and U is small, the vertical advection term is likely to be important.

The value of $\mathcal{R}$ was calculated following a parcel of air along a trajectory from the numerical simulation of the Wokingham and the Hampstead storms. In the inflow, its value is typically of order 100, in region of strong vertical movement, the value of ζ is as high as $10^{-3}s^{-1}$, where the value of the numerator in (3.6) is of the

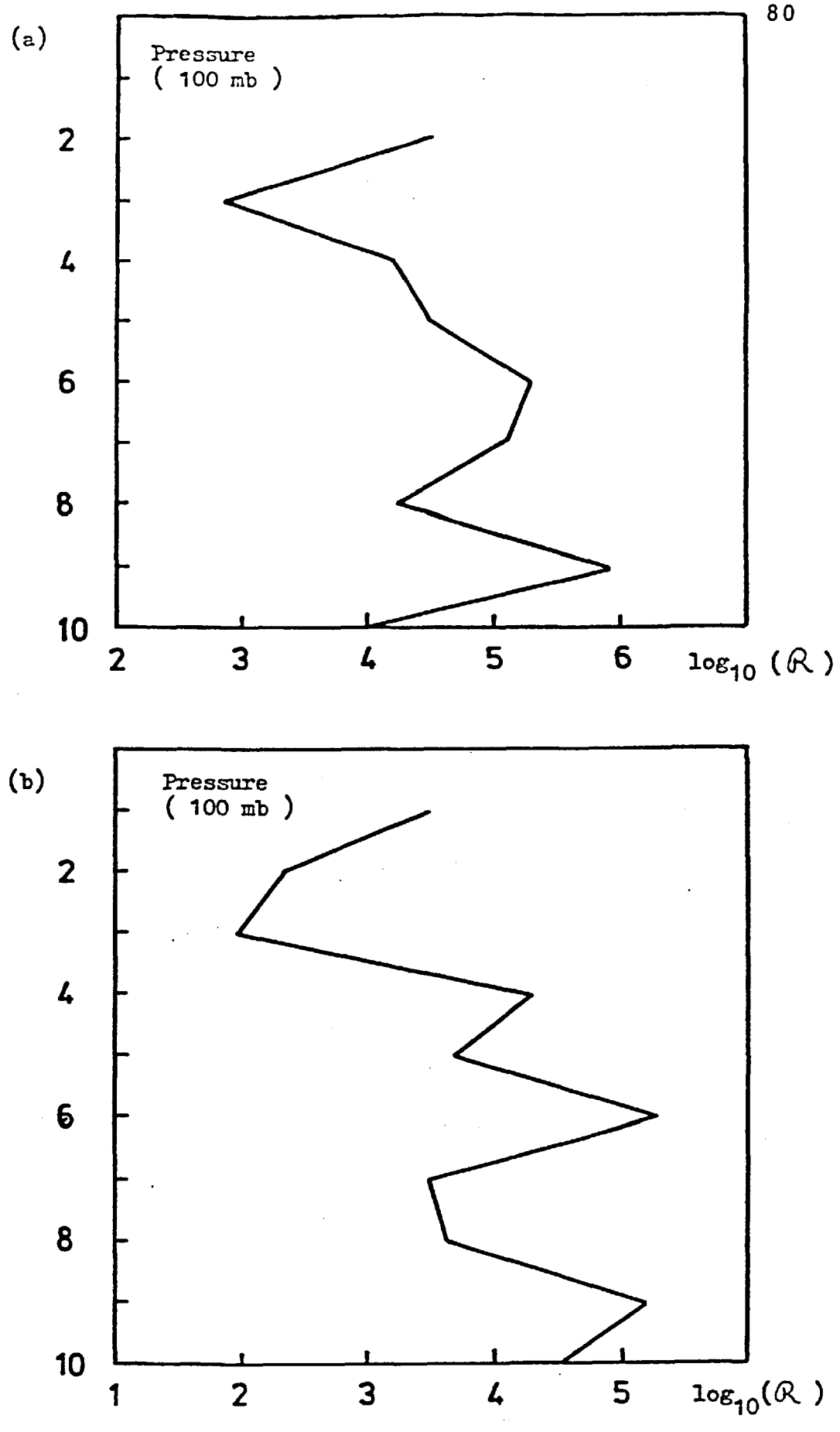

Figure 3.2.2 The computed values of $\mathcal{R}$ in the numerical simulation of (a) the Hampstead storm and (b) the Wokingham storm.

order 10^{-2} to $10^{-1}s^{-1}$. Overall, $\mathcal{R}$ is of order 10 and sometimes much bigger over the entire period the parcel spent inside the cumulonimbus. Thus equation (3.7) without the average is therefore true to better than 10 percent. The values of $\mathcal{R}$ along a trajectory is shown in figure (3.2.3).

At all stages throughout the life history of a parcel travelling through a three-dimensional cumulonimbus, the change in the total energy in the x direction is approximately equal to that in the y direction. It is convenient to separate the path of the parcel into 3 sections as given in figure (2.1).

Region 1 : the parcel of air is approaching the convective cell from infinity. From a large distance away, it is assumed that flow is hydrostatic, and vertical motion is zero. The flow is also irrotational, thus:

$$\frac{D}{Dt_{xz}}\left(\frac{1}{2}u^2 + \frac{\delta p}{\rho}\right) = \frac{D}{Dt_{yz}}\left(\frac{1}{2}v^2 + \frac{\delta p}{\rho}\right) = 0 \qquad (3.8)$$

Region 2 : this is the region where all the convective activity takes place, there is a strong vertical velocity, and a strong pressure gradient. Equation (3.8) can no longer be equated to zero, since flow is rotational. It is a result of generation of buoyancy energy, vertical kinetic energy, and pressure fields. It necessitates a three dimensional treatment.

$$\frac{D}{Dt_{xz}}\left(\frac{1}{2}u^2 + \frac{\delta p}{\rho}\right) = \frac{D}{Dt_{yz}}\left(\frac{1}{2}v^2 + \frac{\delta p}{\rho}\right) \neq 0 \qquad (3.9)$$

At any one point on the trajectory of the air parcel, the change in the x-component of energy approximately equals the change in the y-component of energy.

If X is the total change in the two-dimensional energy along integrated along the path of the parcel, then

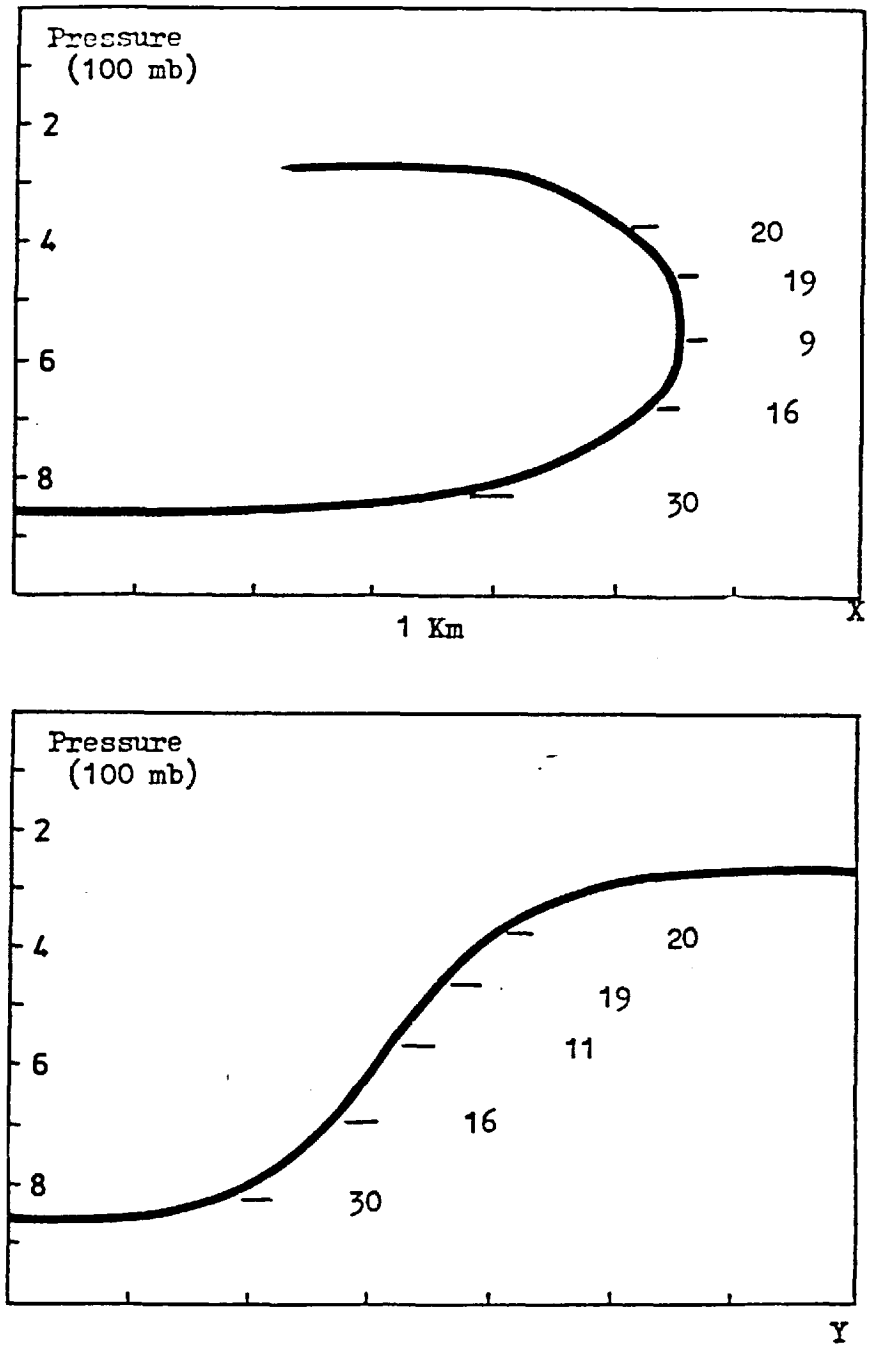

Figure 3.2.3 The computed values of $\mathcal{R}$ along the trajectory of an air parcel.

$$\left[\frac{1}{2}u^2 + \frac{\delta p}{\rho}\right]_{1\,xz}^{3} = \left[\frac{1}{2}v^2 + \frac{\delta p}{\rho}\right]_{1\,yz}^{3} = X \qquad (3.10)$$

for $[X]_1^3$ defined as X, the above equation can be written as

$$\left[\frac{1}{2}u^2 + \frac{\delta p}{\rho} - X\right]_{1\,xz}^{3} = 0 \qquad (3.11)$$

Thus the equation is similar to a two-dimensional Bernoulli energy integral. If G is a function describing the integrated value of terms in equation (3.10) and can be taken inside the D/Dt term, then a conservative quantity in the x-z plane and in the y-z plane can be defined.

$$\frac{D}{Dt_{xz}}\left[\frac{1}{2}u^2 + \frac{\delta p}{\rho} + G\right] = 0 \qquad (3.12)$$

however, the model to be described only considers the remote flow, so only the integrated value of G is the determining factor, which can be deduced from the consideration of the energetics in region 1 and 3.

3.2.3 Equipartition of Convective Available Potential Energy.

From the Bernoulli's energy equation, which is applicable in all three regions. In region 1 and 3

$$\left[\frac{1}{2}u^2 + \frac{1}{2}v^2 + \frac{\delta p}{\rho} - g\int \delta\phi\, dz\right]_1^3 = 0 \qquad (3.13)$$

The change in the horizontal energy is primarily due to the latent energy contained in the parcel which is fixed by its initial property, it is modified by the work done by the pressure field.

Between region 1 and 3, the total horizontal energy equals to the sum total of energy in the two orthogonal component of energy. Thus:

the change of		the change of		total net
energy in x-z plane	+	energy in y-z plane	=	change across
across (1) and (3)		across (1) and (3)		region (1) to (3)

$$\left[\frac{1}{2}u^2+\frac{\delta p}{\rho}-X\right]_{1xz}^{3}+\left[\frac{1}{2}v^2+\frac{\delta p}{\rho}-X\right]_{1yz}^{3}=\left[\frac{1}{2}u^2+\frac{1}{2}v^2+\frac{\delta p}{\rho}-g\int\delta\phi\,dz\right]_{1}^{3} \quad (3.14)$$

thus:

$$X=\left[\frac{1}{2}\frac{\delta p}{\rho}\right]_{1}^{3}-\frac{1}{2}g\int_{1}^{3}\delta\phi\,dz \quad (3.15)$$

The equation can be written in the form of the Bernoulli's energy form :

$$\left[\frac{1}{2}u^2+\frac{1}{2}\left(\frac{\delta p}{\rho}-g\int_{1}^{3}\delta\phi\,dz\right)\right]_{1xz}^{3}=0 \quad (3.16)$$

The calculation above are now shown to be consistent with case studies. The main constraint is on the value of R. Thus a three-dimensional flow through a severe steady convective system can be treated as a composite of two two-dimensional orthogonal flows, with the total convective available potential energy shared equally between them.

There are many instances in nature where partitioning of energy occurs between available degrees of freedom. In many cases, there is no preference between these modes; the total energy is partitioned equally between them: an example is a helium molecule which possesses three degrees of translational freedom. There is no preference as to which direction a helium molecule should move; the internal energy is shared equally between them. This is known as the law of equipartition of energy.

The lack of a particular preference towards a particular mode of freedom implies a lack of constraint, in the case of molecules, the main constraint on a particular mode of freedom is on the size of the gap between successive quantum energy levels, as compared to the magnitude of the internal energy. If the internal energy (given by KT, where K is the Boltzman's constant, and T is the absolute

temperature) is bigger than the energy required in the successive quantum jump in energy levels, there is no constraint on the molecule to choose that particular mode of freedom, which is then allocated with the same amount of energy as the rest.

In the simple cloud model, there is no thermodynamic constraint on the motion along a particular horizontal axis, the two modes of circulation along x and y are equally preferable. If natural laws are universally applicable independent of the scale of motion; it is reasonable that the convective available potential energy available for the two orthogonal circulations should be equally partitioned.

It is shown later that the application of the equipartition of convective available potential energy is valid. The model is able to produce results which agree with observations.

3.3 Observation Modelling

The two-dimensional mid-latitude model of Browning and Ludlam (1962) is capable of explaining many of the observed features in a mid-latitude storm, including a gust front. Subsequent to their suggestion, much work was done on the two-dimensional storm in region of shear. In particular, the analytic work of MG showed that a two-dimensional mid-latitude model defines a realistic steering level, in cases where the ambient flow was near two-dimensional. One of the storms studied by Chisholm (1973) had a near two-dimensional circulation for the updraught. These further reinforce the notion that a two-dimensional structure is adequate in explaining the mid-latitude type storm.

However, Moncrieff (1978) showed that the internal structure of a two-dimensional steering level model had a fundamental problem: the

updraught slope is downshear, and the steady two-dimensional flow field in Browning and Ludlam (1962) model cannot be maintained. It is, however, generally realised that severe storms are three-dimensional structure.

A generalised severe right moving storm was proposed by Browning (1964). It must be stressed here that left-moving storms are just as severe as the right-moving varieties. The airflow model, in this case, is a mirror image of the right moving storm. The new model overcomes the problem of having a near zero inflow velocity for the downdraught which originates near the steering level of the two-dimensional model; and to take into account, for a severe right moving storm, inflows at low and mid level approach the storm from the right. The model is represented in figure (3.3.1), which shows an interlocking structure of updraught and downdraught. One of the features worth noting is that all inflows originate from one side, and outflows on the other. This is, therefore, similar to the tropical circulation. The model also retains the dominant mid-latitude circulation. The same flow structure can be obtained by introducing a sideway propagation speed to the mid-latitude circulation. Similar models were presented in Hammond (1967).

The model made for the Centenial storm (Chisholm (1973)) is shown in figure (3.3.2). The model is similar that of Browning(1964). This is chosen because the Centenial storm is a supercell storm, thus avoiding the ambiguity of some models which are based on a multicell system. The two dominant circulations which were classified as the mid-latitude and the tropical circulations are evident. For ease of illustration, projections of the air flow were made on two orthogonal planes. The mid-latitude circulation lies in the plane where the

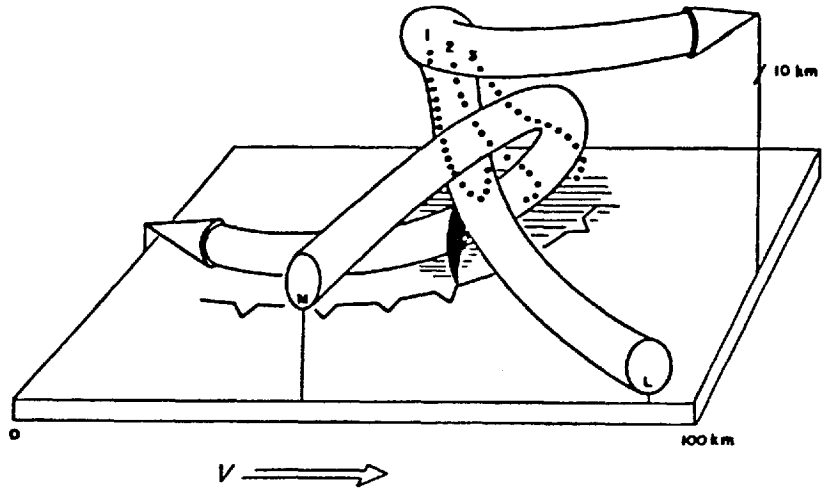

Figure 3.3.1 Schematic diagram showing a 3-dimensional model of the airflow within a severe right moving storm. The L and M refer to low and middle level. (from Browning (1964)).

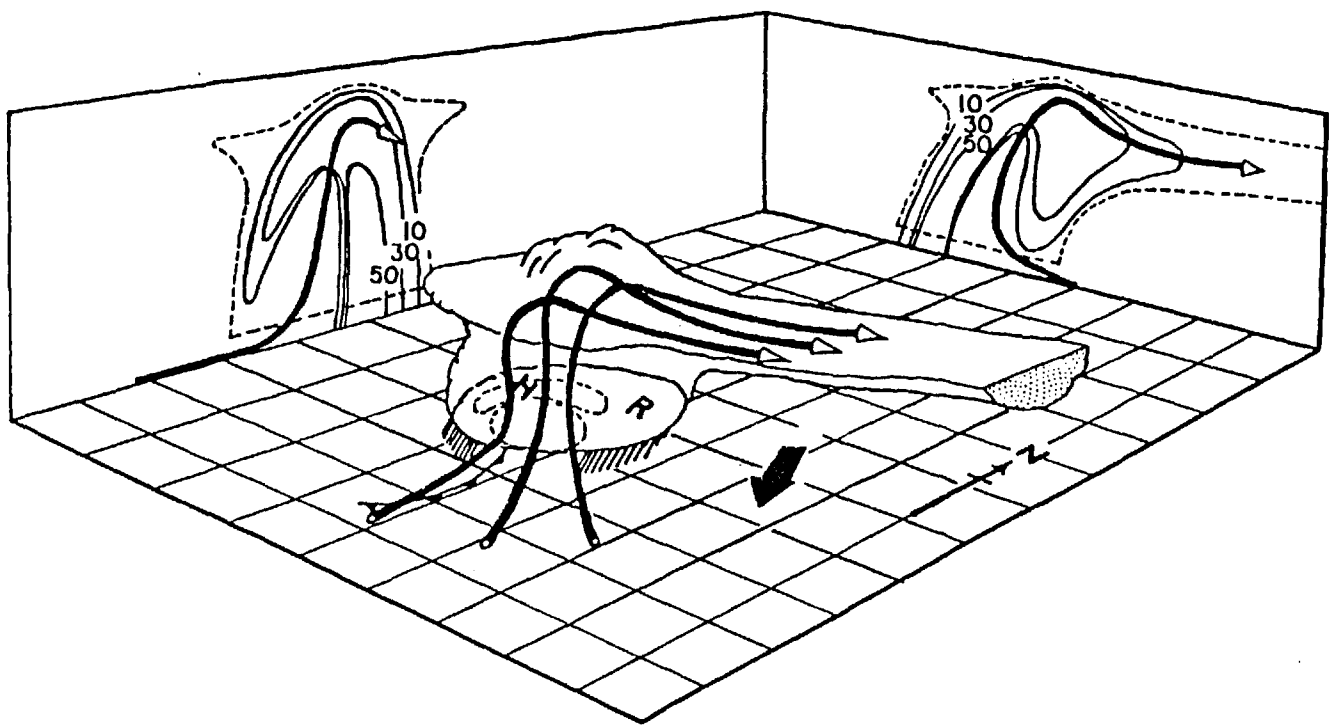

Figure 3.3.2 Perspective view of a supercell (after Chisholm and Renick (1972)).

shear is large, and the tropical circulatin lies in the plane where the shear is small.

The orientation of the updraught in a three-dimensional interlocking system is an important consideration in the maintainance of a steady flow. The downdraught is lying in the downshear side of the updraught, thus, contrary to the two-dimensional circulation which requires an upshear orientation of updraught, the updraught should lie downshear. This is to allow for rain to fall into the downdraught. The two-dimensional mid-latitude circulation study of Moncrieff (1978) can be interpreted as predicting the correct orientation of updraught in such an interlocking structure. It shows a profound connection between two-dimensional and three-dimensional flow representations.

3.4 Numerical Modelling

An alternative to checking observational models is to compare the result with storms produced by numerical simulations; a number of them are available in different degree of sophistication. Among them, Miller (1978) successfully simulated the many features observed in the Hampstead storm notably the model's correct prediction of the location where most rain fell.

The advantage of a numerically simulated storm, for the purpose of determining air flow structure, is that each individual parcel of air can, in principle, be traced throughout the period of simulation. It was found that in Hampstead storm, the downdraught originated from around 600mb, occupied a region between 800 to 600mb and it flowed out below 900mb. The updraught entered the system mostly from the bottom 100mb, though the inflow did extend to 800mb level; the updraught outflow was confined to below 200mb. This is important in the three-layer parameterization model described later.

At 24 minutes of simulation time, the storm was fully developed. The positions of individual air parcel were traced. For the sake of simplifying the picture, only the trajectories of certain parcel of air were chosen. They were selected if they formed part of the inflow into the updraught or the downdraught.

Figure (3.4.1) is taken from the trajectories in the simulated Hampstead storm (Miller (1978)). An interlocking structure of updraught and downdraught similar to that proposed by Browning (1968) is evident. From the plan view of the trajectories, inflow approaches the storm from one side, and outflows leave the storm on the opposite side. The two orthogonal projections of this convective cell are shown in the lower two figures, viewing from the west and from the south with respect to the top diagram respectively. A mid-latitude circulation and a tropical circulation are evident in the two projections. The orientation of the updraught in the mid-latitude circulatin is downshear, an important factor in the maintainance of a steady interlocking structure.

The numerical studies presented a model for a quasi-steady convection which is consistent with the models derived from observations.

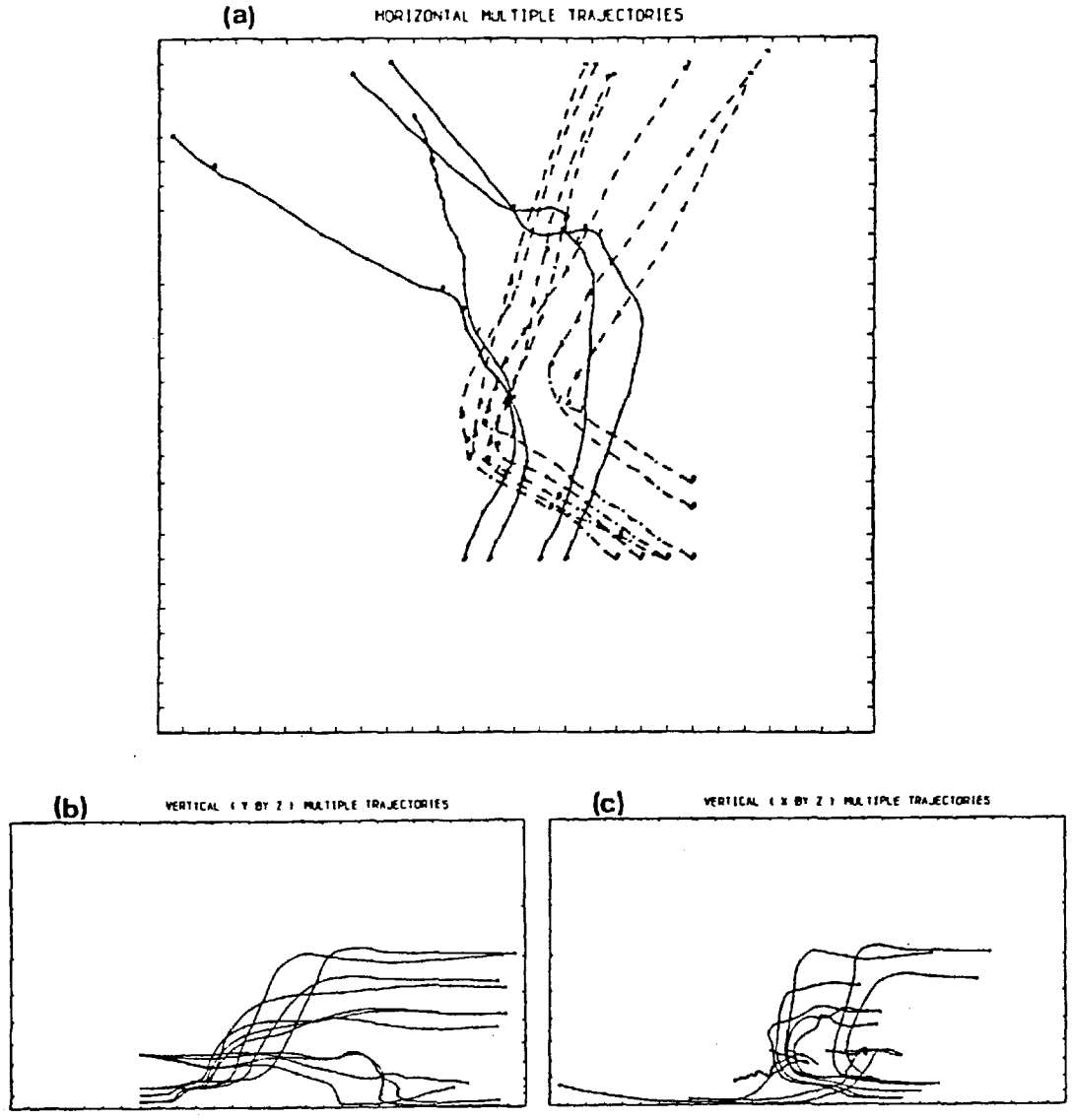

Figure 3.4.1 (a) Trajectories projected onto x-y plane. Dashed lines are updraught, continuous lines are downdraught. The distance between each graduation mark is 1 kilometre.
(b) Same trajectories projected onto the Y-Z plane. The vertical scale is in steps of 100mb starting from 1000mb at ground level.
(c) Same trajectories projected onto the X-Z plane.

3.5 A Simple Three-dimensional Model

The mid-latitude and tropical circulations have hence showed up dominantly in both observational models and in numerical simulations. In the simple three-dimensional model, it is proposed that a three-dimensional circulation can be resolved into two quasi-two-dimensional circulations : the mid-latitude and the tropical circulation.

3.5.1 Orientation of the Two Orthorgonal Components.

It is expected that the environment in which the storm is to develop would give an indication of the orientation of the two components. Consider a simple atmosphere with unidirectional uniform constant wind shear extending from the bottom to the top of the troposphere. A wind hodograph for such an environment is a straight line, figure (3.5.1). There are two distinct directions. Along A-B the wind shear is a maximum, and is zero in a direction perpendicular to it.

In MG and MM the two circulations were found to be governed by a parameter R which is similar to R_m, but different to R_t considered in chapter 2.

$$R = \frac{CAPE}{(AH)^2}$$

where CAPE = convective available potential energy.

A = shear

H = height of the convective system.

The value of R, in mid-latitude circulation, needs to be small; Moncrieff (1978) showed that $-0.25 \leq R \leq 1$ is the condition for the existence of a free boundary between the updraught and the

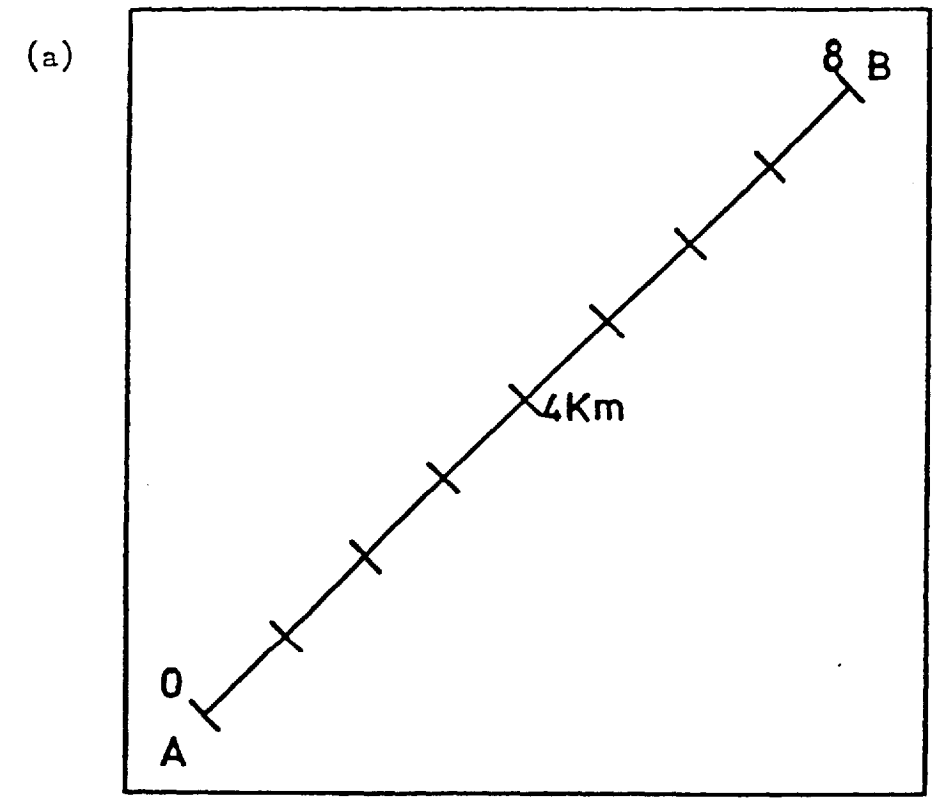

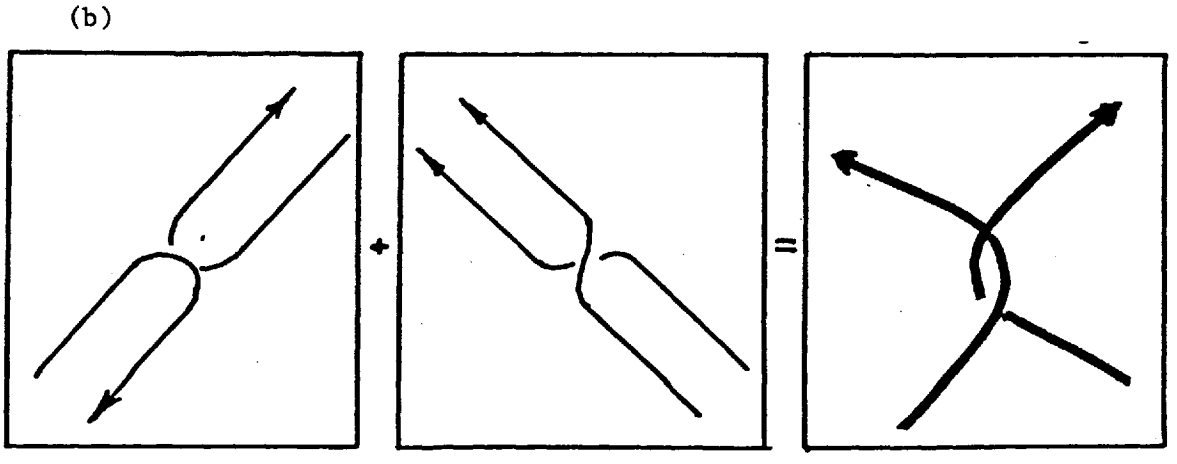

Plan view of the mid-latitude circulation. the tropical circulation. the 3-d interlocking structure.

Figure 3.5.1 (a) A linear constant shear hodograph.
(b) Schematic diagrams showing if a mid-latitude circulation and a tropical circulations were superposed, an interlocking flow is resulted.

downdraught. For the tropical circulation, however, a large value of R is preferred.

Along A-B, R is a minimum, and perpendicular to A-B, R is a maximum. If a severe storm cell is to develop in this environment, the two widely different values of R in orthorgonal directions provide the ideal conditions for the mid-latitude and the tropical circulations. Thus a convective cell can be thought of as having a component of mid-latitude circulation along A-B and a component of tropical circulation along a direction perpendicular to A-B.

Figure (3.5.1.b) shows schematically, the plan view of the two circulations. It can be visualised that they can, in principle, be superposed. The resultant flow field has a similar structure to that proposed by Browning and others; and those observed in numerical simulations.

A typical wind hodograph is, however, seldom a straight line. In general, it is observed that severe storms develop in region where the shear is large, and directions of maximum and minimum shear can be defined without difficulty. In many cases, the hodograph is almost straight except at the bottom kilometre or so, where the effect of surface drag produces the familiar Ekman spiral. In all the severe storms studied here, there is a strong directional shear present.

3.5.2 Framework Of The Model.

The proposed model is for a basic unit of dynamically dominant convective cell, which is assumed to be in a quasi-steady state. In this way, the flow within the cell can be treated practically as steady over the time interval necessary for an air parcel to travel through the cell. The effect of earth's rotation can safely be

ignored since the time involved for an air parcel to traverse through the convective system is less than that of the Coriolis force. However. The earth's rotation has a fundamental effect on a larger time scale -- establishing the boundary layer Ekman shear profile.

The dynamics of the updrauht is, for the purpose of analytic modelling, to be treated as separate orthorgonal two-dimensional flows; the directions are along and perpendicular to the direction of maximum mean wind shear. The circulation along the maximum wind shear is of a mid-latitude type; and that perpendicular to it is of a tropical type. In keeping with Ludlam's observation that shear is an important factor for organization of severe storms, boundary conditions in the tropical circulation are to match those generated in the mid-latitude circulation. Thus the steering height in the mid-latitude circulation marks the upper limit of the updraught inflow. This height is a function of shear and convective available potential energy. The extreme inflow height in the tropical circulation is to matched that of the mid-latitude circulation. (since they are part of the updraught, they are also referred to as components).

The velocity of the cell is made up of two components -- due to the mid-latitude and the tropical modes. The definition of mean wind direction is along the direction of maximum average shear in the depth of the troposhere concerned. There is a velocity component along this direction as given by the mid-latitude circulation; another velocity component is given by the tropical component which is always travelling in a direction perpendicular it. Thus the velocity of a convective cell is in general deviatory. The direction in which the cell deviates depends on the velocity profile resolved along the

direction of the tropical component. The magnitude of deviation depends on the shear, the wind speed , and the convective potential energy.

3.5.3 Preferred Direction Of Propagation.

Convective cells are often observed to move to the left or right of the mean wind, sometimes they move both to the left and to the right. The latter is a splitting storm, which does not occur frequently. There is an underlying constraint imposed by the environment, which determines the preferred leftward or rightward movement.

The propagation velocity of the mid-latitude circulation is fixed by the wind velocity at some level. The tropical circulation, however, requires inflow into the circulation at all levels. Thus it can either propagate faster or slower than the mean flow along the direction of minimum shear. The question of whether a convective cell travels to the left or the right of the mean wind depends on the direction of propagation of the tropical component.

In an environment with a constant shear straight hodograph one may postulate that both directions are equally preferable, and a splitting storm type convection would result. In a real environment, the profile of the hodograph plays a vital role in determining the preferred direction of propagation.

3.5.3.1 Linearized Theory Of Unstable Waves.

Miles and Howard (1961) shows that the speed of an unstable wave always lies between the maximum and the minimum flow speed of the propagating medium. For example, for a mean flow with a parabolic profile (figure (3.5.2)), the phase speed is more than V_o for $\frac{d^2V}{dz^2}$

positive and less than V_o for $\frac{d^2V}{dz^2}$ negative. The difference between the phase speed c and V_o, according to the Miles and Howard theorem, is less than the maximum difference ΔV.

Linearized theory is generally applied to disorganised convection. A steady, deep convection is an organised flow, and is necessarily of finite amplitude, and therefore, a non-linear phenomenon. The developing stage, however, is disorganised, the linear mode of the convection at this stage can play a major role in determining the subsequent behaviour of the organised mature stage.

3.5.3.2 Definition Of A Hodograph

A hodograph is a curve which passes through the end points of the horizontal wind vectors at all heights. Thus in referring to the clockwise turning of the hodograph, it means that when one moves along the hodograph toward the direction of increasing height, the curve turns to the right. This is not equivalent to the veering or backing of wind.

3.5.3.3. A Simple Case: A Parabolic Profile

The hodograph is usually curved. Figure (3.5.3) is a simplified hodograph. It turns clockwise with height. A-B and C-D defines the direction of maximum and minimum shear respectively. The profile is such that it gives a uniform constant shear along A-B as shown in figure (3.5.4), and a parabolic profile along C-D as in figure (3.5.5).

The tropical circulation is to take place along C-D. During the developing stage, the convection, if organised by waves, would travel slower than V_o along the direction C-D figure (3.5.5). The organised tropical circulation developed along this plane later would,

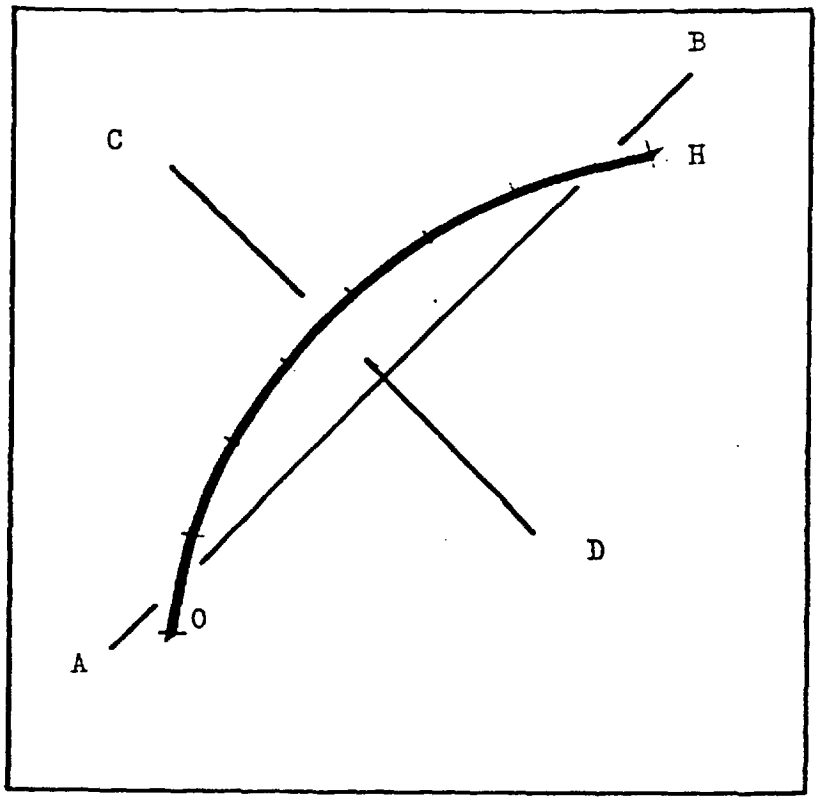

Figure 3.5.3 A clockwise turning hodograph.

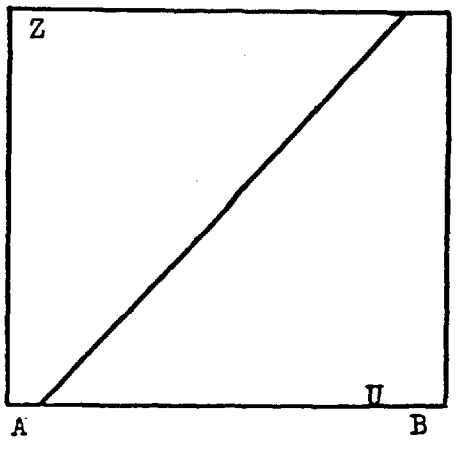

Figure 3.5.4 The constant shear velocity profile along AB.

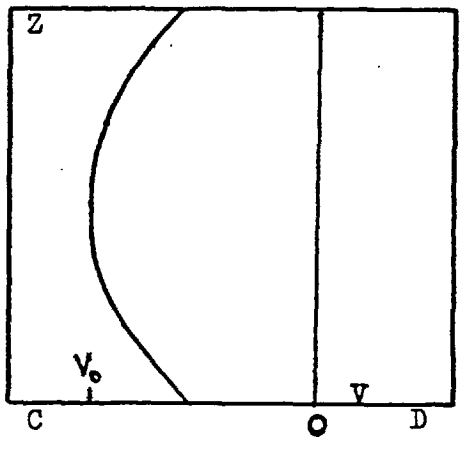

Figure 3.5.5 A parabolic velocity profile along CD.

therefore, be travelling slower than V_o. The tropical component propagates towards C-D. The resultant velocity of the convective cell, is a velocity vector pointing to the right of the mean wind vector which is directed along A-B. Similarly, a hodograph which turns in an anticlockwise direction, supports a left moving convective cell. One example is the Lawton storm (Hammond (1967)); the constituent cells moved towards the left of the wind. The hodograph, in this case, turns anticlockwise with height, see figure (3.7.5).

Klemp and Wilhelmson (1978) performed a series of experiments in a three-dimensinal numerical model. They found that if the wind hodograph turned clockwise with height, a single right moving convective cell evolved from a parent convective cell. Similarly a left moving convective cell is favoured in an environment in which the hodograph turned anticlockwise.

3.5.3.4. More Complicated Profiles.

The linearized theory argument is applicable to any profile with a well defined maximum or minimum wind speed V_o, the parabolic profile is a simple example to draw a particular conclusion on the propagation direction of the tropical circulation. Figure (3.5.6) shows some example of the likely velocity profiles that favours a tropical component which propagates slower than V_o. If these profiles are to superpose onto a constant shear profile in the perpendicular direction. The resultant hodograph is more complicated. There is not a constant turning in the hodograph. In the case of (3.5.6.a) the hodograph turns clockwise initially,then anti-clockwise, and then clockwise again. In (3.5.6.b) it turns clockwise, then anti-clockwise. They are simplified profiles of the Hampstead (Ham7) and Rimbey storms, their hodographs are shown in figure (3.7.7) and

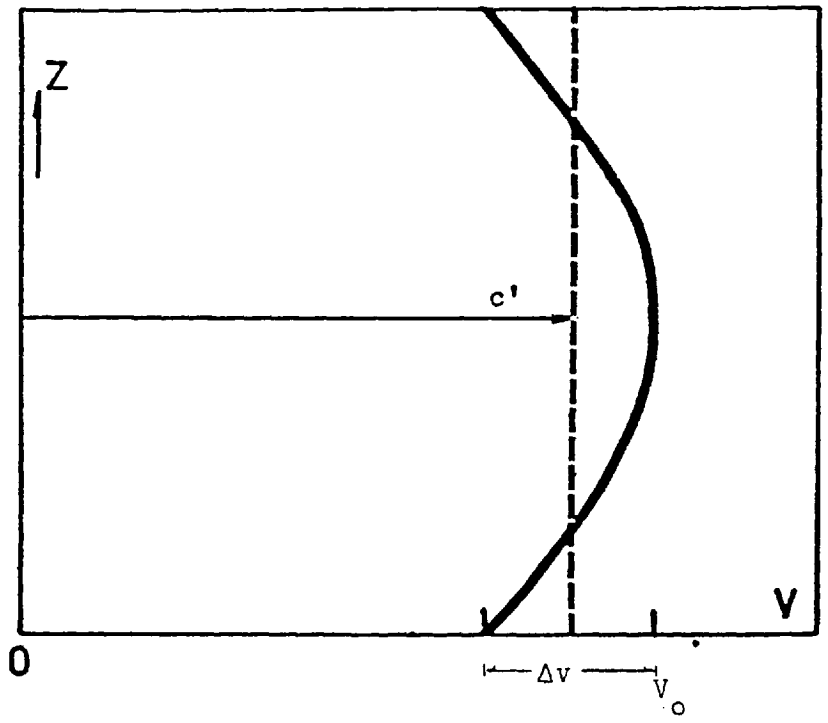

Figure 3.5.2 The phase speed c' of an unstable wave in a medium with a parabolic velocity profile.

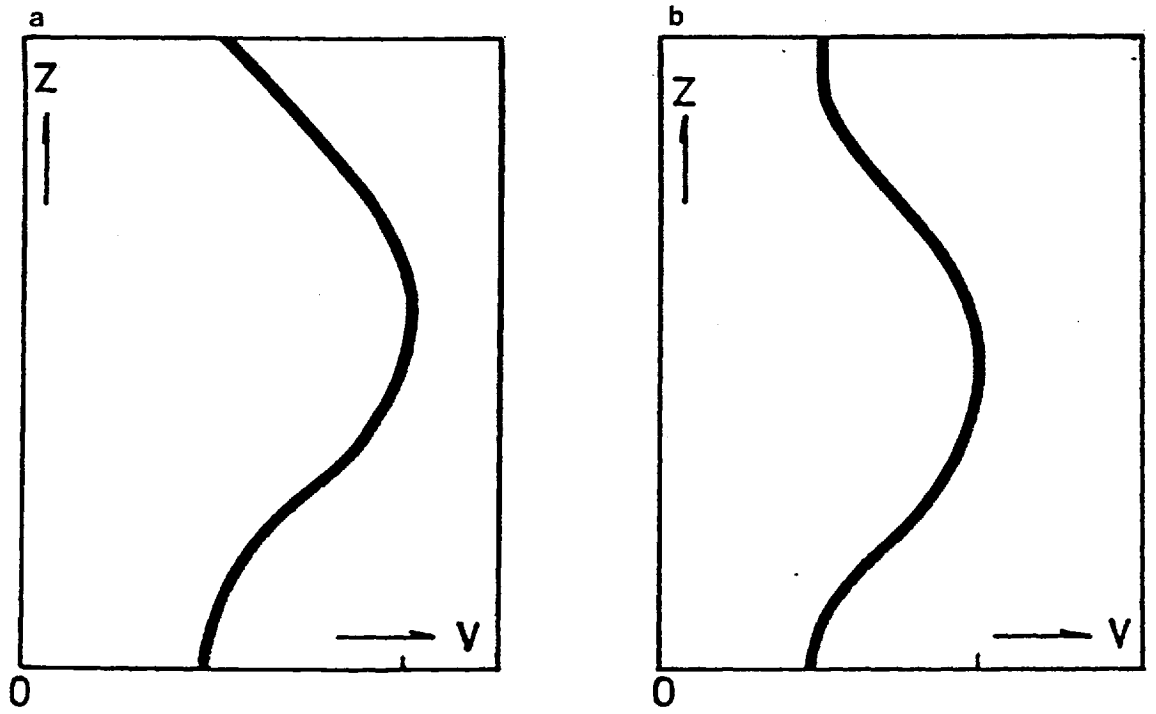

Figure 3.5.6 Examples of more complicated velocity profiles.

(3.7.2) respectively. They are consistent with the description above. In the Rimbey storm, the cells deviated towards the left as predicted.

The conclusion of Klemp and Wilhelmson (1978) is that the shape of the hodograph determines a right or left moving storm cell, and not the actual turning of wind. The analysis presented here agrees with their general conclusion: it, however, goes futher to point out that it is the velocity profile of the tropical component that is the determining factor.

Hammond (1967), likes many others, attributed the left moving characteristics of the Lawton storm to the anticlockwise turning of wind at the bottom kilometre, putting forward the theory of deviatory motion of Newton and Katz (1958). When a convective cell is in a quasi-steady state, the dynamics of the cell prevails. The vertical extent of the convective cell is from the ground level to the top of the troposphere. It is likely that the convective cell be affected by the profile of the whole depth of the troposphere, rather than by the lowest kilometre.

The deviatory motion of the storm due to new cell growth is due to the interaction of the downdraught with the sourroundings, therefore influenced by the velocity profile at the low level. Chapter 4 is devoted to this phenomenon.

3.6 Notes on the Case Studies.

In common with the observation of Ludlam (1962), the severe storms studied here occured in regions of high shear. The magnitudes of convective available potential energy involved are different, ranging from a large value of 2000 JKg^{-1} to just under 350 JKg^{-1}. Their severity , however, seem to be similar in terms of

damage caused, and the long duration. In the dynamical formulation of the mid-latitude circulation, the parameter R_m governs the behaviour of the circulation, and it lies within a restricted range. This indicates that there is a constraint on the environment if severe storms are to develop, namely the ratio of convective available potential energy to that of the shear. This is likely to be the case, as most of the storms studied had a value of R_m less than 1, typically around 0.5. The immensely damaing Centenial storm developed in an environment with $R_m = 0.1$. Included in the study is a computer simulated non-severe storm, Hamll, (Thorpe and Miller (1978)). The value of R_m is found to be 4; the storm was made up of a number of cells which did not reach mature stage at all, spending most of its lifetime in the growing and decaying phases. Thus R_m can be useful as an indicator for an environment capable of supporting a severe storm.

Many severe storms produce hail. The usual predicting technique of an impending severe storm is to observe a hook shape echo inside the storm region on the radar screen. This region is referred to as the weak echo region (WER for short). Browning paid much emphasis on the importance of the WER in the observation of severe storm and hail growth. Inside the WER, it is thought that air rises at a very high speed. The water droplets which condense out as the air rises cannot be accumulated at a high enough density to give a strong radar image. The high speed updraught is responsible for supporting hailstones and supplying them with moisture and water droplets. In order for hail of any significant size to reach the ground, the updraught has to maintain its high vertical speed for as long as it takes for hail stones to grow to a required size; the time period required is much longer than the typical time a parcel takes to pass through the cell.

Thus hail fall is a good indicator that a severe storm is in a quasi-steady state, but not visa versa. Many of the cases studied here were observed with large hail.

3.7 Case Studies

3.7.1 The wokingham storm.

This storm occured in south-east England, and was subjected to intense radar studies. The mid-latitude storm model, and later the severe right moving storm model were based on these studies. Each cell had a typical life time of an hour on the radar screen with clear WER at some stage. The thermodynamics sounding and the hodograph are shown in figure (3.7.1).

CAPE = 390 ± 39 JKg^{-1}

R_m = 0.3

D = 1.5

The estimated 10 percent error in CAPE is due to the uncertainty in the measurements, it is included in the following cases. Thus giving velocities of the :

mid-latitude component = 18 ms^{-1} towards $29^{o}N$.

Tropical component = 1 ms^{-1} towards $119^{o}N$.

The predicted velocity of the convective cells is 18 ± 0.5 ms^{-1} towards $32 \pm 2^{o}N$.

The observed velocity of the cells is 19 ms^{-1} towards $29 \pm 10^{o}N$.

3.7.2. The Rimbey Storm (16th July 1969)

This storm was a multicell system. The propagation velocity of the storm and those of the cells were quite different. This

difference is discussed later. The damage it caused was small, the hail was mainly pea size. It was on the threshold of being considered as severe. The rather large value of R_m suggests that the convective cell was not as well organised as the Wokingham storm. Figure (3.7.2) shows the environment around the storm.

CAPE = 760 ± 76 JKg^{-1}

R_m = 1.9

D = 1.3

thus giving velocities of the

mid-latitude component = 5.8 ms^{-1} towards $55^{o}N$.

Tropical component = 7.1 ms^{-1} towards $325^{o}N$.

Thus the predicted velocity of the cells is 9.2 ± 0.7 ms^{-1} towards $14 \pm 3^{o}N$. It agrees almostly exactly with observed value of 9 ± 2 ms^{-1} towards $15 \pm 10^{o}N$.

3.7.3 The Centenial Storm (29th June 1967)

In this case, there was a high directional shear in the whole depth of the troposphere, an average value of shear is $0.075s^{-1}$. It falls into the severely sheared supercell grouping under the classification of Marwitz (1973). It occured near the frontal zone where there was an intense jet aloft. The high magnitude of shear was due to this jet.

CAPE = 340 ± 34 JKg^{-1}

R_m = 0.12

D = 0.9

It is worth noting that the value of CAPE was very small (figure(3.7.3)) and the storm extended to only 7 kilometres, which accounts for the low value of D.

Thus giving velocities of the

mid-latitude component = 9.4 ms^{-1} towards $105^{o}N$.

Tropical component = 2 ms^{-1} towards $195^{o}N$.

The predicted velocity is 9.6 $\pm$ 0.5 ms^{-1} towards 117 $\pm$ $2^{o}N$. It agrees exactly with the observed values.

3.7.4 The Horsham Storm (5th September 1958)

This was the severest of storms that occured over Sussex, with the heaviest hail fall in history over Horsham. Its development was watched by radar, the resolution of which was coarse. Velocity was estimated at between 24 to 30 knots in a general direction of $230^{o}N$.

The soundings used were made many hours before the passage of the storm, the shear was small which accounted for the big value of R_m. This is the only case where the severity of the storm is associated with such a big value of R_m. The sounding used may not be representative of the environment the storm was in. They are shown in figure (3.7.4).

CAPE = 960 $\pm$ 96 JKg^{-1}

R_m = 1.5

D = 1.5

thus giving velocities of the

mid-latitude component = 12 ms^{-1} towards $185^{o}N$.

Tropical component = 5.6 ms^{-1} towards $275^{o}N$.

The predicted velocity is thus 15 $\pm$ 1 ms^{-1} towards 218 $\pm$ $2^{o}N$. The observed velocity was 12 to 15 ms^{-1} 230 $\pm$ $10^{o}N$.

3.7.5 The Lawton Storm (23rd April 1964)

In contrast with many observations in which a storm turned to a severe right moving storm during its most severe stage, it turned to a severe left moving storm. It was as severe as many right moving storms.

The measured value of CAPE is 1850 JKg^{-1} which is large. The shear on this occasion was also very large, due to a jet stream aloft, giving a low value of R_m. The thermodynamic sounding and wind hodograph are shown in figure (3.7.5).

R_m = 0.48

D = 1.5

the velocities of the

mid-latitude component = 17 ms^{-1} towards 68°N.

Tropical component = 7.8 ms^{-1} towards 338°N.

The predicted velocity is 18.2 $\pm$ 1 ms^{-1} towards 43 $\pm$ 2°N., which compares very well with the observed value of 18 $\pm$ 2 ms^{-1} towards 40 $\pm$ 10°N.

3.7.6 The Union City Storm (24th May 1973)

This was a splitting storm that occured over Union City. It developed early in the afternoon. Soon after it reached a mature stage, it evolved into two supercells which travelled in two different directions. The leftward moving cell travelled at a similar velocity to that of the parent cell. There is a major difference

in this case: the velocity profile in the tropical component (figure (3.7.6)) is such that a preferred direction of propagation of the tropical component cannot be defined. The soundings are shown in figure (3.7.7).

CAPE = 1100 ± 110 JKg^{-1}

R_m = 0.54

D = 1.5

thus giving velocities of the

mid-latitude component = 13.8 ms^{-1} towrards $108^{o}N$.

Tropical component = 0 and 9 ms^{-1} towards $18^{o}N$.

The predicted velocities for the left moving cell is 16.5 ms^{-1} towards $75^{o}N$ while for the right moving cell it is 13.8 ms^{-1} towards 108^{o} the left moving storm was observed to travel at 15.3 ms^{-1} towards $66^{o}N$ the right moving cell travelled at 11 ms^{-1} towards $106^{o}N$.

3.7.7 Ham7

This is a numerical simulated storm as presented in Miller (1978), the temperature and wind profiles used in the simulation are presented in figure (3.7.8). A system structure was observed.

CAPE = 970 ± 97 JKg^{-1}

R_m = 2.0

D = 1.4

thus giving velocities of the

mid-latitude component = 9.3 ms^{-1} towards 43°N.

Tropical component = 1 ms^{-1} towards 317°N.

The predicted velocity is 9.4 ms^{-1} towards 37°N. The cell was observed to travel at approximately 11 ms^{-1} towards a general direction of 30°N.

3.7.8. Ham 11

This is another numrically simulated storm as presented in Thorpe and Miller (1978). The thermodyanamic sounding used was the same as that for the Ham7 simulation, the wind profile was different, and it is shown in figure (3.7.9).

CAPE = 750 $\pm$ 75 JKg^{-1}

R_m = 4

D = 1.4.

Thus giving the velocities of the

mid-latitude component = 9.4 ms^{-1} towards 336°N.

Tropical component = 4.9 ms^{-1} towards 66°

the predicted velocity is 10.6 ms^{-1} $\pm$ 1.1 towards 3.5 $\pm$ 8°N. The observed velocity is 4.8 ms^{-1} towards 21°N.

The big discrepancy which exists in this case is not surprising. The cells were observed to spend all of their lifetime in the growing and dissipating phases. They grew to a height of around 6 kilometres, and began to dissipate. This is in contrast with the rest of the case studies in which the convective cells were long lived and spent the major part of their life in the mature stage.

3.8 General Remarks

One of the main aims of modelling is to explain, from the point of view of the model, the features observed. Propagation velocity is one of the characteristics considered. A comparison between predicted and observed velocities of convective cells is presented in figures (3.8.1) and (3.8.2).

The 2-dimensional mid-latitude model was based on careful observation. On occasions, a three-dimensional storm model was judged to be necessary. The main difference in these two types of storms observed lies in the value of CAPE available. Wokingham and Centenial storms were described as near 2-dimensional. The value of CAPE is of the order $400 JKg^{-1}$. In a severe 3-dimensional storm, such as the Lawton storm, the value of CAPE is large -- $2000\ JKg^{-1}$.

The characteristic deviatory motion of convective cells is due to the dynamics of the whole circulation and the related environmental wind profile. The apparent motion due to the process of regeneration is the subject of the next chapter.

(a) The temperature sounding

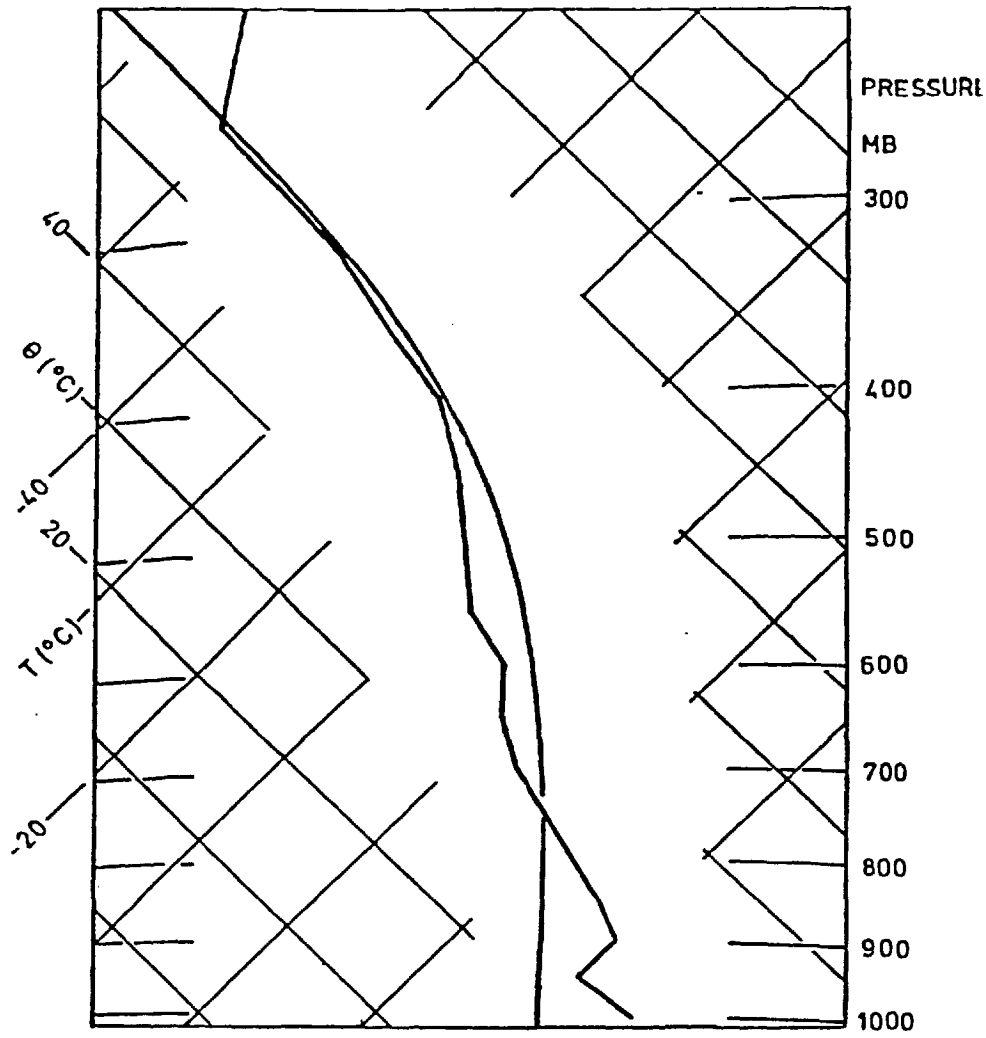

(b) The hodograph

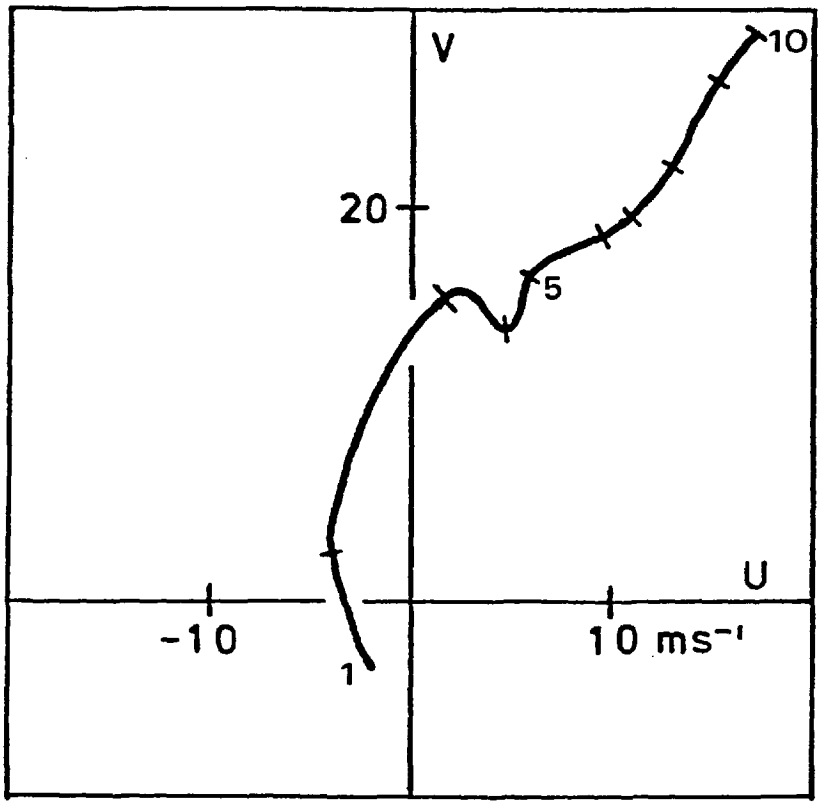

Figure 3.7.1 The Wokingham Storm.

(a) The temperature sounding

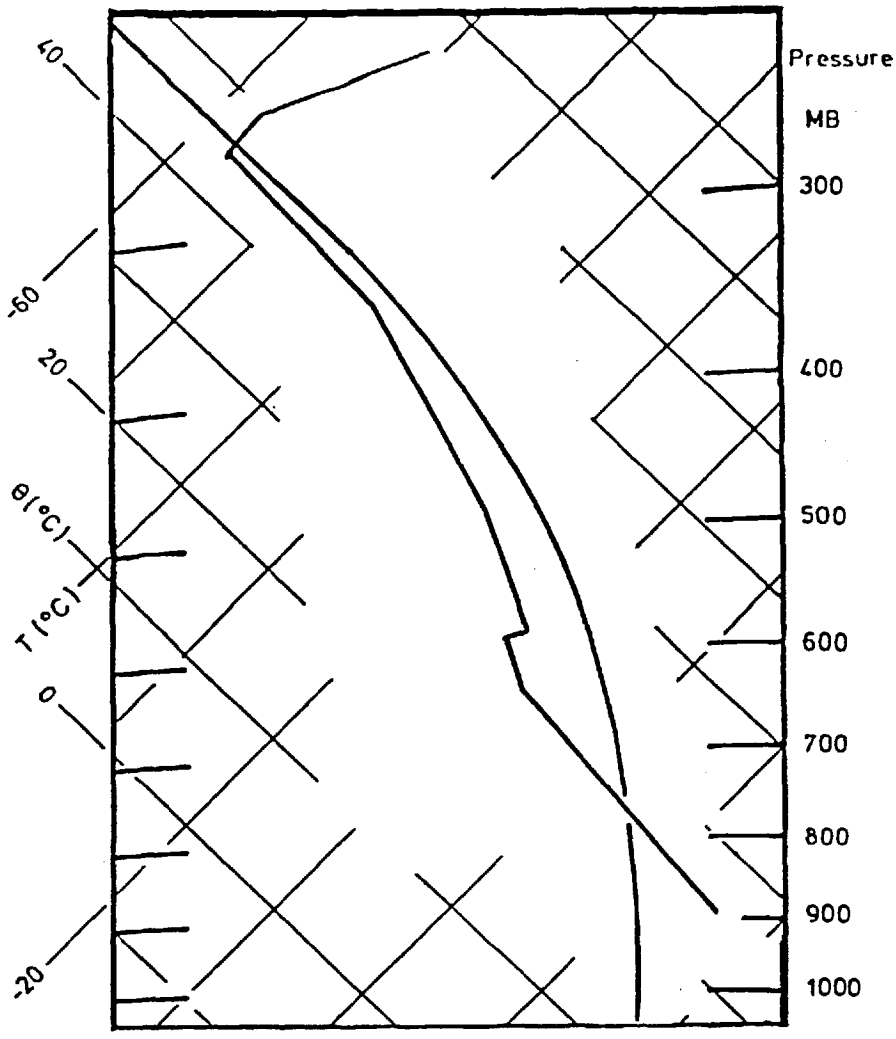

Figure 3.7.2 The Rimbey Storm.

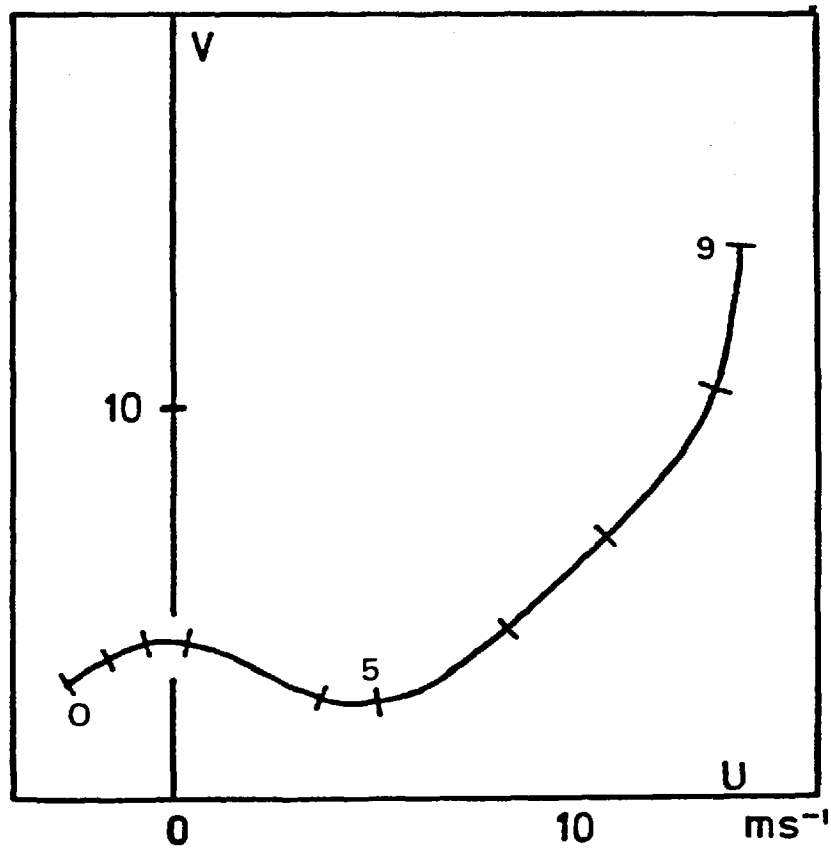

(b) The hodograph

(a) The temperature sounding

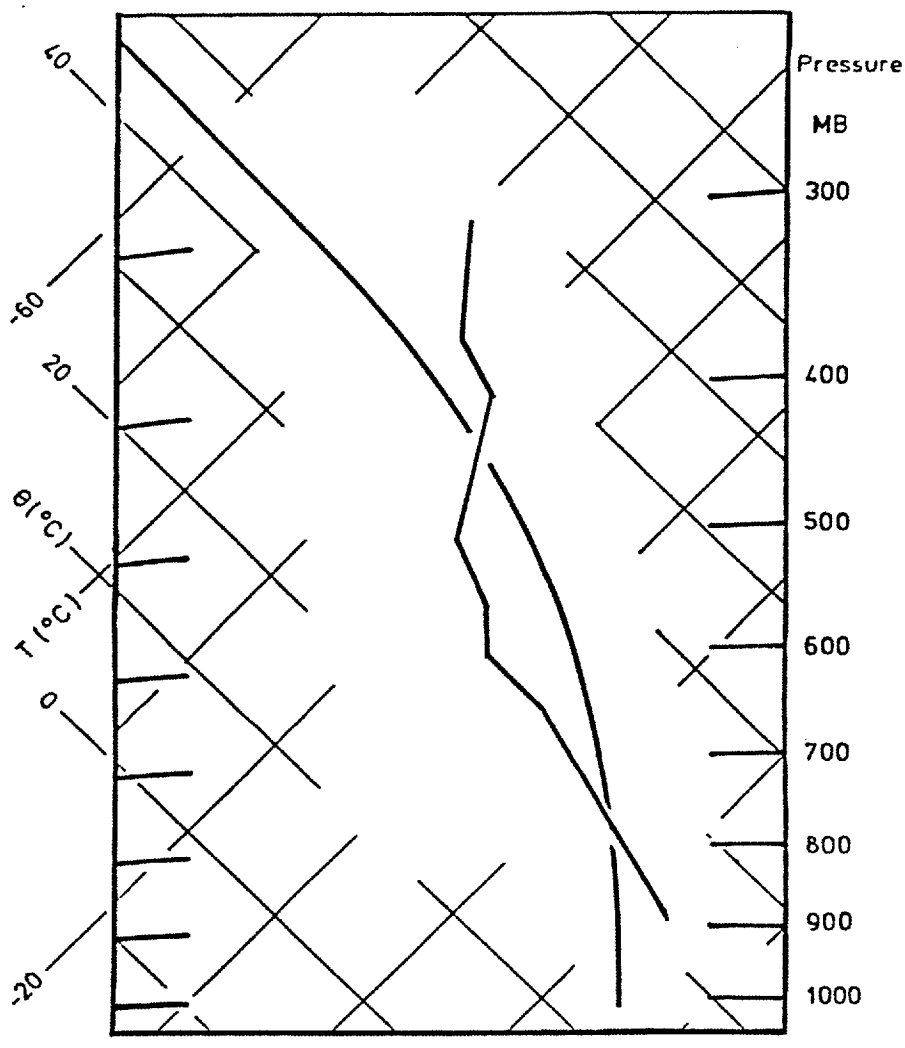

Figure 3.7.3 The Centenial Storm.

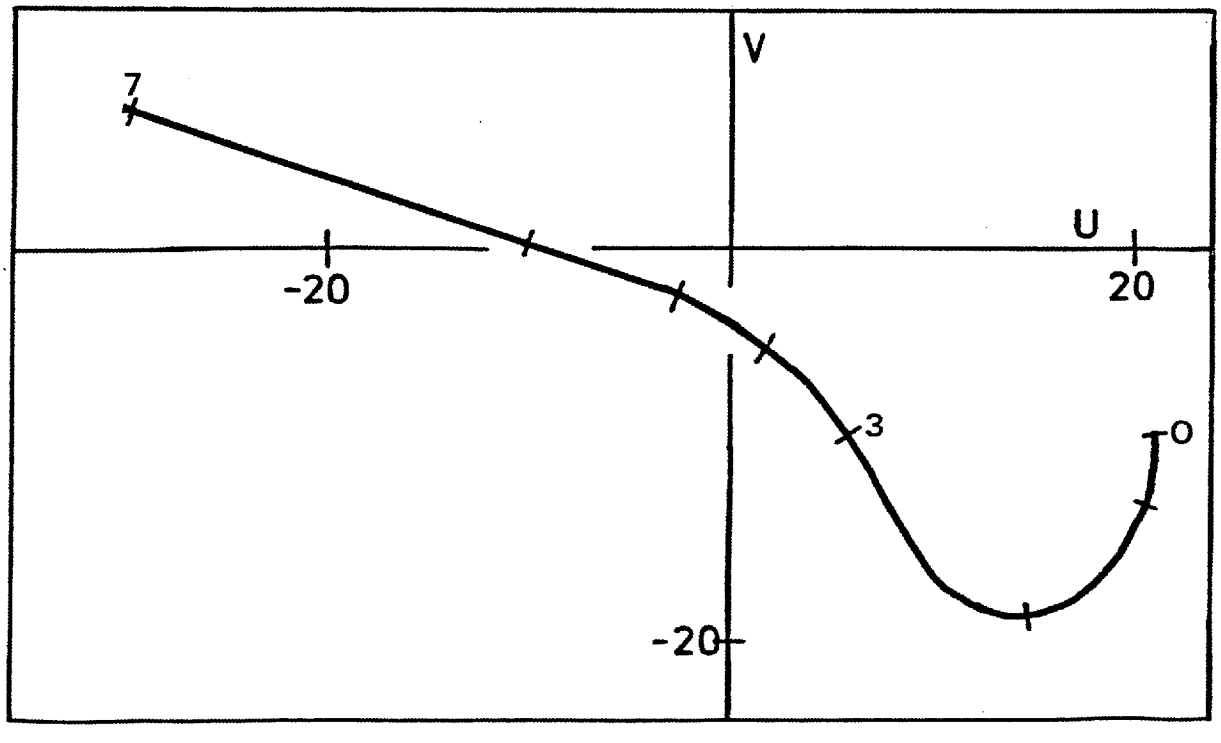

(b) The hodograph

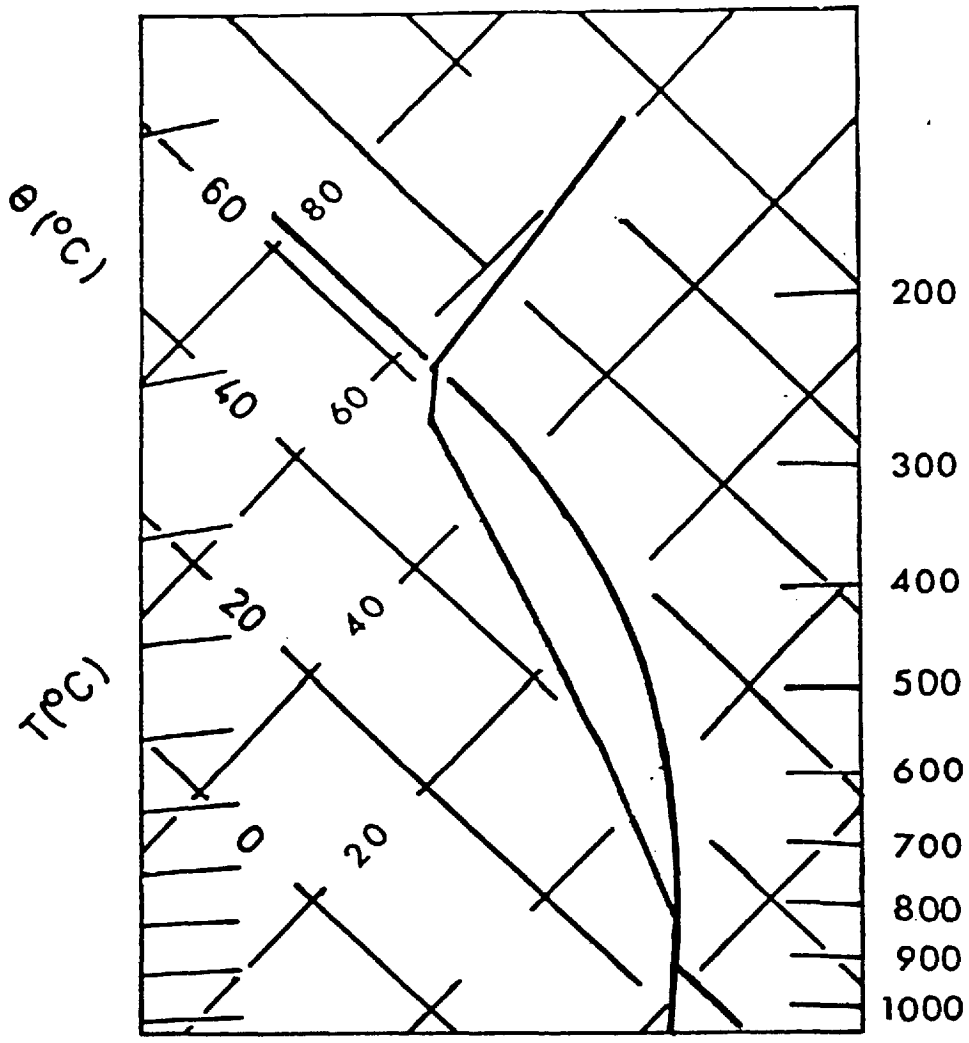

Figure 3.7.4 The Horsham Storm.

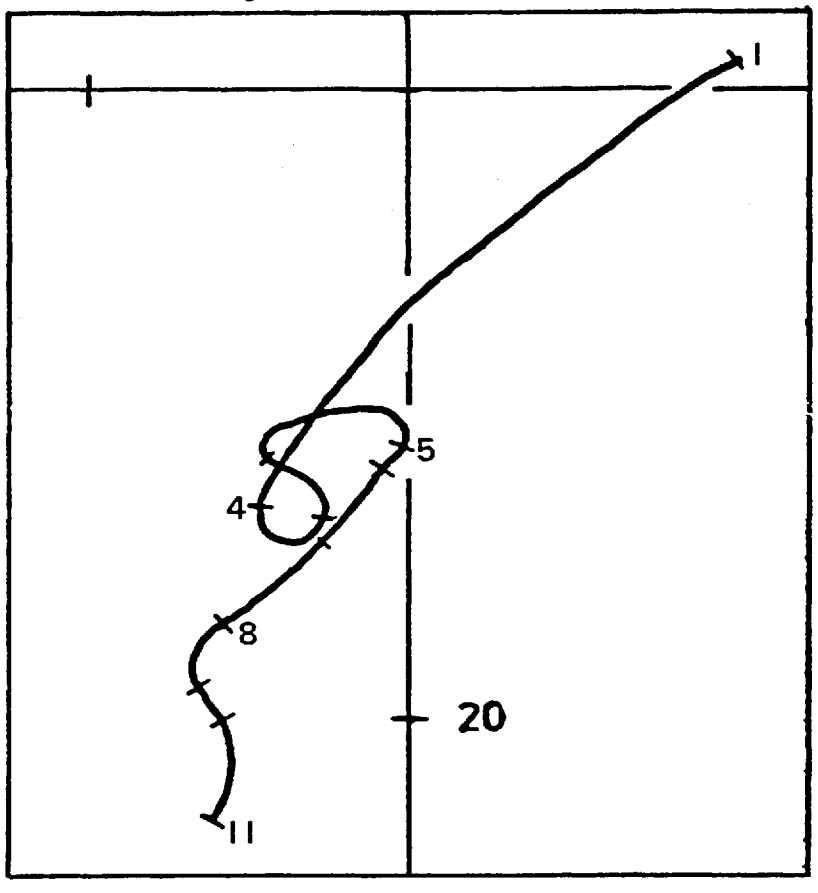

(b) The hodograph

(a) The temperature sounding

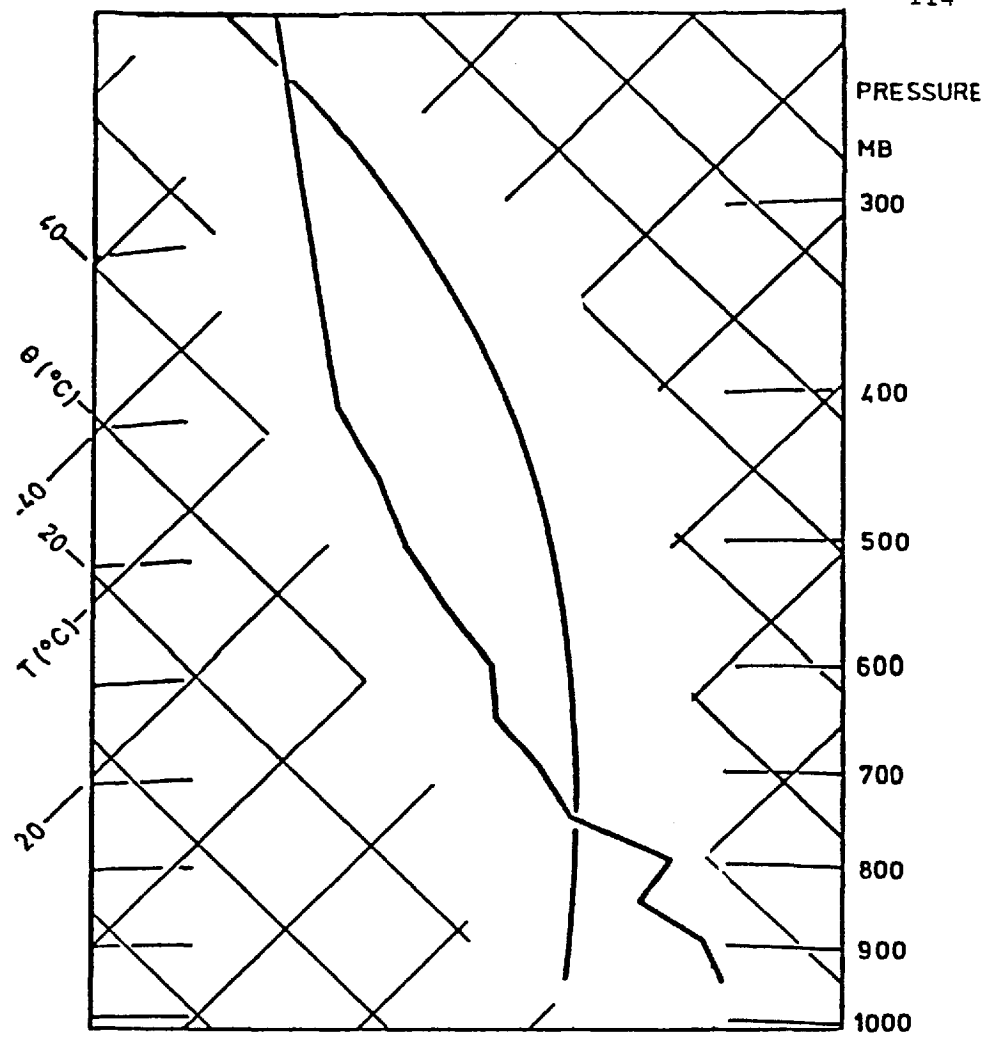

Figure 3.7.5 The Lawton Storm.

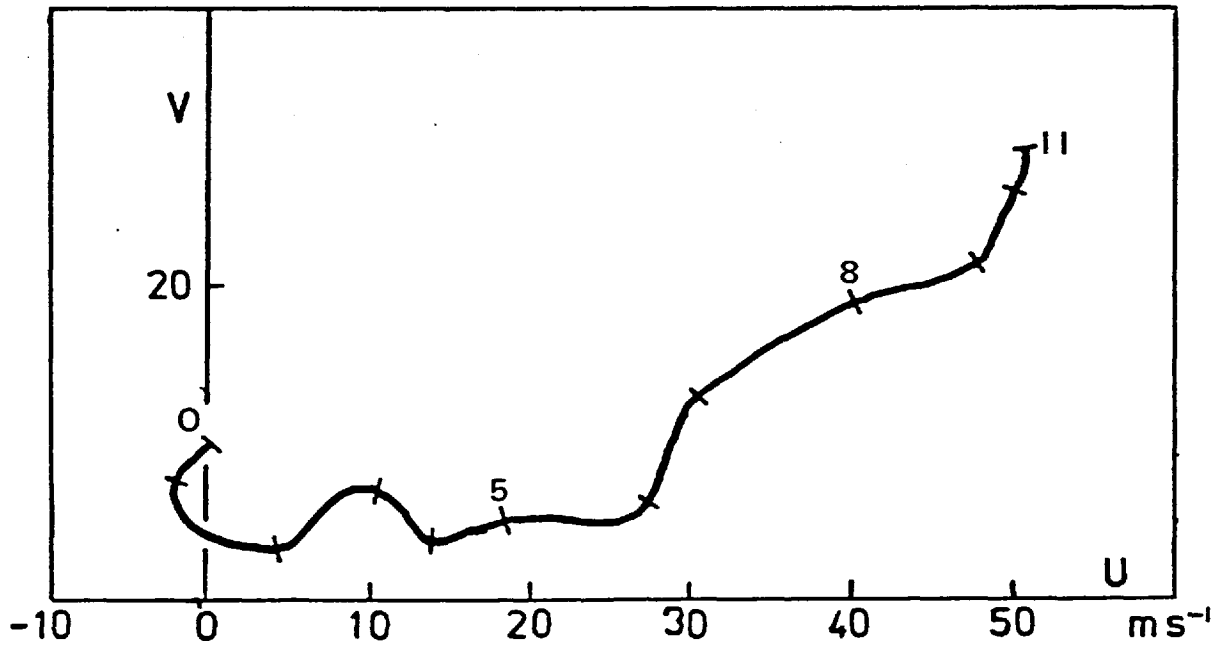

(b) The hodograph

(a) The temperature sounding

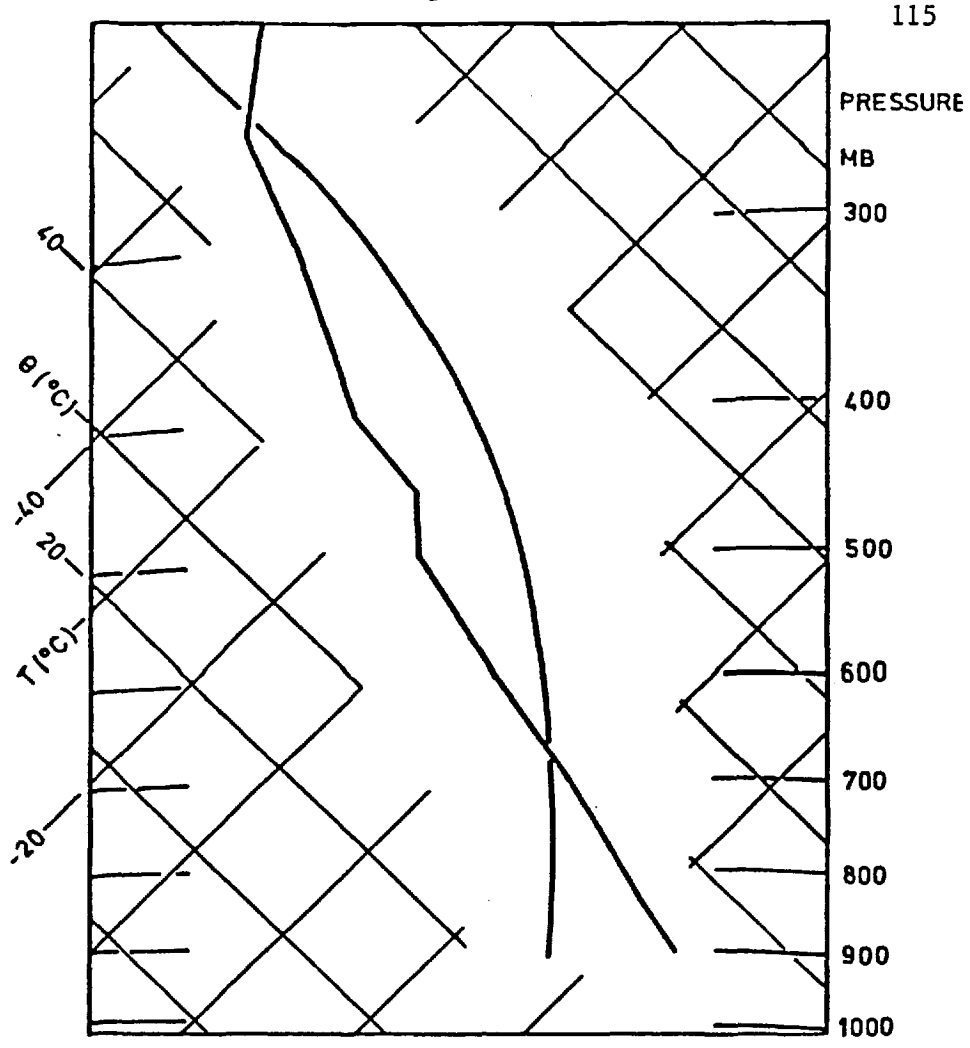

Figure 3.7.7 The Union City Storm.

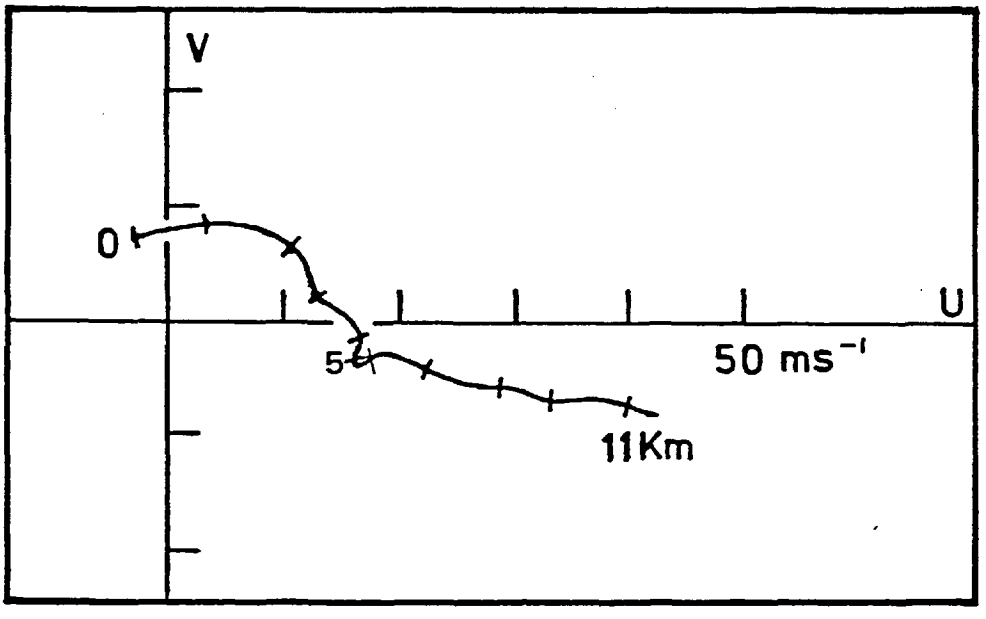

(b) The hodograph

(a) The temperature sounding

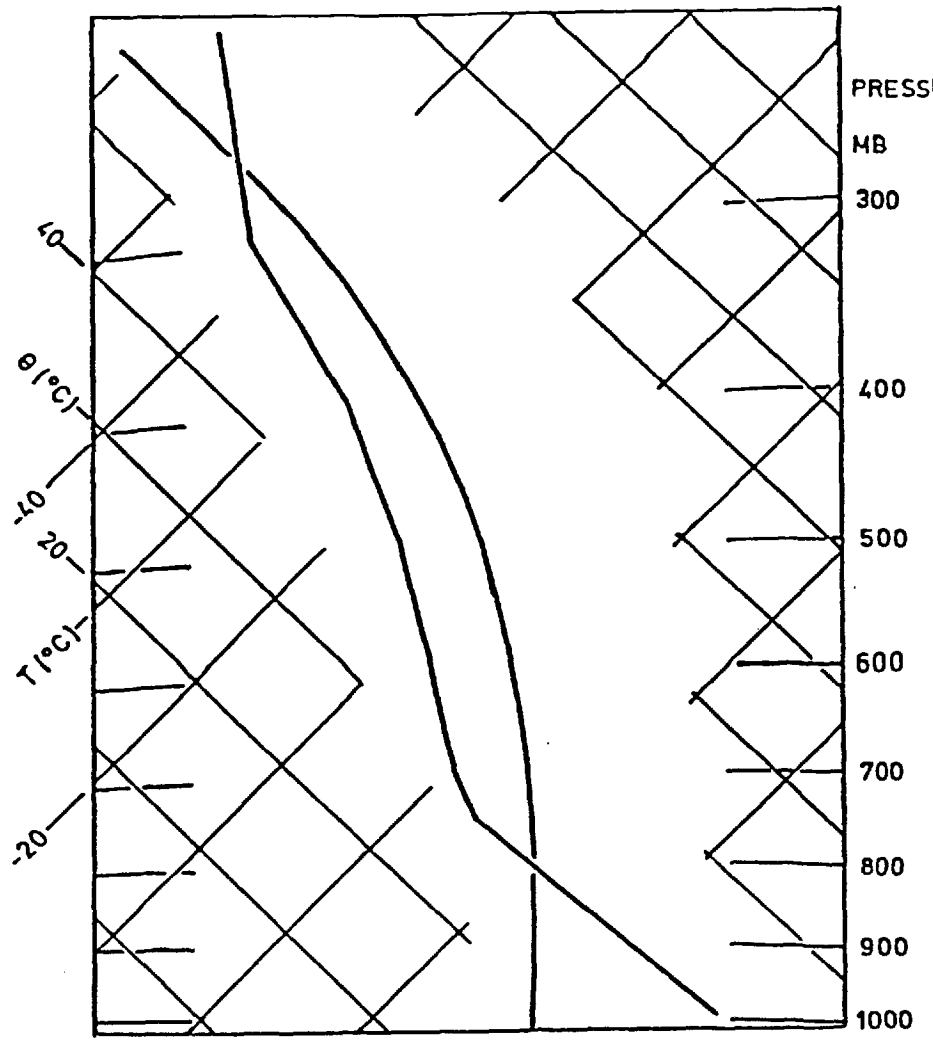

(b) The hodograph

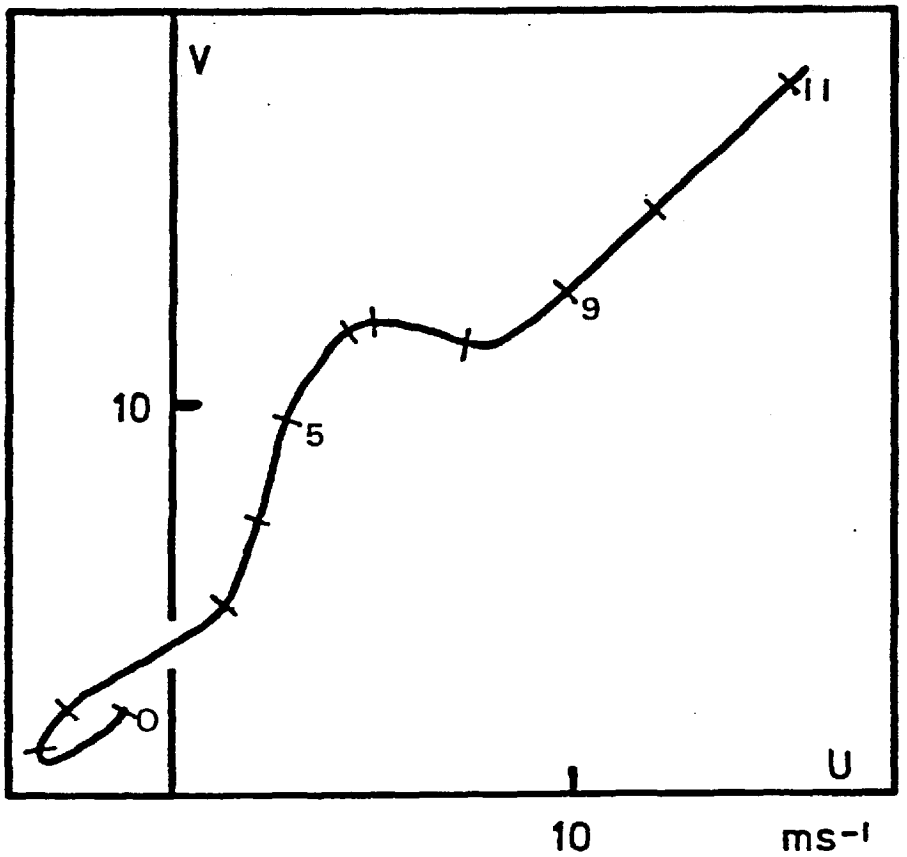

Figure 3.7.8 The numerical simulated storm - HAM7 .

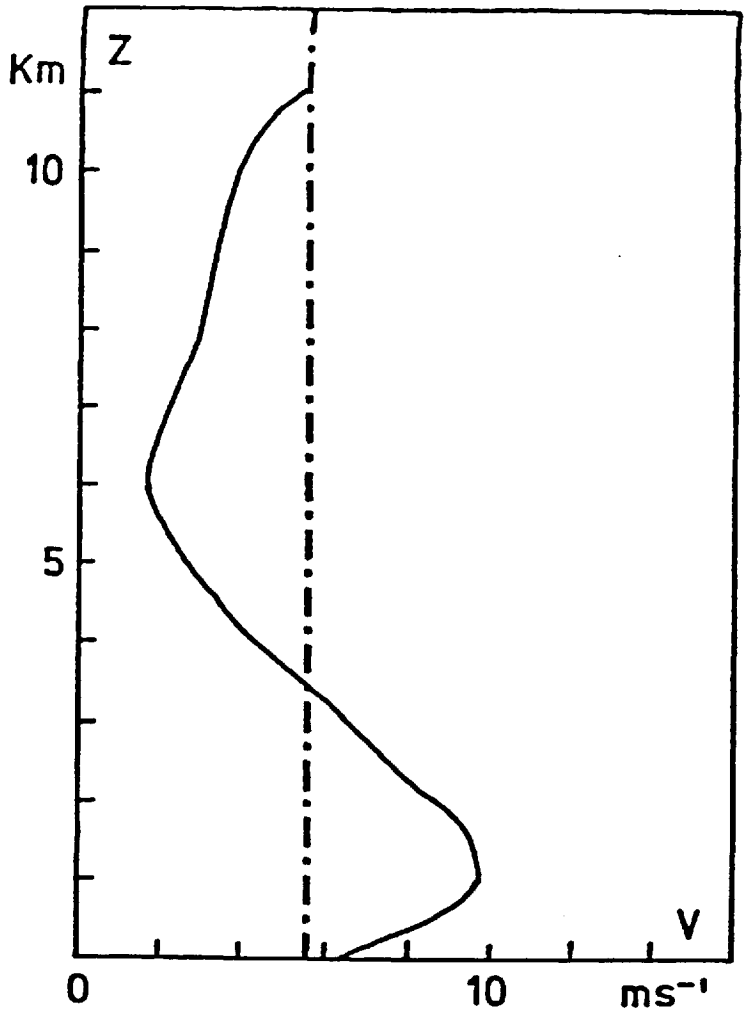

Figure 3.7.6

The velocity profile in the direction of minimum mean shear.

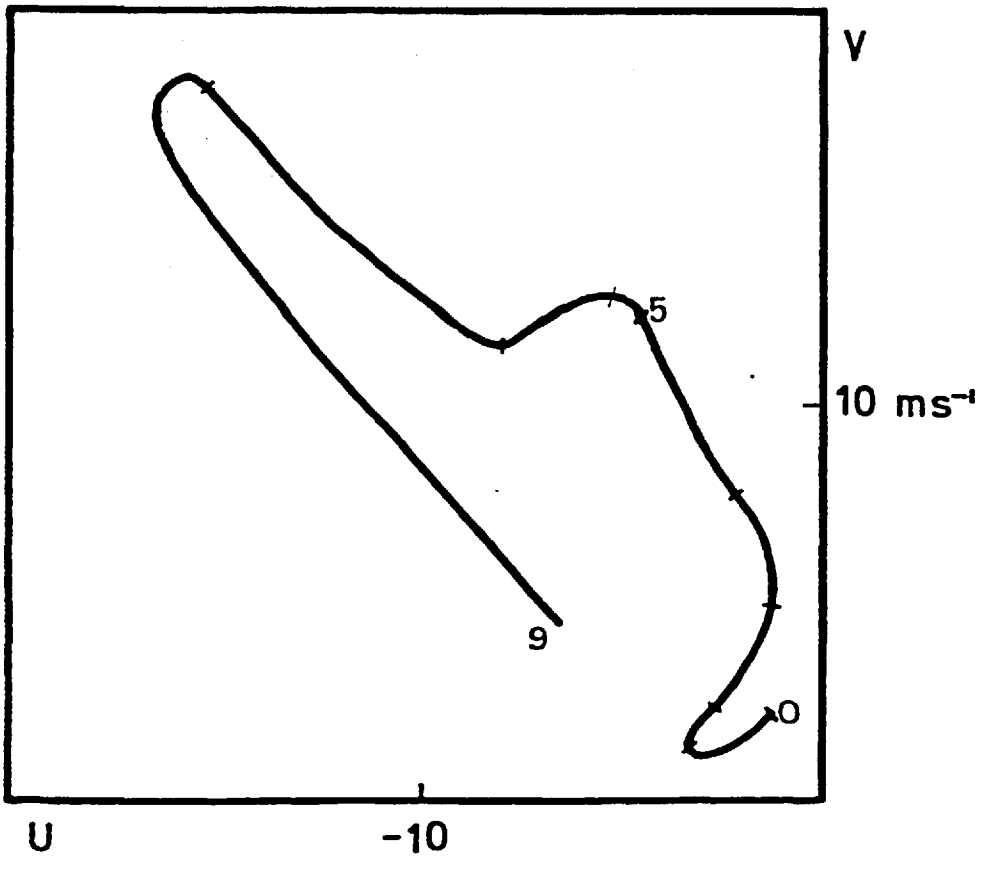

Figure 3.7.9 The numerical simulated storm - HAM11 .

Figure 3.8.1 Observed and predicted speeds.

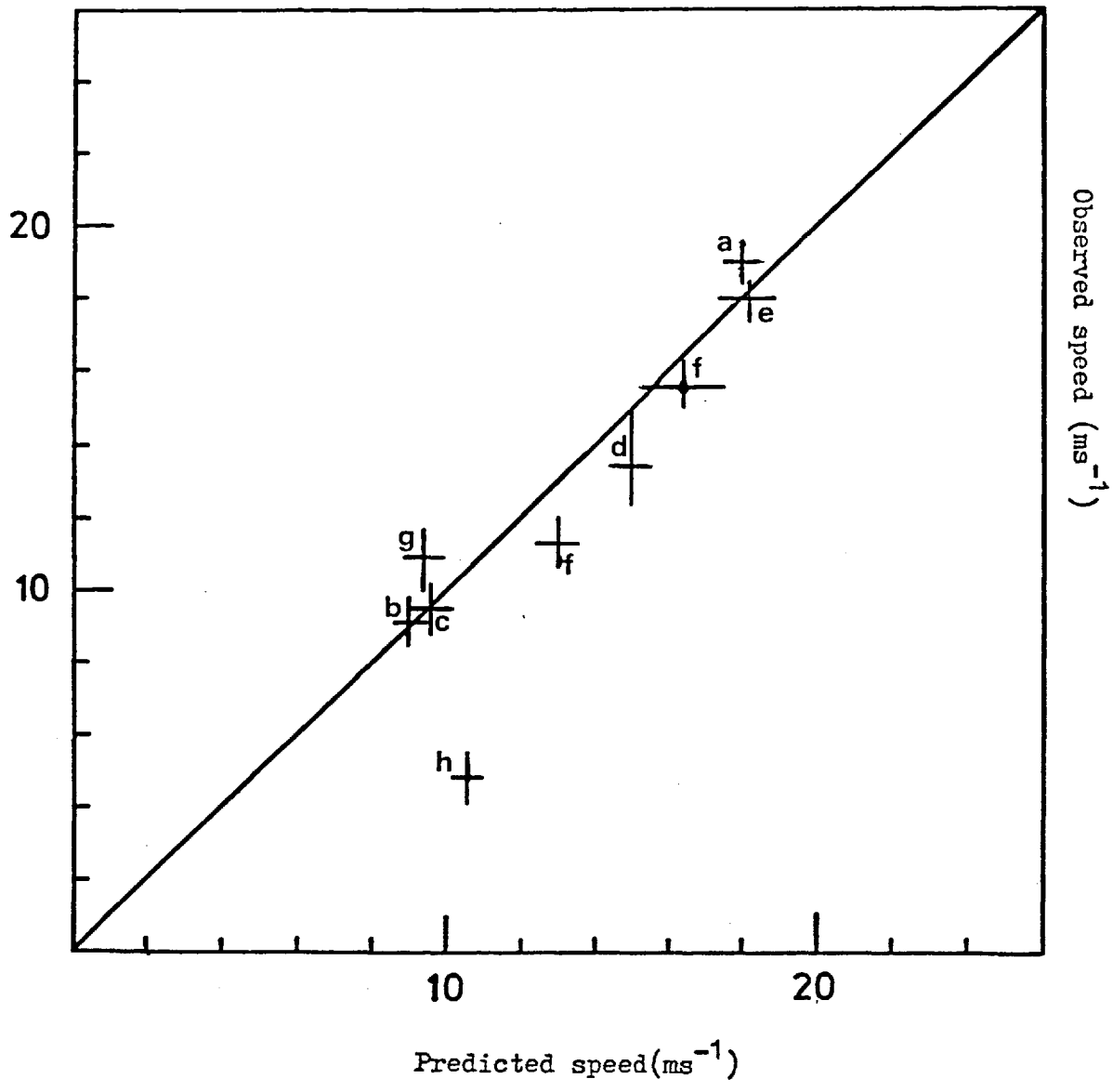

(a) The Wokingham Storm

(b) The Rimbey Storm

(c) The Centenial Storm

(d) The Horsham Storm

(e) The Lawton Storm

(f) The Union City Storm

(g) HAM 7.

(h) HAM 11.

Figure 3.8.2 Observed and predicted directions.

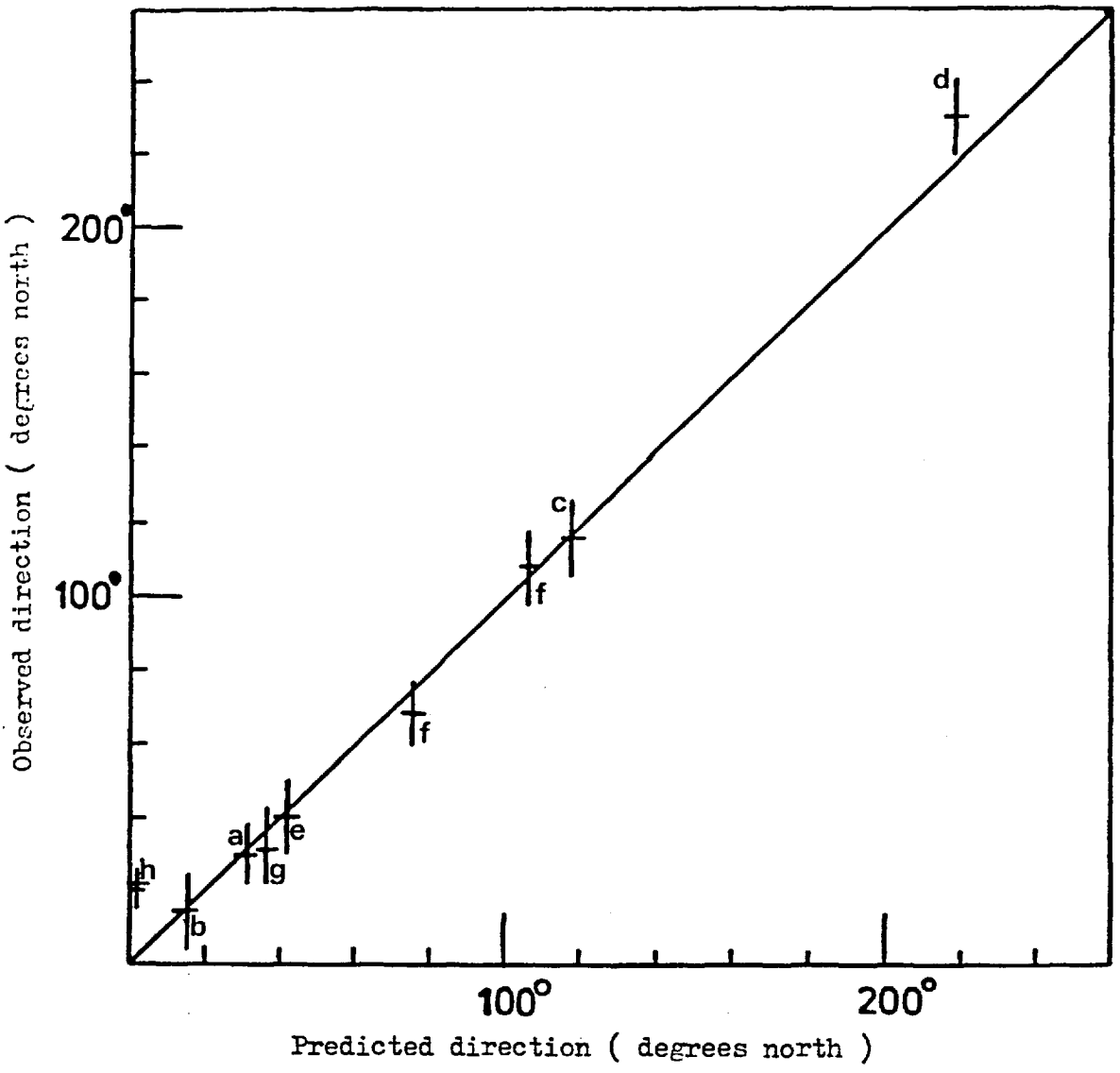

CHAPTER FOUR

PROPAGATION VELOCITY OF STORM : ROLE OF DOWNDRAUGHT.

4.1 Introduction

The velocity of a storm is sometimes different from its constituent convective cells. The difference is due to an apparent movement which leads to an additional velocity component. It is due to a process of generation of new cells on one flank, and the decay of older cells on the opposite flank. The velocity resulted from this process alone is called the discrete propagation velocity. It was observed in the Wokingham storm by Browning (1962) and in the Lawton storm by Hammond (1967). The cells were assumed to travel with the mean wind, the deviatory motion was then explained in terms of the discrete propagation process. This was despite their observations that the constituent cells did not travel with the mean wind, in other words the cells were deviatory. The propagtion velocity of the cell is governed by the internal dynamics of the cell, the discrete propagation velocity of a storm depends on the interaction of the downdraught outflow with the environment. This chapter is devoted to the latter process.

4.2 Discrete Propagation Due to Water Budget Requirement.

Newton and Fankhauser (1964) investigated the movement of storms due to the process of generation of cells by considering the water budget requirement of the system. They postulated that a storm moved in such a way that balanced the supply and demand requirements of the water budget. The amount of water vapour intercepted by the storm is proportional to its diameter, and its velocity relative to the air at the low level. They suggested that since the water lost through

precipitation was proportional to the area of the storm --- the square of the diameter, in order that the water budget should balance, a large storm was required to travel faster relative to the low level air in order to intercept more moisture than a smaller one. In other words there is a maximum adjustment of the moisture flux into the storm. In an environment where wind veers with height, a storm should tend to move discretely towards the right.

When the results were compared with observations, the scatter between predicted and observed velocities was large. Hammond (1967) applied this result to the Lawton storm, and found that the theory predicted a right moving storm with a propagation speed less than that of the mean wind speed. The storm was observed to propagate discretely towards the left, and travelled faster than the mean wind. There is a major inconsistency in the analysis, the discrete deviatory motion of the storm is recognised by the authors to be due to the process of regeneration of new convective cells preferentially on one flank. This motion, however, is also interpreted as an additional velocity component serving to increase the relative inflow speed of the air at the low level. It is clear that this apparent movement of the storm mass makes no contribution to increasing the inflow. The volume of inflow is governed by the velocity of the cell.

4.3 Density Current -- A Mechanism of Generation of New Cells.

It has been recognised that the downdraught is important in maintaining convection and in generating new convection. Miller and Betts (1976) studied the role of a density current --- the outflow of downdraught at the surface -- in the maintainance of a long lasting squall line. They found that under certain circumstances, the density

current front could travel at the same speed as the squall line, such that the density current front was stationary relative to the updraught. The numerical simulations of the effect of the density current on activating new cells growth was presented in Thorpe and Miller (1978). It was observed that new convective cells grew in the region of density current front. Cells grew in regions where the boundary layer convergence was greatest. The net movement of the storm is towards the direction of maximum convergence relative to the cell. It determines the direction of the discrete propagation.

4.4 A Simple Disorganized Downdraught.

A downdraught, in models predicting deviatory motion such as Newton and Katz (1958), can be thought of as a column of air moving vertically downward relative to the cell. As the air parcel approaches the ground, it spreads out in all directions. The region of maximum convergence is where the downdraught outflow meets the low level relative flow head on. Thus the direction where new convection is expected to grow, is opposite to that of the relative velocity vector between the cell and the low level flow. Assuming that the cell was travelling with the mean wind, Newton and Katz (1958) found that when wind veered with height, a storm tended to propagate discretely towards the right. However, it was observed in the Lawton storm, where there was a veering of wind, the preferred direction of new cells growth was towards the left instead of towards the right. If the cells are assumed not to be steered by the mean wind, and the actual velocity of the cell is used, the predicted directions for discret propagation are, in most cases, incorrect.

In the case of the updraught, the direction to which the deviatory

propagation is directed depends on the profile along the direction of minimum mean shear -- the tropical component; or crudely the shape of the hodograph. The turning of wind as seen by an observer at a stationary ground station is not representative of the wind profile as seen by the convective system.

4.5 A Simple Organised Downdraught Model.

The downdraught is often modelled as an unorganized flow; often too much emphasis has been paid on extracting details concerning the outflow region, the analysis of the density current is one of the examples. While these studies provide valuable information, they leave questions unanswered such as whether a particular downdraught causes new convection on the right or the left of the mature convective cell. A more appropriate approach is to model a downdraught circulation as an entity.

It is easy to perceive an updraught circulation through the formation of cloud masses, but a downdraught has the disadvantage of being difficult to observe. It can be deduced, however, through temperature and vertical velocity measurements taken across the convective cell or system. Its intensity and steadiness are confirmed by all such measurements. The knowledge of downdraughts from observation is still incomplete ; there is no agreed maximum downdraught inflow height for example ; and its effect on the intensity of convection is still not well understood.

From the trajectory tracing of Miller (1978), it can be seen that the downdraught circulation can be an organized circulation similar in many respects to the updraught circulation. The behaviour of the updraught is found to be determined by its dynamics. The downdraught,

being similar to the updraught, may be a dynamically dominant circulation. As such, it may be modelled in a similar fashion ; that is, the downdraught is resolved into two orthorgonal two diminsional circulations -- a mid-latitude circulation along the plane of maximum directional shear, and a tropical circulation along the direction of minimum shear. The magnitude of shear in the low level is usually fairly large, thus providing an organizational effect.

4.6 Boundary Conditions

4.6.1 Lower Boundary

The lower boundary remains the same as that for the updraught --- the ground at $z = 0$.

4.6.2 Upper Boundary.

The vertical extent of the downdraught has been recognised to be smaller than the updraught and inflows occur somewhere at mid level. The upper boundary of the downdraught inflow is open to dispute. It is, however, in general agreement that it originates from mid-levels. There is, however, no reason to assume the downdraught to originate from a fixed level as in Ryan and Carson (1978) in their treatment of the squall-line downdraughts. The inflow into the downdraught needs to be chilled by evaporative cooling: a process which requires transfer of the moisture condensed inside the updraught to the downdraught. The updraught is saturated, therefore, evaporative cooling can only occur outside the updraught, and below the minimum updraught outflow level. The maximum inflow level of the downdraught is limited by the depth of the updraught outflow. In the model, for convenience, the downdraught maximum inflow height is to be taken to be the steering level of the mid-latitude component of the updraught branch. Miller (1978) observed

in the numerical simulation of the Hampstead storm that downdraught originated as high as 600 mb using trajectory tracing technique. This level is close to the calculated steering level of the mid-latitude component of the updraught .

4.7 Convective Available Potential Energy

The value of CAPE for the downdraught is calculated from the integral $\int g \delta\phi \, dz$. The value of $\delta\phi$ depends on the particular thermodynamical path followed by the parcel and the temperature profile of the environment. To a first approximation, the parcel can be assumed to descend wet adiabatically. The value of CAPE can be measured from a tephi-gram, or by a numerical method described in the appendix. It is worth noting that the value of CAPE is not equal to that of the updraught, in most cases, it is smaller.

4.8 Mid-latitude Circulation

From the analytic results in 2.2

$$\lambda_{*_d} = \frac{1}{(1 + \beta_d)} \tag{4.1}$$

where

$$R_{m_d} = 2\beta_d(\beta_d - 1) \tag{4.2}$$

The superscript d denotes variables that belong to the downdraught all updraught variables, from now on, will contain a superscript u. This is omitted in earlier chapters for clearer illustration.

$$R_{n_d} = \frac{CAPE_d}{(\Delta U_d)^2} \tag{4.3}$$

The steering level in the mid-latitude component of the downdraught is defined by λ_{*_d}. The magnitude of height is normalised with respect to the downdraught height scale, which is that of the

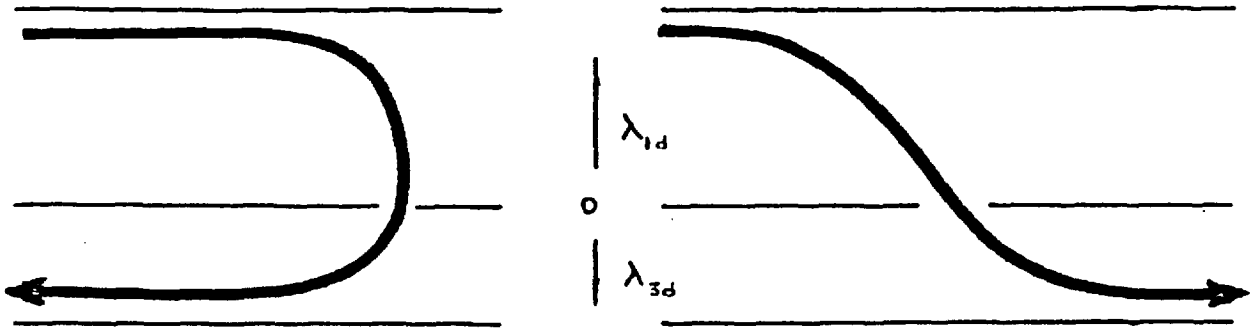

Figure 4.5.1 Schematic diagrams showing the mid-latitude and tropical circulations in the downdraught.

updraught steering level. The actual height of the steering level of the downdraught :

$$Z_{*d} = \frac{1}{(1+\beta_d)} \frac{\beta_u}{(1+\beta_u)} H \qquad (4.4)$$

4.8.1 Effect Of Density Stratification.

The numerical solution to the updraught circulation indicates that the steering level is depressed when the ratio of the height of the convection and the density scale height, D is non zero. The relationship for the updraught is described in equation (2.32). This relationship extends to ranges where D is negative. In the formation of the downdraught circulation, the air parcel descends from a high level to a lower level, the effect of density stratification has the effect of increasing the distance between z_{*u} and z_{*d}. The net result is a depression of the steering level of the downdraught mid-latitude circulation relative to the bottom boundary. Thus:

$$Z_{*d} = Z_{*d}\Big|_{D=0} - \cdot 11 D_d H \qquad (4.5)$$

4.8.2 Tropical Circulation

The circulation is determined from the boundary conditions imposed by the mid-latitude component of the downdraught, together with CAPE. The outflow profile and propagation can be obtained from the equations in section 2.3.

In incompressible case (D=0) and since $\alpha_d = \lambda_{*d}$

$$\lambda_{*d} = C_d \sinh^{-1} \frac{1}{C_d} \qquad (4.6)$$

the relationship obtained for D positive is applicable for D negative. Thus

$$C_d = f(\alpha_d)\,(30\alpha_d)^{-.17 D_d} \qquad (4.7)$$

The steering level of the mid-latitude circulation of the downdraught is different to that of the updraught, so is the propagation velocity of the tropical component. Thus the downdraught circulation tends to to have a different propagation velocity.

4.9 The Downdraught as a Dynamical Circulation

As a dynamically dominant circulation, the downdraught tends to propagate in a different velocity from that of the updraught. However, the energy for convection in the downdraught is derived from the evaporation of the water droplets which fall from the updraught. Thus when the downdraught moves away from the updraught, its energy source, it decays; the downdraught is, in this case, constantly renewed. The net effect of the downdraught is to co-exist with the updraught, but tends to propagate towards a different direction.

The function of downdraught in the steady state updraught/downdraught system is well known. The updraught provides the necessary energy for convection to the downdraught, while the downdraught provides a region of strong local convergence to effect a large uplift of air into the updraught -- this picture is consistent with observation and numerical simulations. The observed region of highest convergence caused by the downdraught outflow is not necessarily in the direction of updraught inflow. In the Lawton storm, for example, this region of high convergence is on the left side of the cell, while the updraught inflow is from the right side. This is a surprising result if one considers downdraught maximises the updraught inflows and visa versa. It is seen that the dynamics of the updraught and downdraught is responsible.

The dynamically dominant downdraught circulation tends to move

with a different velocity from the convective cells. The direction with which the downdraught tends to propagate towards determines the region of highest convergence at the low level; this can be thought of as analogous to the case of an object moving through a fluid, there is a region of strong convergence just ahead of the moving object. The importance of downdraught in affecting the intensity, and the behaviour of the storm are to be discussed.

4.10 Intensity Of Convective Cells.

In a steady state system with updraught and downdraught, it is conceivable that a strong updraught can be maintained only when the local surface convergence in the direction of updraught inflow (relative to the cell) is large. A weaker updraught conversely requires a weaker convergence at the low level. Given a downdraught, the strongest surface convergence is in the direction the downdraught tends to propagate towards; the strength of the convergence falls off in either direction. The intensity of the updraught, thus depends on the difference in direction between the updraught inflow vector and the direction towards which the downdraught tends to propagate. If the difference is small, an intense updraught can be maintained; hence an intense convection results.

One ideal case to study is the Union City storm. It started off as a single convective cell, which at a later stage splitted into two cells. These travelled in two different directions. The left moving cell travelled at similar velocity to that of the parent cell, the right moving cell in a direction 40 degrees to the right. The left moving cell continued for an hour with no appreciable growth in size or intensity. Its characteristics were similar to those of the parent

cell. The right moving cell, however, grew in both size and intensity. The radar echo of the right moving cell was four times larger than that of the left moving cell; with large hail and tornadoes which were absent in the left moving cell. The downdraught circulation is found tending to propagate towards the right of the mean wind, the difference in direction relative to the low level flow between the propagation velocity of the cell and that of the downdraught was small for the right moving cell, and big for the left moving cell. Thus a stronger uplift was provided by the downdraught to the right moving cell than that provided to the left moving one. This accounts for the difference in intensities of the two split systems.

This result is generally true for all the cases studied. The Wokingham storm, for example, had its downdraught tending to propagate in a similar direction as the convective cell, thus leading to an intensive storm. The Rimbey storm, however, had its downdraught tending to propagate in a direction 80 degrees to the right of the velocity vector of the cell --- it is a rather weak storm, just on the threshold of being classified severe.

4.11 Downdraught Circulation --- A Case Study

A downdraught cannot be detected by the usual techniques such as radar. By virtue of its lower temperature and the pressure anomaly it creates at the surface, the downdraught and its behaviour can be inferred from measurements on the ground. In Hammond (1967), a dense array of recording stations totalling 47 were arranged in a checkerbord fashion, with horizontal spacing between 10 to 15 nautical miles. Pressure, temperature, relative humidity, precipitation, and wind velocities were continuously measured. From these readings, surface

distribution maps of all the measured variables were plotted at a given instance as well as continuously.

The passage of the convection through the network was marked by a pressure surge followed by a mesohigh which remained under the main body of the radar echo. The pressure surge was strongest on the left of the storm, figure (4.8.1). There was a sharp temperature drop accompanied the pressure surge on the left flank, figure(4.8.2). The position of the gust front was close to the pressure surge front.

It was found that the location of the cold cell, the mesohigh, and the gust front remained in the same position relative to the main part of the radar echo. The cold pool, temperature drop and the gust front can be interpreted as the region where the downdraught was reaching the ground. A similar pattern was observed at various times, indicating the convective system was in a steady state. The direction where the gradient of pressure surge, or of the temperature or of the wind, was greatest can be interpreted as the direction along which the downdraught tended to propagate. The direction is found to be towards 13 degrees north.

From the simple organized downdraught model, the propagation velocity was found to be 9 ms^{-1} towards 14 $\pm$ 3^{o}N. The two directions agree very well. It is worth noting that if the downdraught were a disorganised column of downward moving air relative to the convective cell, the maximum convergence is along 84^{o}N. If, however, one regards the storm as a convective unit, the direction of maximum convergence is along 58^{o}N. In both cases the region of maximum convergence are on the right side of the storm.

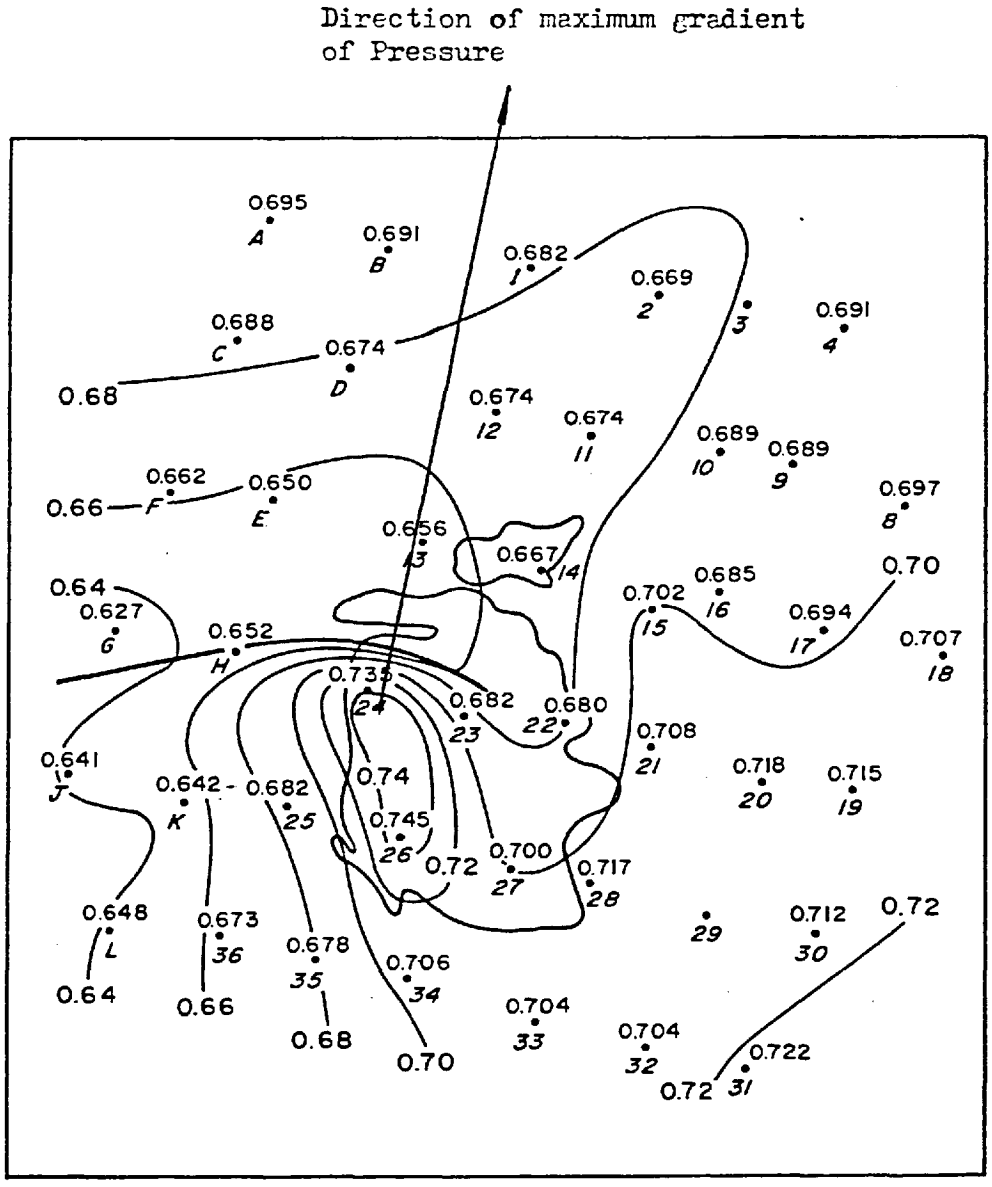

Figure 4.8.1 Pressure-isochrone-amplitude analysis of the Lawton Storm. The location of ground stations, the outline of the radar echo (at full gain and at 0^{o} elevation angle), the pressure surge line, and the direction of maximum pressure gradient at the pressure surge front are shown.

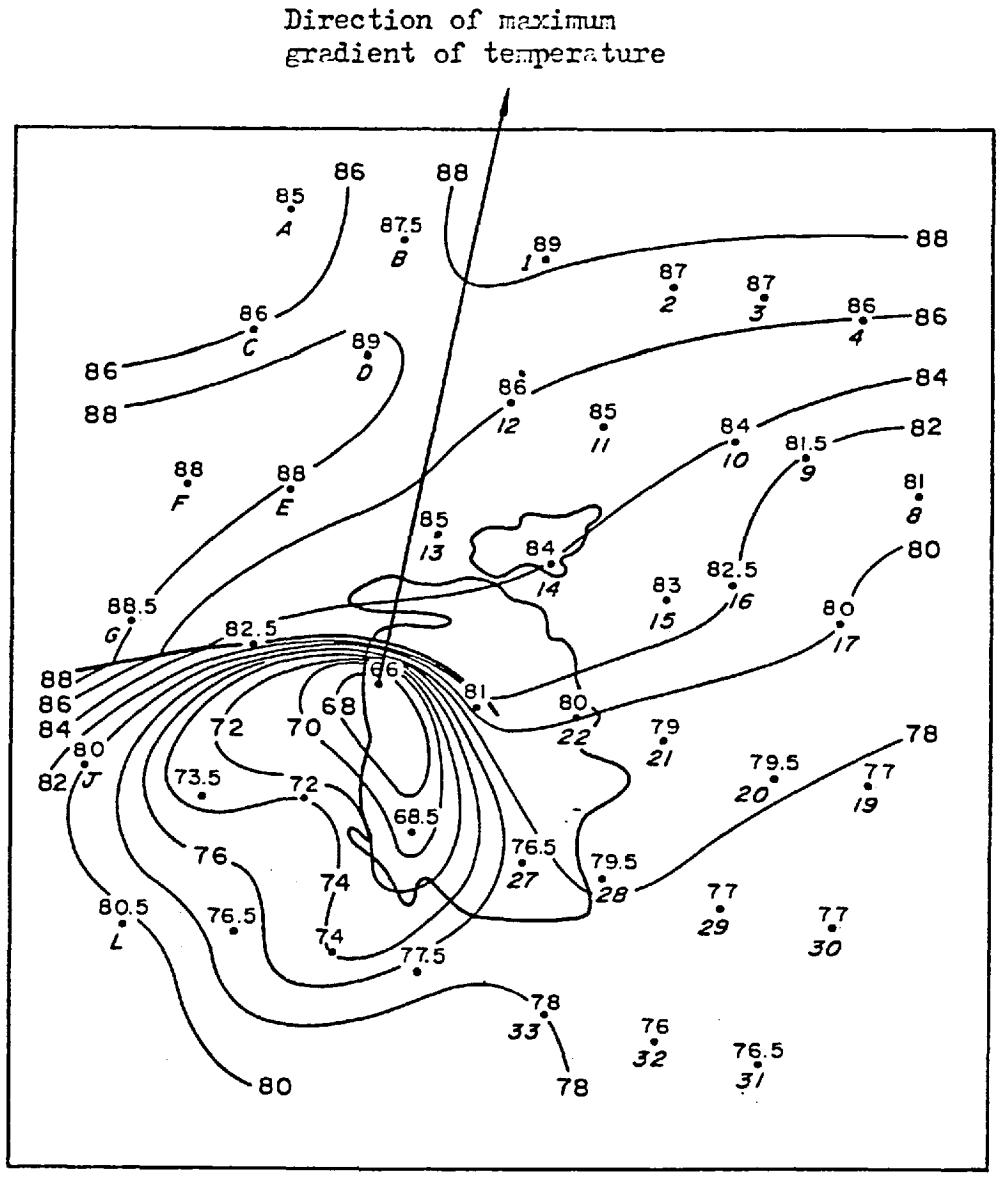

Figure 4.8.2 Temperature-isochrone-amplitude analysis of the Lawton Storm. The temperature drop line and the direction of maximum temperature gradient are shown. (from Hammond (1967))

4.12 discrete propagation of storm cells

The discrete propagation is a process not describable by the internal dynamics of circulation through individual convective cell, or the net circulation through the whole storm mass. It can, however, be inferred from the effects of the downdraught, which indicates the direction where further regeneration of convective cell should occur. It was discussed that this direction cannot be determined from a disorganised downdraught model.

The dynamics of the downdraught is determined by the shear, and the velocity profile in the tropical component direction. The region of maximum surface convergence is determined by the downdraught dynamics, hence the direction where new convective cells are encouraged to grow can be determined.

A precise value of the discrete propagation velocity cannot be determined. If the convective cells that made up the storm are assumed to be uniform in size and in spacing, and if the life time of the cell τ is also constant. Then the speed of discrete propagation is,

$$V_p = \frac{d}{\tau} \qquad (4.8)$$

where d = distance between cells.

For the typical cell size of 15 kilometres, and τ = 1 hour. $V_p = 4\ ms^{-1}$.

4.13 Case Studies

4.13.1 The Lawton Storm

The downdraught was found to propagate towards 140^{o}_{N} giving a

preferential growth region on the left of the mature convective cell. The cells were travelling at 18 ms^{-1} towards $40^{o}N$; and the generation rate was one cell per hour --- which gives a discrete propagation speed of 4 ms^{-1}. The predicted velocity of the storm mass is 18.4 ms^{-1} towards $27^{o}N.$, which compares favourably with the observed value of between 18.5 to 20 ms^{-1} towards $25^{o}N.$

4.13.2 The Wokingham Storm

The downdraught tended to propagate towards $50^{o}N.$, with respect to the low level flow, the prefered direction for further convection is to the right. The cells were travelling at 19 ms^{-1} towards $29^{o}N.$, with a discrete propagation speed of 4 ms^{-1} towards the right. The predicted storm velocity is 19.5 ms^{-1} towards $41^{o}N.$, which agrees with the observed value of 20 ms^{-1} towards $45^{o}N$.

4.13.3 The Rimbey Storm

There is a large directional difference between the convective cell propagation vector, and that of the downdraught --- 80^{o} to the right compared with about 20^{o} to the right in the Wokingham storm. The cells were travelling towards the left at 9.2 ms^{-1} towards $14^{o}N.$, the rate of generation of new cells was irregular. The lifetime of individual cells was about 30 minutes -- thus giving a large discrete propagation of 8 ms^{-1}. The predicted storm velocity is 12 ms^{-1} towards $57^{o}N.$ The observed value of the storm is 11 ms^{-1} towards 70^{o}_{N} .

4.13.4 The Horsham Storm

The velocity of the storm was traced on a radar screen for several hours. The reported velocity was that of the storm system. It is likely that during those hours, regeneration processes took place. If the cells were assumed to propagate with the predicted velocity given in 3.7.4, and the cells lasted an hour. The velocity of the storm is predicted to be 15 ms^{-1} towards $230^{o}N.$, which agrees with the observed value.

The comparison of observed and predicted speeds are shown in fig (4.9.1) and directions in figure (4.9.2). It can be seen that the comparison is within observational error.

Figure 4.9.1 Predicted speed and observed speed

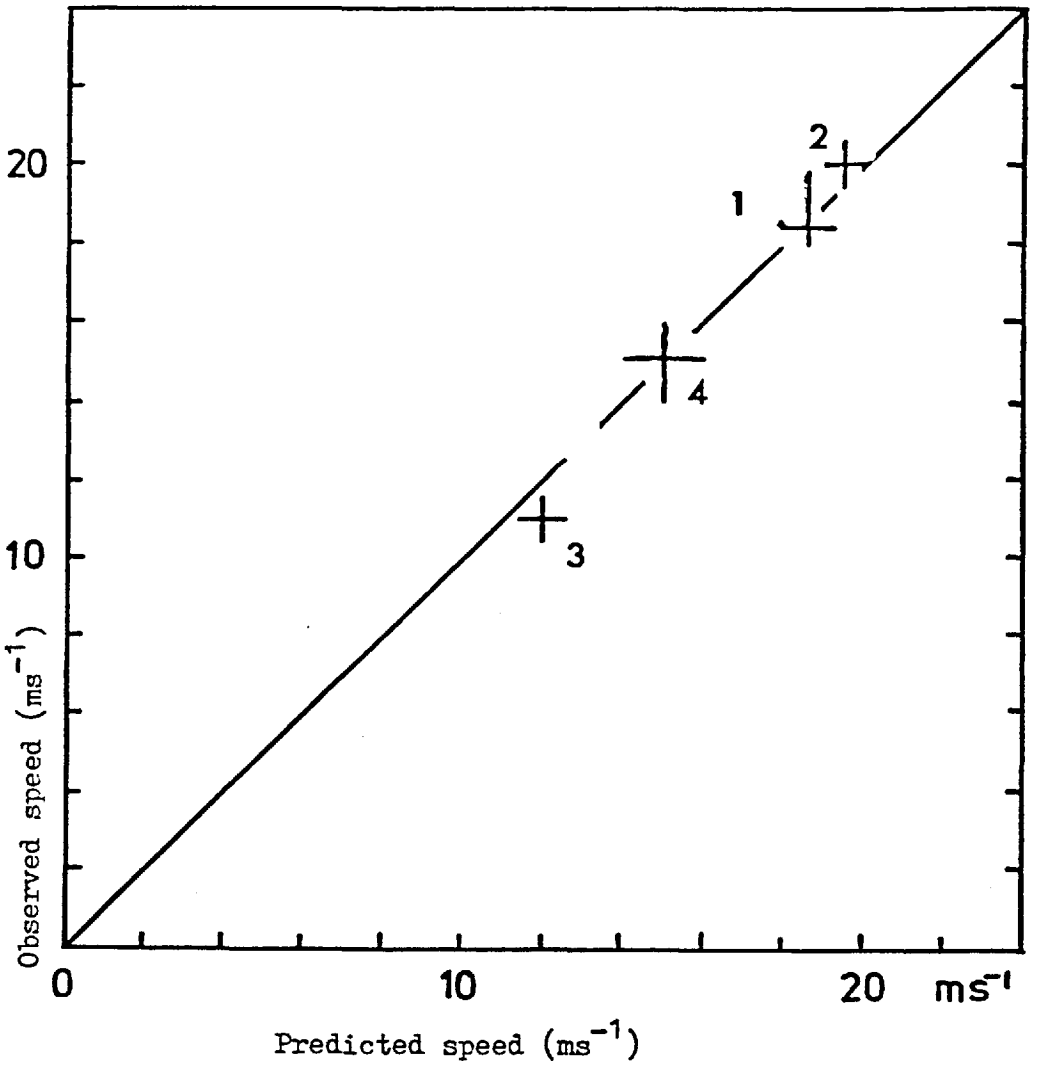

(1) The Lawton Storm
(2) The Rimbey Storm
(3) The Wokingham Storm
(4) The Horsham Storm.

Figure 4.9.2 Predicted direction and observed direction.

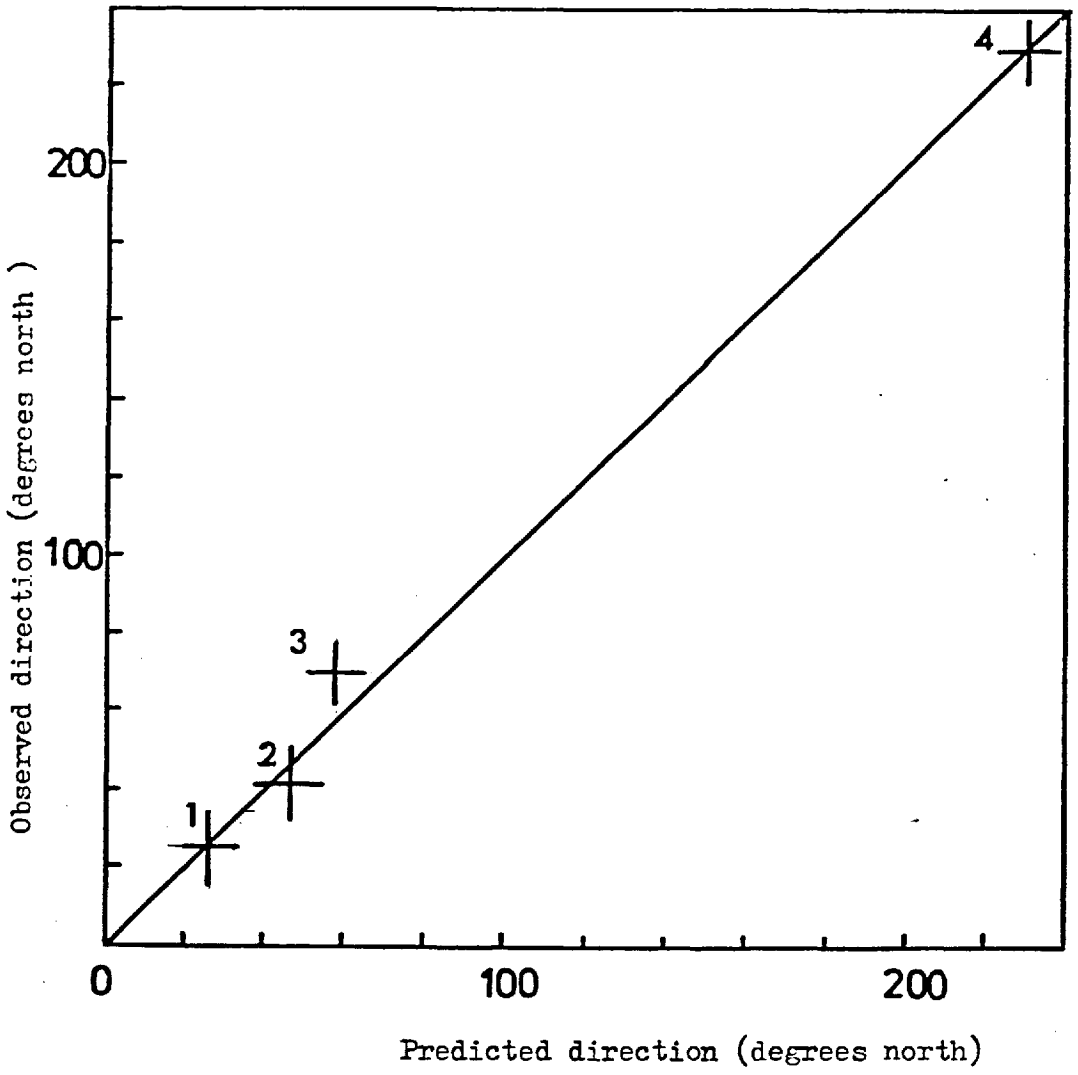

CHAPTER FIVE: PARAMETERISATION : A THREE-LAYER MODEL

5.1 INTRODUCTION : TURBULENCE.

Turbulence is a convenient word used to describe some scale of motion which cannot be precisely defined, moreover, it would not be useful to have a precise description because it would be too complicated. It is, therefore, difficult to find a definition which is universally applicable. One of the definitions is that turbulent motion is dispersive, just as it disperses smoke from a chimney; on occasions some complicated wave motions may have the appearance of turbulence but fail to disperse anything at all.

Lamb in his book "Hydrodynamics" in 1895 wrote that " Turbulence remains to call attention to the chief outstanding difficulty of our subject". This implies that someday, this "outstanding problem" would be fully understood and solved. However, it was realised that it took more than a lifetime to study the infinite details of the flow of one unique occasion which may not happen again when the experiment was carried out at a later time. More and more, we come to realise our limitation, and the degree of complexity of a system is chosen so that it is describable in terms of a mean flow plus a random motion. The random part of the motion is another definition of turbulence, it implies that it contains details which will not be enquired into.

In numerical models, motion with a space and a time scale smaller than twice the grid length and twice the integrating time step is not represented if there are several eddies, one very large and some small, then samples obtained from different parts of this big eddy would merely serve to review the shape of the big eddy, which would be seen as part of the mean motion. The small eddies, the scale of which is very

different from the sampling scale sort themselves into random fluctuations. The sampling scale is the grid length in the numerical model, eddies smaller than the grid scale are, therefore, turbulence.

In mesoscale models, turbulence is represented in a very much simplfied way, parameterized in terms of grid variables. The mixing length notions and K-theory are widely used, assuming the motions are truely random. Its application in molecular diffusion is very successful owing to the random movement of molecules. The objecive of this chapter is to represent the transfers of a steady deep convection as an organized structure.

5.1.1 Mathematical Representation Of Turbulence.

The quantities at any grid point can be expressed in terms of a mean quantity and a small randomly fluctuating quantity.

$$q = \bar{q} + q' \tag{5.1}$$

where q is any quantity, thus the three velocity components are express as :

$$\begin{aligned} u &= \bar{u} + u' \\ v &= \bar{v} + v' \\ w &= \bar{w} + w' \end{aligned} \tag{5.2}$$

where bar quantities denote mean values, and dash quantities denote random fluctuations.

The properties of this representation in particular the definition of the average demands that

$$\overline{q'} = 0 \tag{5.3}$$

it follows that

$$\bar{\bar{q}} = \bar{q} \tag{5.4}$$

and any odd power of q′ when averaged is zero.

From the momentum equation

$$\frac{D}{Dt}\underset{\sim}{v} + \text{grad}\frac{\delta p}{\rho} - g\delta\phi\,\underset{\sim}{k} = 0 \tag{5.5}$$

the equation can be separted into a mean and a fluctuating part, thus

$$\frac{D}{Dt}\bar{\underset{\sim}{v}} + \text{grad}\frac{\overline{\delta p}}{\rho} - g\overline{\delta\phi}\,\underset{\sim}{k} =$$

$$\frac{D}{Dt}\underset{\sim}{v}' + \underset{\sim}{v}'.\text{grad}(\bar{\underset{\sim}{v}}+\underset{\sim}{v}') + \text{grad}\frac{\delta p'}{\rho} - g\delta\phi'\,\underset{\sim}{k} \tag{5.6}$$

where

$$\frac{D}{Dt} = \bar{u}\frac{\partial}{\partial x} + \bar{v}\frac{\partial}{\partial y} + \bar{w}\frac{\partial}{\partial z} \tag{5.7}$$

multiply (5.6) with $\bar{\underset{\sim}{v}}$ vectorially and then average over space,

$$\frac{D}{Dt}\frac{1}{2}\bar{\underset{\sim}{v}}^2 + \bar{\underset{\sim}{v}}.\text{grad}\frac{\delta p}{\rho} - \bar{w}g\overline{\delta\phi} = -\bar{\underset{\sim}{v}}.\left(\underset{\sim}{v}'.\text{grad}\,\underset{\sim}{v}'\right) \tag{5.8}$$

$\underset{\sim}{v}'.\text{grad}(\underset{\sim}{v}')$ can be written as $\text{div}(\underset{\sim}{v}'\underset{\sim}{v}')$ which is a stress tensor. The term on the right hand side represents the work done by the stress on the large scale motion. Putting div v′ = 0, this term can be re-arranged into $\underset{\sim}{v}'\underset{\sim}{v}'.(\text{grad}\,\bar{\underset{\sim}{v}})$, in the atmosphere $\frac{\partial}{\partial x}$ and $\frac{\partial}{\partial y}$ of $v << \frac{\partial}{\partial z}v$. The term reduces to the familiar form of

$$u'w'\frac{d}{dz}\bar{u} + v'w'\frac{d}{dz}\bar{v} \tag{5.9}$$

which are the basic terms used in the mixing length and K-theory transfers of kinetic energy is limited to up and down gradient. If equation (5.8) is integrated across the grid volume, i.e. From x to x + Δx, from y to y + Δy, and from z to z + Δz.

$$\frac{\partial}{\partial t}\left\{\bar{K}\right\} + \bar{\underset{\sim}{v}}.\text{grad}\left\{\bar{K}\right\} + \left\{\bar{K}.\bar{P_m}\right\} - \left\{\bar{P}.\bar{K}\right\} = \left\{\kappa'.\bar{K}\right\} \tag{5.10}$$

where $\left\{\bar{K}\right\} = \iiint \frac{1}{2}\bar{\underset{\sim}{v}}^2\,dx\,dy\,dz$

the mean kinetic energy.

$$\{\bar{K}.\bar{P}_{re}\} = \iiint_{\Delta x\Delta y\Delta z} \bar{\underset{\sim}{v}}.\,\mathrm{grad}\,\frac{\overline{\delta p}}{\rho}\,dx\,dy\,dz$$

transfer of mean K.E. To pressure field.

$$\{\bar{P}.\bar{K}\} = \iiint_{\Delta x\Delta y\Delta z} g\bar{w}\,\overline{\delta\phi}\,dx\,dy\,dz$$

transfer of mean potential energy

to mean kinetic energy.

$$\{K'.\bar{K}\} = -\iiint_{\Delta x\Delta y\Delta z} \bar{\underset{\sim}{v}}.\,\overline{(\underset{\sim}{v}'.\,\mathrm{grad}\,\underset{\sim}{v}')}\,dx\,dy\,dz$$

transfer of turbulent kinetic energy

into large scale kinetic energy.

5.1.2 Turbulent Kinetic Energy

$\underset{\sim}{v}'$. Equation (5.7) and average

$$\frac{D}{Dt}\frac{1}{2}\overline{\underset{\sim}{v}'^2} + \overline{\underset{\sim}{v}'(\underset{\sim}{v}'.\mathrm{grad})\bar{\underset{\sim}{v}}} + \overline{\underset{\sim}{v}'.\mathrm{grad}\,\frac{\delta p}{\rho}'} - \overline{gw'\delta\phi'} = 0 \qquad (5.11)$$

integrate over a grid volume of$\Delta x,\Delta y,\Delta z$.

$$\frac{D}{Dt}\{K'\} + \{K'.\bar{K}\} + \{K'.P_{re}'\} - \{P'.K'\} = 0 \qquad (5.12)$$

where

$$\{K'\} = \iiint_{\Delta x\Delta y\Delta z} \frac{1}{2}\overline{\underset{\sim}{v}'^2}\,dx\,dy\,dz$$

total kinetic energy of motions with

The subgrid space scale.

$$\{K'.P_{re}'\} = \iiint_{\Delta x\Delta y\Delta z} \overline{\underset{\sim}{v}'.\,\mathrm{grad}\,\frac{\delta p}{\rho}'}\,dx\,dy\,dz$$

Work done by

The sub-grid eddies on pressure fields.

$$\{K'.P'\} = \iiint_{\Delta x \Delta y \Delta z} g\overline{w'\delta\phi'}\, dx\,dy\,dz$$

the conversion of sub-grid scale kinetic energy into sub-grid scale of temperature changes.

Figure (5.1.1) shows schematically the flows of energy between large and sub-grid scale motions. The sub-grid kinetic energy K' is supplied by means of the P box, and dissipates through the pressure and frictional boxes. The basic kinetic energy $\bar{K}$ receive energy from $\{K'.\bar{K}\}$ transformation and loses it through pressure and dissipation. A positive $\{K'.\bar{K}\}$ implies a transfer of kinetic energy from a small scale to a larger scale motion, a negative value indicates transfer in the other direction. Ramdom motions represented by the K-theory produces a downgradient transfer in which case, $\{K'.\bar{K}\}$ is negative. Deep convection in the presence of shear produces a positive $\{K'.\bar{K}\}$. Asai (1964) found that this is the case for small amplitude dry and moist convection; Ogura (1963) found similar results.

It is important to realise that the transports may not be of a diffusive type, and this is indicated by the organised nature of the cloud models. In this chapter, it is shown how these transports can be represented in a simplified three-layer model. Although it is oversimplified nevertheless it gives a method by which more complicated formula can be derived.

5.2 The Three-layer Model

The parameterisation scheme described is based on a three-layer model; the outflows in the mid-latitude circulation partition the transfer properties of the convection into three distinct regions. They correspond to the three regions in the three-layer model, with positive, zero, and negative transfers.

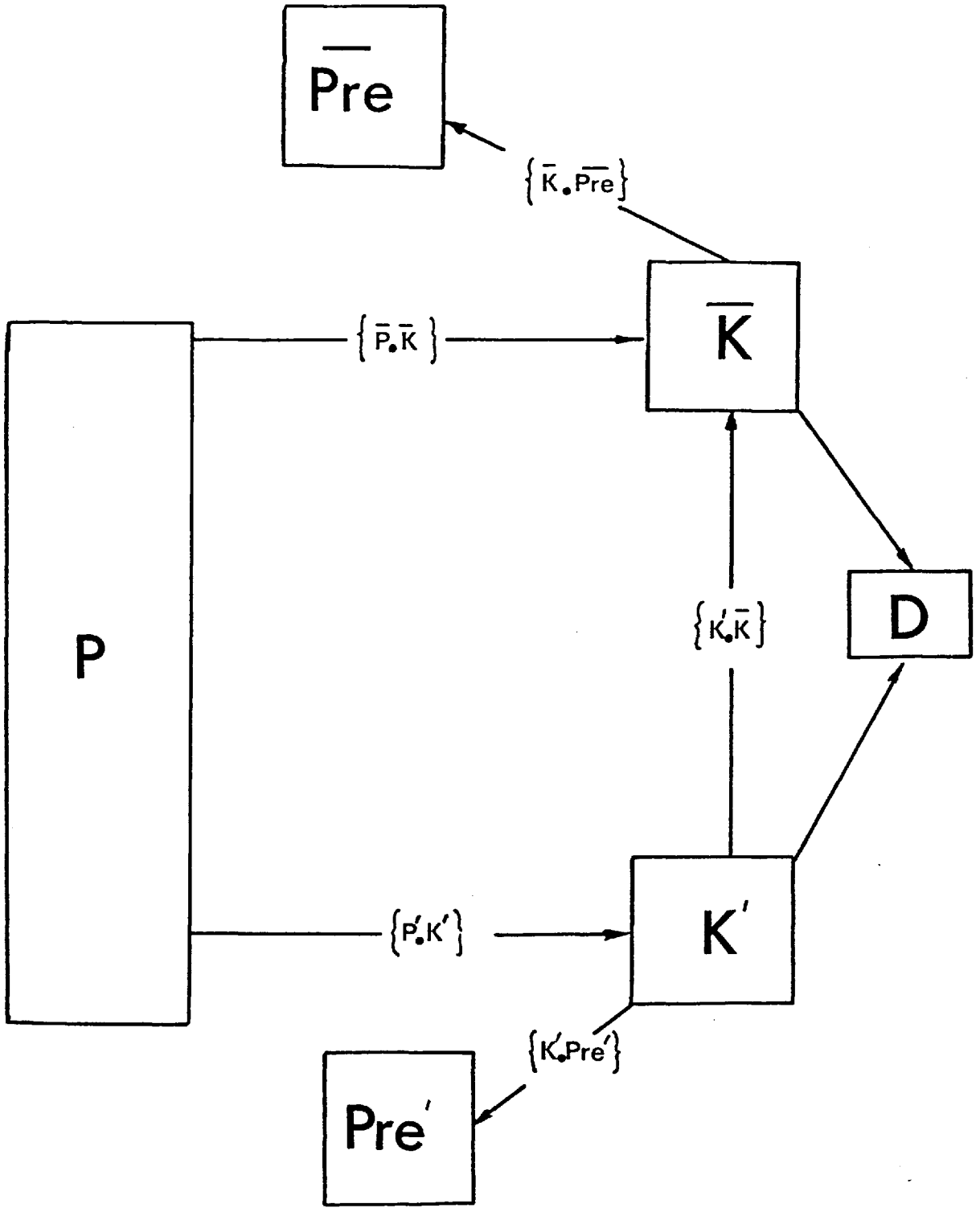

Figure 5.1.1 Energy flow diagram.

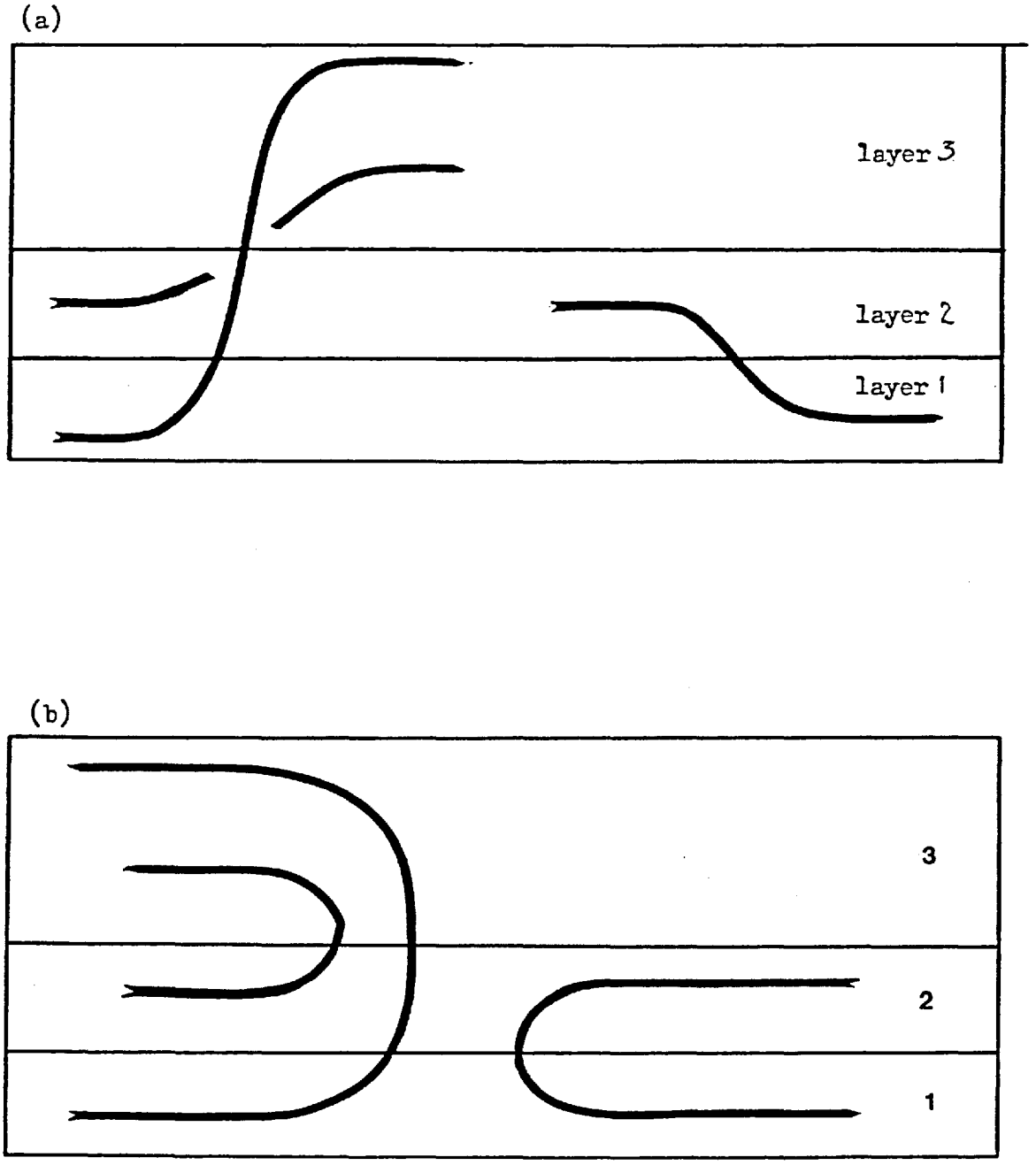

Figure 5.2.1 Schematic diagram showing the flow of fluxes in the three layers.

The updraught inflow originates from layer 1 and layer 2, and flows out into layer 3. The height that marks the boundary of layer 2 and 3 is determined by the steering level of the mid-latitude circulation of the updraught. The downdraught circulation occupies layer 1 and 2, with inflow originates at layer 2, and outflow into layer 1. The boundary between layer 1 and 2 is similarly determined by the height of the steering level of the mid-latitude circulation of the downdraught. Figure(5.2.1) depicts, schematically, the transfers resulting from the up and downdraught in the three-layer model.

In an incompressible atmosphere with a constant shear, linear hodograph, the transfers for both circulations can be obtained analytically. In the mid-latitude circulation, the outflow shear is enhanced. Figure (5.4.1). In the three layer model, it is represented as the total momentum transfer into the layer . The modifications of the atmosphere by the tropical component is similarly arranged into the three layers (figure (5.4.1)). The height and thickness of these layers are function of R_m; typically z_*=H/2, and z_{*d} = H/4.

The modifications are effected directly into layer 1 and 3, layer 2 is modified indirectly. This is a result of mass balance which occurs in a larger scale than the cumulonimbus convection. Layer 2 is altered through large scale subsidence, which leads to a warming; this is described in Miller and Betts (1976) who called this subsidence the system downdraught.

5.3 Equivalent Width : Closure For The Scheme.

The equivalent width of a convective system is a measure of the extensiveness of the convection.

The activities of deep convection are customarily represented by a cloud covered area ratio. It is a ratio of the cloud covered area to the area covered by a typical grid, and is usually assumed to be small, say 1 to 5 percent. It is used in the parameterisation model of deep convection when a plume type cloud model is used. The cross sectional area of the plume can be taken as the cloud covered area of the plume. It is worth noting that the area of cloud cover predicted from the boundary conditions in the plume type model bears no resemblance to the actual cloud covered area in the real atmosphere given that all conditions are the same. It is, however, a graphic term in describing the extensiveness of the convection.

In a cloud model which is made up of two-dimensional circulations as described in this thesis, the cloud covered area does not have the same importance as that of a plume type model. While a plume type cloud model uses the updraught variables explicitly, the two dimensional models are essentially a "black box" type model which deals with the updraught implicitly. For a system dominated by the processes of entrainment and detrainment, the updraught variables must be defined explicitly, since the atmosphere is modified through the process of turbulent mixing. In the case of severe, deep convection, the updraught and downdraught cores remain undiluted, turbulent mixing plays a minor role. The dynamical system as a whole is the dominant factor in effecting changes in the atmosphere. The extensiveness of convection can be defined from the amount of air taking part in the updraught or downdraught circulations.

An equivalent width, in the three layer model, measures the volume of air directly involved in the convection. A wider inflow ensures a

bigger mass of air taking part in the convection, a bigger cloud mass and a bigger cloud covered are assured.

5.3.1 Equivalent Width of the Updraught.

Convection derives its energy from the convective available potential energy due to the amount of heat and moisture present in the lower troposphere. The extent of the convection is controlled by the amount of moisture available to be taken into the cumulonimbus. Hence the equivalent width is related to the convective available potential energy and available moisture.

As a cumulonimbus propagates along, air in the lower troposphere with high moisture content is ingested into the updraught from which the energy for convection is released. A downdraught replaces the lower troposphere with air mass containing a lower dry and moist static energy; thus the air provided by the downdraught cannot take part in further convection without an injection of energy, until replenished by boundary layer fluxes of sensible and latent heat.

The moisture flux into the cumulonimbus is given by:

$$M_q = \int_{\Delta x}\int_{\Delta y}\int_{0}^{z} \mathrm{div}\left(\bar{\underset{\sim}{v}}\, q(z)\right)\, dx\, dy\, dz \qquad (5.13)$$

where Δx, Δy are the horizontal grid length and

$q(z)$ is the mean distributin of moisture in the vertical.

The extensiveness of convection depends on the available moisture for convection. The large scale convergence provides the initial forcing, thus it is a factor in controlling the extensiveness of convection.

For the case of a linear straight hodograph, the moisture flux can

be written in terms of the organised circulations as follows, and it defines the equivalent width L.

$$M_q = L_m \int q A (z_{*u} - z)\, dz + \int L_{t_d} C q \, dz \qquad (5.14)$$

where L_m = equivalent width of the mid-latitude circulation.

L_t = equivalent width of the tropical circulation.

C = propagating velocity of the tropical circulation.

The value of M_q would in principle be determined from the large scale model equations.

5.3.2 Vertical Profile of Equivalent Width.

The amount of CAPE available to the two circulations are the same by the principle of equipartition of energy described previously. One of the implied conditions is that the mass flux into the two circulations is the same also. This arises because the same parcel of air is taking part in both circulations.

The mass flux into the mid-latitude circulation is

$$= L_{mu} A(z_{*u} - z)) \qquad (5.15)$$

The mass flux into the tropical circulation is

$$= L_{tu} C \qquad (5.16)$$

For the two mass flux to be equal, L_t is a function of z.

$$L_{t_u} = L_{m_u} \frac{A}{C} (z_{*u} - z) \qquad (5.17)$$

if L_m is a constant, L_t is a linear function of z. Thus the extensiveness of the storm can be expressed as a function of L_m only, and it can be defined as

$$M_q = 2\int_0^{z_{*u}} L_{mu} A \left(z_{*u} - z\right) q \, dz \qquad (5.18)$$

5.3.3. Equivalent Width Of Downdraught L_d

The mass flux into the downdraught circulation is

$$2\int_{z_{*d}}^{z_{*u}} L_{md} A \left(z - z_{*d}\right) dz \qquad (5.19)$$

The intensity of the updraught and downdraught are similar; this means that there is a cloud scale mass balance as opposed to the large scale subsidence required by the plume model. The downdraught can be thought of as compensatory mass balance in the scale of the culumonimbus. The mass flux in layer 1 is thus balance by the updraught and downdraught. Thus from the two previous equations and for L_m to be a constant,

$$L_{mu} = \varepsilon L_{md} \qquad (5.20)$$

where

$$\varepsilon = \frac{\int_0^{z_{*d}} \left(z_{*u} - z\right) dz}{\int_{z_{*d}}^{z_{*u}} \left(z - z_{*d}\right) dz} \qquad (5.21)$$

ε is the ratio of the areas of the upper and lower part of a segmented triangle.

It can be expressed in terms of β only.

$$\varepsilon = \frac{1 + 2\beta_d}{\beta_d^2} \qquad (5.22)$$

Since β_d is always bigger than 1, $\varepsilon > 1$. For example, when $R_m = 1$, $\varepsilon = 1.6$. Schematic diagrams showing the two circulations with the above considerations are presented in figure (5.3.1) and (5.3.2).

5.4 Transfers

The transfer properties of the convection is discussed in three separate regions in the three layers.

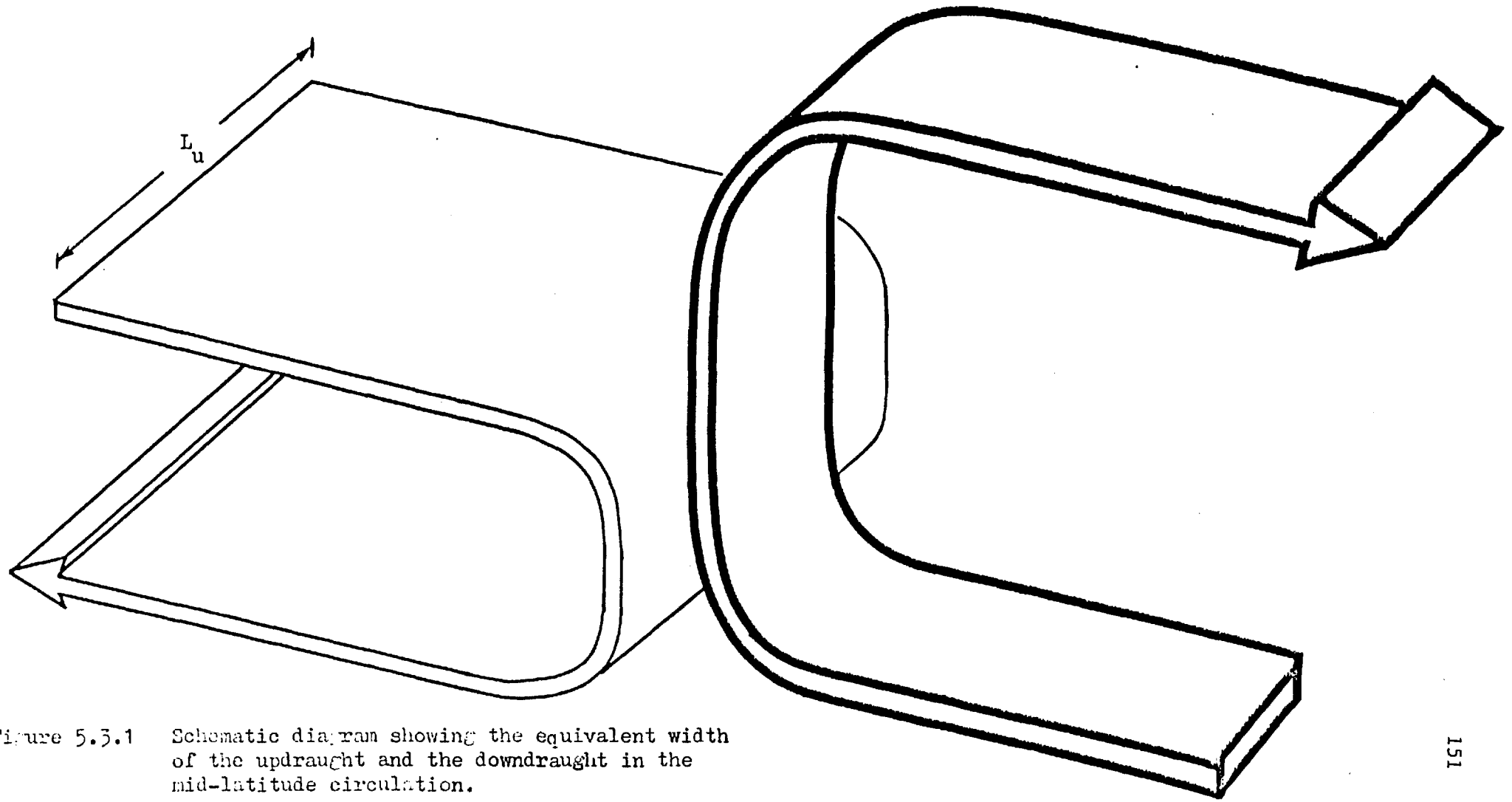

Figure 5.3.1 Schematic diagram showing the equivalent width of the updraught and the downdraught in the mid-latitude circulation.

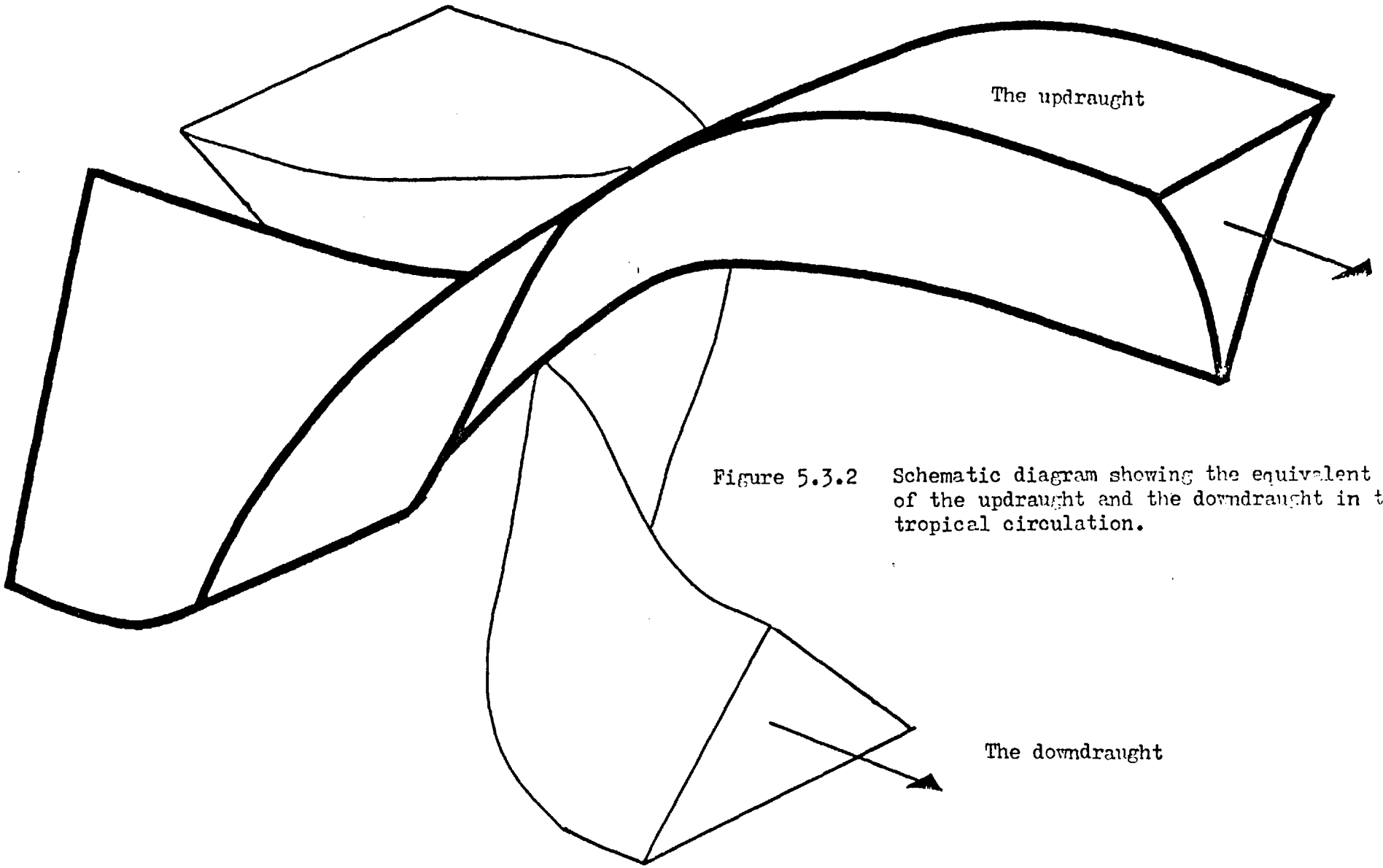

Figure 5.3.2 Schematic diagram showing the equivalent width of the updraught and the downdraught in the tropical circulation.

5.4.1 Momentum Transfers

5.4.1.1 Layer Three: Mid-latitude Component.

The outflow profile of velocity is

$$u_3 = \beta_u^2 A (z - z_{*u}) \tag{5.23}$$

therefore the momentum transfer is

$$\int_{z_{*u}}^{H} \rho L_{m_u} (u_3 - u_1)^2 = \rho \frac{A^2 H^3}{3} \frac{(\beta_u - 1)(\beta_u^2 + 1)}{(1 + \beta_u)^2} L_{m_u} \tag{5.24}$$

Tropical Component.

The velocity outflow profile is

$$V_3 = C_u \left(2 - \cosh \frac{\lambda_3}{C_u}\right) \int (CAPE) \tag{5.25}$$

where

$$C_u \left[\ln\left(\frac{1}{C_u}\left(1 + \sqrt{(1 + C_u)}\right)\right)\right] = \frac{2}{3 + \sqrt{(1 + 2R_{m_u})}} \tag{5.26}$$

momentum flux is

$$\rho A^2 H^3 C_u^4 \sqrt{R_{m_u}} \int_0^{\alpha} \left(2 - \cosh \frac{\lambda_3}{C_u}\right)^2 \left(\lambda_3 - C_u \sinh \frac{\lambda_3}{C_u}\right) d\lambda_3 \tag{5.27}$$

A discontinuity in the outflow velocity profile in the tropical component does not show up in the momentum flux profile since the mass flux at the point of discontinuity is zero. It can be shown that

$$= A^2 H^3 L_{m_u} C_u^2 \sqrt{R_{m_u}} \, \sigma_u$$

where $$\sigma_u = \frac{1}{4}(9\alpha^2 + 7) - 4\alpha + \frac{1}{2}\alpha \cosh \frac{\alpha}{C_u} - \frac{1}{3} C_u \left(\cosh^3 \frac{\alpha}{C_u} - 1\right) \tag{5.28}$$

The fluxes of momentum transfered by the two circulations are illustrated in figure (5.4.2). The contributions from the mid-latitude component is larger than that of the tropical component. This is due to the outflow characteristics of the latter. It transfer positive momentum flux to the lower part of layer 3, and a negative flux to the

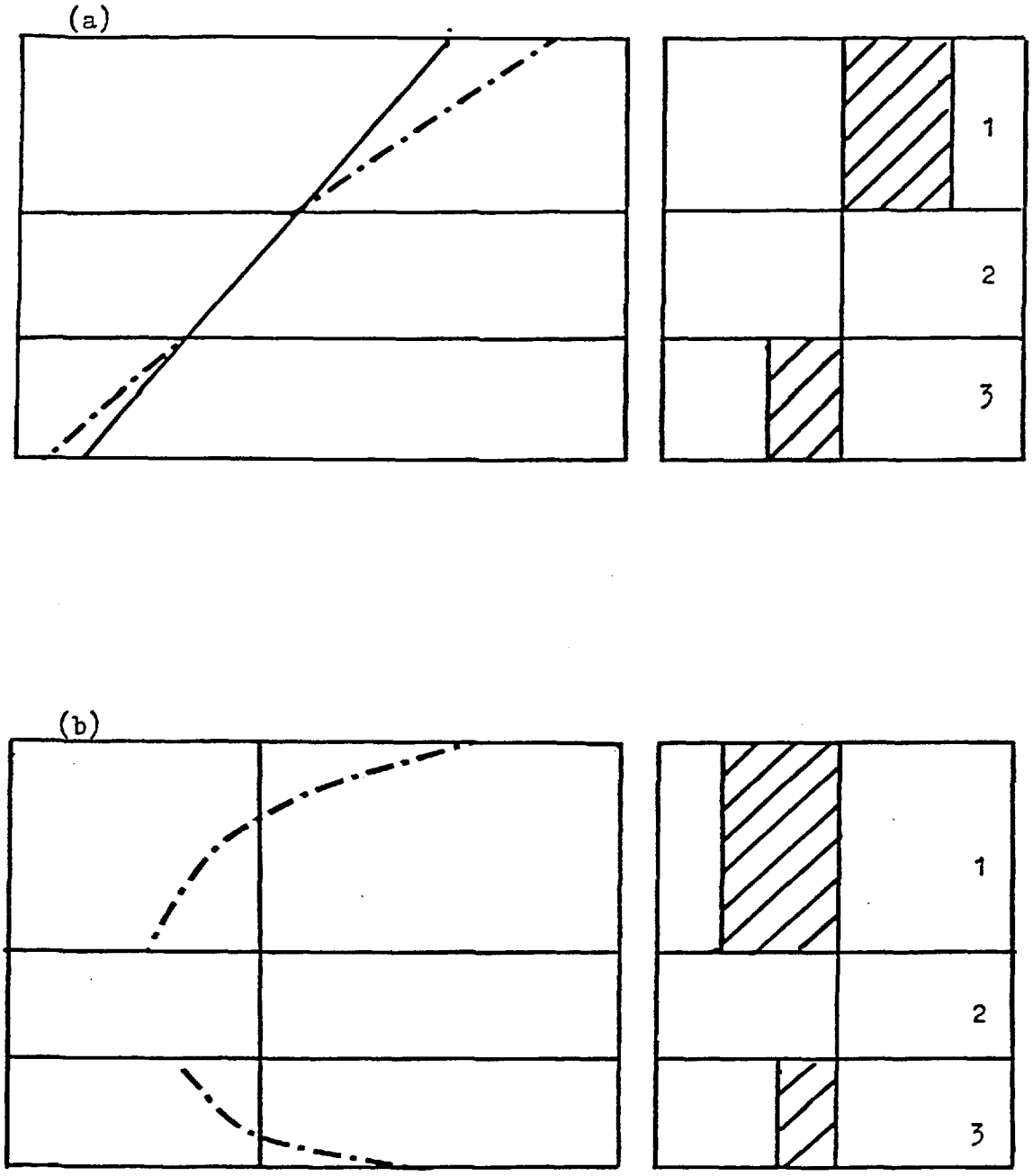

Figure 5.4.1 Schematic diagram showing the representation of momentum fluxes in the three layers , (a) due to the mid-latitude circulation , and (b) due to the tropical circulation.

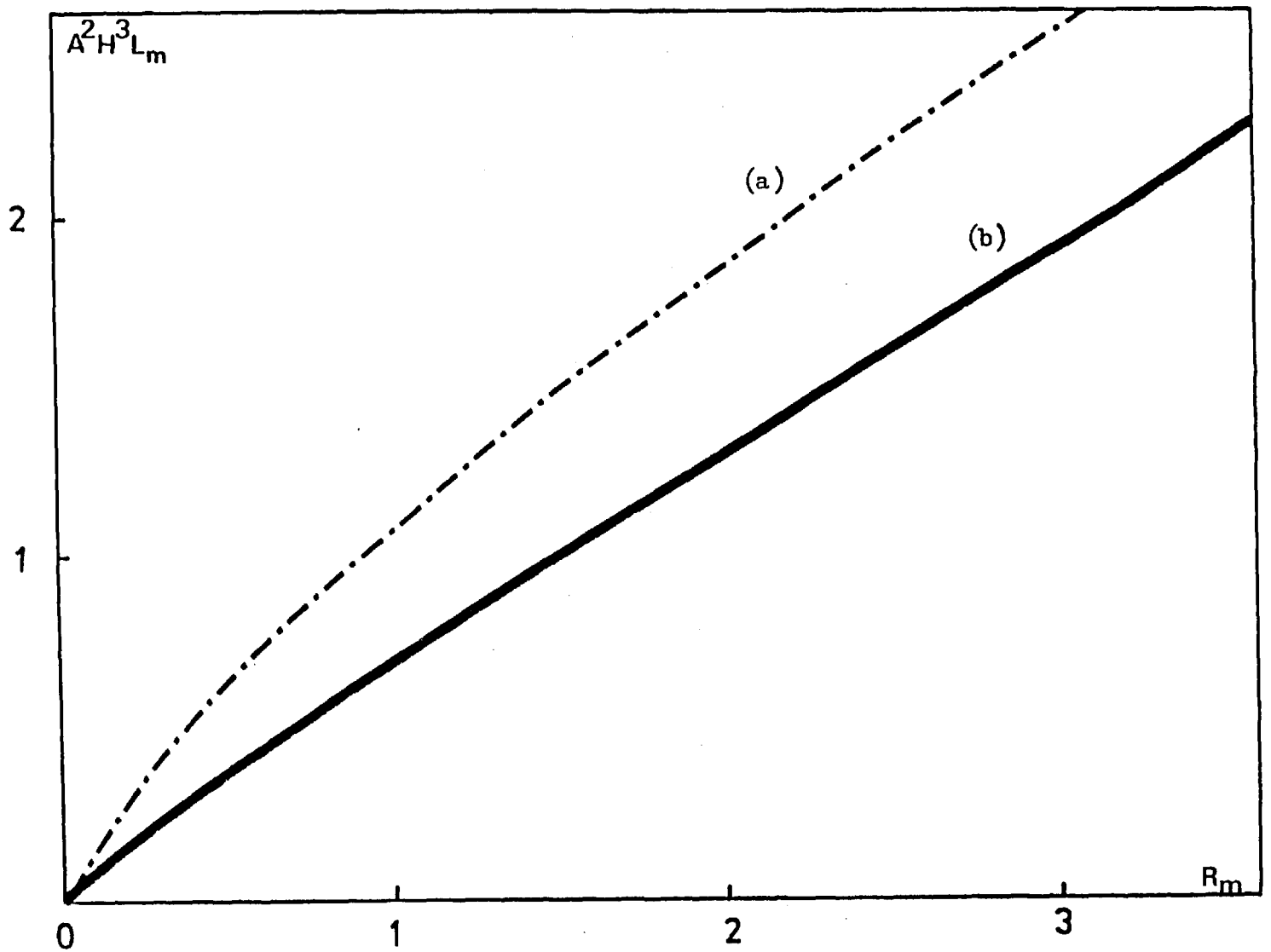

Figure 5.4.2 Schematic diagram showing the flow of fluxes in the three layers, (a) due to tropical circulation and (b) due to mid-latitude circulation.

top part. Thus the integrated flux in the layer is reduced. The magnitude of the two contributions from the two components is similar.

5.4.1.2 Layer Two

There is no net transfer of momentum.

5.4.1.3 Layer One: Mid-latitude Component.

The outflow profile is

$$M_{3_d} = -\beta_d^2 A \left(z_{*_d} - z\right) \tag{5.29}$$

thus the momentum transfer into this layer is

$$= -\frac{1}{3}\rho A^2 H^3 L_{m_d} \frac{\beta_d^4 - 1}{(1+\beta_d)^3} \frac{\beta_u^3}{(1+\beta_u)^3} \tag{5.30}$$

Tropical Component.

The problem is symmetrical, thus the function derived for the updraught is applicable here, except for the change of updraught constant into downdraught constants.

$$A^2 H^3 L_{m_d} C_d \sqrt{R_{m_u}}\ \sigma_d \tag{5.31}$$

The updraught and downdraught in the tropical component increases momentum at the top and bottom of the troposphere , the changes being of the same sign in contrast with the changes introduced by the mid-latitude component which is of the opposite sign, figure (5.4.1).

5.4.2 Entropy Flux

5.4.2.1 Layer Three: Mid-latitude Component

The entropy profile is integrated across the whole layer.

$$C_p \int \rho(\gamma - B)(z - z_{*_u})\, \beta_u^2 A\, (z - z_{*_u})\, L_{m_u}\, dz$$

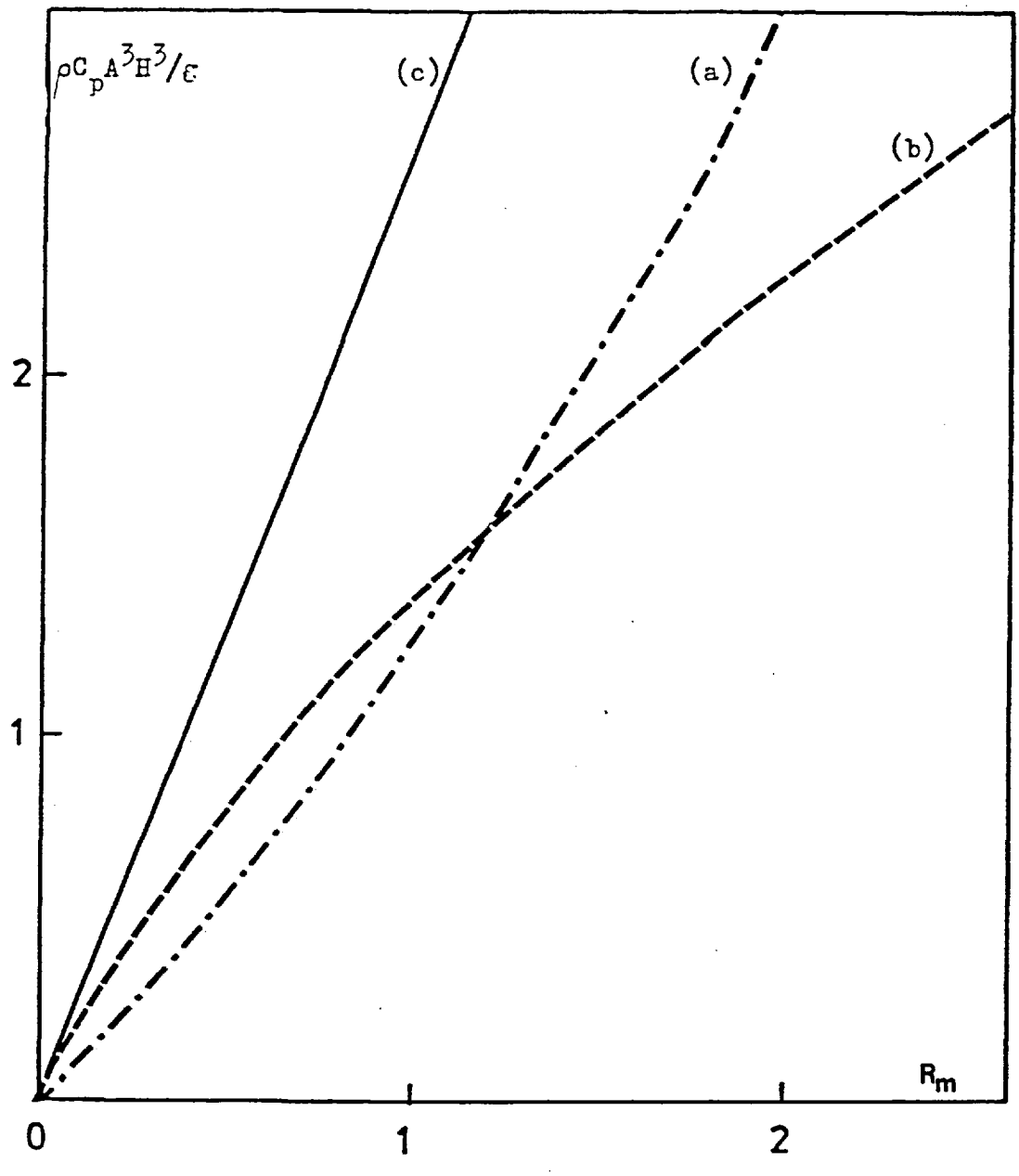

Figure 5.4.3 Entropy fluxes as a function of R_m.
(a) Flux from the mid-latitude circulation.
(b) Flux from the tropical circulation.
(c) Total flux from (a) and (b).

$$= \frac{1}{3}\frac{\rho C_p A^3 H^3}{g} L_{m_u} \frac{\beta_u^2}{(1+\beta_u)^2} R_{m_u} \qquad (5.32)$$

Tropical Component.

$$C_u H^2 \int (CAPE)\, \rho C_p (\delta - \bar{\theta}) \int L_{t_u}(\lambda_3 - \lambda_1)\left(2 - \cosh\frac{\lambda_1}{C_u}\right) d\lambda,$$

$$= \frac{\rho C_p A^3 H^3}{g} L_{m_u} R_{m_u} \left\{\left(\frac{15}{2}\ln(2+\sqrt{3}) - \frac{11\sqrt{3}}{2}\right)C_u^3 + 2C_u^2(1-\alpha_u) + \frac{\alpha_u}{4}(1+2C_u^2) + \frac{C_u}{3}\left[\frac{3}{4} - 2\alpha_u\right]\sqrt{1+C_u^2}\right\} \qquad (5.33)$$

The term inside the bracket can be approximated to $0.93C_u$ with less than 1 percent error throughout the whole range of R_m and C_u encounted. Thus the entropy flux is

$$= .93 \frac{\rho C_p}{g} C_u \int (R_{m_u})\, A^3 H^3 L_{m_u} \qquad (5.34)$$

The fluxes of the two circultion are of the same magnitude, figure (5.4.3). It can be seen that while the rate of change of entropy flux of the mid-latitude circulation is increasing with R_m, the opposite is true for the tropical circulation. Their sum total can be described by a linear relationship with R_m.

$$\text{Entropy flux into layer 3} = .27 R_{m_u} \frac{\rho C_p A^3 H^3}{g} L_{m_u} \qquad (5.35).$$

5.4.2.2 Entropy Flux Into Layer 1

Mid-latitide Component.

Similar to the updraught, we have

$$-\frac{1}{3}\frac{\rho C_p A^3 H^3}{g} L_{m_d} \frac{\beta_d^2}{(1+\beta_d)^2} \frac{\beta_u^3}{(1+\beta_u)^3} \qquad (5.36)$$

Tropical Component

The problem is symmetrical for the updraught and the downdraught, using the result derived for the updraught.

$$-.93 \frac{\rho C_p}{g} C_u \int (R_{m_d})\, A^3 H^3 L_{m_d} \qquad (5.37)$$

The sum of entropy flux into layer one is

$$-.27\, R_{m_d} \frac{\rho C_p A^3 H^3}{g} \left(\frac{\beta_u}{1+\beta_u}\right)^3 \varepsilon L_{m_u} \qquad (5.38)$$

It is less than the entropy flux into layer 3 when $R_{mu} = R_{md}$, the flux of entropy into layer 3 is four times that of the flux into layer 1.

5.4.3 Moisture Fluxes

The moisture budget is balanced assuming that there is no precipitation. Precipitation efficiency is a ratio of amount of water precipitated as compare to the amount of water vapour taken into the updraught. It is found to be small, around 10 to 20 percent, indicating either a very efficient transfer of water into the downdraught, thus the cumulonimbus is able to maintain a strong downdraught. Or, a very large moisture flux into the top layer of the troposphere. In view of the low temperature at the top of the troposphere, it is more likely that most of the water content is transfered to the downdraught.

As a parcel descend from a height z_3 to z_1. The change in dry static energy is

$$\rho C_p \theta_3 - \rho C_p (1+\delta\phi)\theta_1 \qquad (5.39)$$

which is proportional to the amount of water absorbed. Thus the total amount of moisture taken into the downdraught is

$$\frac{1}{L_v} \int \rho C_p \left\{(\theta_3 - \theta_1) - \delta\phi\theta_1\right\} v\, dz \qquad (5.40)$$

θ_3 and θ_1 are in general a complicated function of z. The integral can be simplified if the potential temperature in each layer is considered as a constant, that is a layer average.

The first term in the previous equation is the product of the difference

in dry static energy and the mass flux into layer 1, while the second term is proportional to the entropy flux into layer 1.

$$M_{q_d} = \rho C_p A H^2 \varepsilon L_{m_u} \left\{ (\bar{\theta}_2 - \bar{\theta}_1) \frac{\beta_d^2}{(1+\beta_d)^2} + \frac{\bar{\theta}_1 A^2 H}{g} (.27 R_{m_2}) \frac{\beta_u}{1+\beta_u} \right\} \left(\frac{\beta_u}{1+\beta_u} \right)^2 \quad (5.41)$$

5.4.3.1 Moisture Flux Into Layer 1 (M_{q_1})

It is due to the moisture contained in the inflow air with moisture evaporated into the downdraught subtracted from it.

$$M_{q_1} = 2L_{m_d} \int_{z_{*d}}^{z_{*u}} v \rho_a \, dz + M_{q_d} - 2 \int_0^{z_{*d}} L_{m_u} A (z_{*u} - z) \rho_a \, dz \quad (5.42)$$

5.4.3.2 Layer 2 (M_{q_2})

It is the total moisture taken into the updraught and downdraught.

$$M_{q_2} = 2L_{m_u} (1+\varepsilon) \int_{z_{*d}}^{z_{*u}} u \rho_a \, dz \quad (5.43)$$

5.4.3.3 Layer 3

$$M_{q_3} = \int_0^{z_{*u}} 2L_{m_u} u \rho_a \, dz - M_{q_d} \quad (5.44)$$

5.5 Modification in the Region of Influence.

Cumulonimbus convection can be thought of as being made up of two regions: A region of active convection which is occupied by the updraught and downdraught; and the region of influence. In the active convective region, mass fluxes are balanced at certain levels only: in the levels at which updraught and downdraught co-exist together. In layer 1, the mass flux is balanced within the active convective region.

At layer 3, there is only an updraught outflow, so there is a net mass flux into layer 3 within the convective region. The overall mass flux is balanced over the area affected by the cumulonimbus convection.

The region of influence is a mechanism to balance mass flux by subsidence. The result of this forced subsidence is a warming and drying in the region.

If the rate of subsidence = w , $\bar{A}$ is the area of the region of influence, and M(z) the mass of flux out of the active convective region. Then

$$\rho \bar{A} w = \int_z^H M(z)\, dz \qquad (5.45)$$

The entropy flux across an area at the level z is

$$\rho \bar{A} w \, \delta\phi$$

but $$\delta\phi = B \int w \, dt$$

The area of the region of influence surrounding the active convective region is not of a static nature. The propagating nature of the cumulonimbus means that the material within the region of influence is renewed continuously. Thus

$$= \rho \bar{A} B \, w \int w \, dz$$

$$= \rho \bar{A} B \, w^2 \Delta\tau \qquad (5.46)$$

where $\Delta\tau$ represents the time period through which the cumulonimbus had its region of influence renewed.

It is expected that in this region,the modification is different, there is a continuous warming of the troposphere from the top to z_* .

The entropy fluxes through any level is

$$\Delta\tau \, \rho \bar{A} B w^2 \qquad (5.47)$$

Thus the entropy flux into layer 2 is

$$\frac{4A^2H^4}{\bar{A}} \frac{\beta_u^4}{(1+\beta_u)^4} L_m^2 B \Delta z \qquad (5.48)$$

5.6 Concluding Remarks

The transfers are functions of R_m and A, both of which can be determined from large scale variables. Putting R_m = 1 and A = $0.003s^{-1}$, the momentum flux F_m, is of order A^2H^2, = $900 kgm^{-1}s^{-2}$. The corresponding entropy transfer, F_h, is $300 kg°C^{-1}s^{-3}$.

These fluxes can be expressed in the familiar form

$$F_m = -\rho K_m A \quad \text{and} \quad F_h = -\rho C_p K_h \frac{d\theta}{dz}$$

where K_m and K_h are transfer coefficients. They can be calculated from values of R_m and A. Using the above values of R_m and A, $K_m = 10^5 m^2 s^{-1}$ which is four order of magnitude bigger than the typical value of turbulent eddy transfers near the ground. The value of K_h is of order $10^5 kg s^{-1} J g°C^{-1}$ which is four order of magnitude larger than those of shallow cumulus convection. These high values of transfer coefficient highlight the importance of cumulonimbus transfers in a numerical global circulation model.

CHAPTER 6: CONCLUDING REMARKS

Considerable simplification on the mathematical treatment of a 3-dimensional cumulonimbus circulation is achieved through the approximation that a three-dimensional circulation can be represented by two orthogonal 2-dimensional circulations. This approximation is applicable when the time scale of the flow is much smaller than that given by the vertical component of vorticity. This is found to be the case from numerical studies. From observational and numerical studies, the two 2-dimensional circulations are the mid-latitude and the tropical circulation it leads to an analytic three-dimensional circulation model.

Experiments on the behaviour of the two 2-dimensional circulations on a variety of velocity profiles were carried out. These profiles were gentle deviation from a constant shear profile and low level jet profiles in the mid-latitude circulation; a parabolic profile and low level jet profiles in the tropical circulation. These profiles are common features exhibited in the wind field of an environment in which a severe organised circulation develops. The parabolic profile corresponds to a clockwise or anti-clockwise turning of the hodograph. The low level jet profile resembles the wind profiles in the Centenial, the Rimbey and the Wokingham storm. The results of these experiments showed that in the mid-latitude circulation, the steering level (hence the propagation speed) is raised when the profile deviates from the constant shear profile. However, this is found to be small when a realistic deviation from the constant shear profile is considered. The effect of positive and negative deviations on the steering level is similar, though the

resultant outflow profiles are quite different.

In the tropical circulation, a deviation from the constant velocity profile changes the propagation speed in a linear manner. Thus, a positive jet causes the speed of the tropical circulation to increase, and vice versa. In both circulations, the effect of density stratification (D) is to reduce the propagation speed of the circulation. In the mid-latitude circulation, the steering level decreases linearly with D. While in the tropical circulation, the relations is described by a power law.

A 3-dimensional circulation can be thought of as being a vector sum of these two 2-dimensional circulations. The propagation velocity of the cell is thus a vector sum of the mid-latitude and the tropical circulation. The good agreement between observed and predicted velocities suggests that the approximation is valid.

The deviatory nature of cell propagation is due to the propagation of the tropical component. Its velocity depends on the velocity profile in that plane. One particular result is that in an environment in which the wind hodograph turns clockwise with height, a right-moving cell is favoured. And when the hodograph turns anti-clockwise with height, a left-moving cell is preferred. Klemp and Wilhemson (1978) obtained similar results in their numerical simulation of convection. In general, however, the direction of deviatory motion is determined by the velocity profile in the plane of the tropical circulation.

The velocity of a storm mass is made up of two factors --- the propagation velocity of its constituent cells, and an apparent motion

due to the generation and decay of cells at opposite flanks. The latter is due to the interaction between the downdraught outflow with the low level flow. Evidence suggests that a downdraught is a dynamically dominant circulation, therefore it tends to propagate towards a different direction from that of the updraught. If the downdraught tends to propagate towards the left of the cell, a leftward discrete propagation would result, and visa versa. Correct directions of discrete propagation and realistic storm velocities were predicted.

The concept of a 3-dimensional circulation being a composite effect of the mid-latitude and the tropical circulation is applied to the parameterisation of cumulonimbus transfer in the form of a 3-layer model. The mid-latitude circulation is found to enhance the mean shear. The tropical component transfers positive momentum to the top and bottom layers. Both circulation cause a warming in the top layer, and a cooling in the bottom layer.

The transfers effected by organised cumulonimbus is many order of magnitude bigger than those of shallow cumulus and turbulent eddies near the ground. It highlights the importance of cumulonimbus in the numerical global circulation model. The three-layer parameterisation model can be generalised to include the effect of density stratification. The calculation is more complicated, however, a basic three-layer structure is maintained. Since on can obtain a continuous function of transfers from the cloud model, a parameterisation scheme with any number of layers can be derived.

The infrequent occurence of severe storms implies that there are many conditions the ambient environment has to satisfy before an

intense severe storm can develop. These constraints can be expressed as a set of rules with which meteorologists can predict the occurence likelyhood, the severity and the area affected by the storm. One such constraint is R_m. It is found to be small in the cases studied here, and in studies of severe storms in the Arabian gulf and in India. The severity of the predicted storm can be inferred from the difference in propagation directions between the updraught and downdraught.

APPENDIX

CONVECTIVE AVAILABLE POTENTIAL ENERGY

The simple definition of the convective available potential energy involved in the overturning in cumulonimbus is by the parcel theory of convection; in which small volume of air is considered to rise adiabatically through an undisturbed environment with the conversion of potential energy into kinetic energy through the release of latent heat and buoyancy forces. At the core of the updraught, this simple definition of convective available potential energy is sufficient since the parcel inside the updraught ascend wet adiabatically, and mixing with environmental air is negligible.

It can be defined as

$$\int_{l.c.l.}^{H} g\,\delta\,\phi\,dz \qquad (a.1)$$

Where l.c.l. Is the lifting condensation level, and H is the height of the equilibrium level.

This integral can be evaluated by measuring the area enclosed by the parcel lapse rate curve and the environmental temperature profile on a tephi-gram. The value of CAPE is proportional to that area. This method can be tedious. A mathematically method is described below.

Equation of states:

$$TdS = dE + PdV \qquad (a.2)$$

which can be written as

$$c_p \delta T - \frac{\delta P}{\rho} + L \delta r = 0 \qquad \text{(a.3)}$$

Where L = latent heat

r = mass of water vapour in a unit mass of air.

From the definition of , equation (a.3) can be written as:

$$c_p \delta \theta + \frac{\theta}{T} L \delta r = 0 \qquad \text{(a.4)}$$

It forms the basic definition of equivalent potential temperature when the above equation is expressed in the substantial derivative form. Rewrite equation (a.4)

$$C_p \frac{d}{dX}\theta + \frac{X_o}{X}\frac{d}{dX} r = 0 \qquad \text{(a.5)}$$

Where $X = P^{\gamma}$

$X_o = P_o^{\gamma}$

$\gamma = C_p - C_v / C_v = 0.285$

After integration between two pressure levels : 1 and 0

$$C_p X_1 \theta_1 - \int_o^1 C_p \theta \, dX + L X_o r_1 = C_p X_o \theta_o + L X_o r_o = H_o \qquad \text{(a.6)}$$

Where subscripts 0 and 1 denote the values of the respective variables at level 1 and 0. H_o is the pressure weighted moist static energy (pwmse) of the parcel.

Equation (a.6) showed that the location at which the latent heat of vaporization is released affects the final value of potential temprature attained by the parcel. It is best explained in an energy-pressure (E-X) diagram, (figure(a.1)). It consists of two

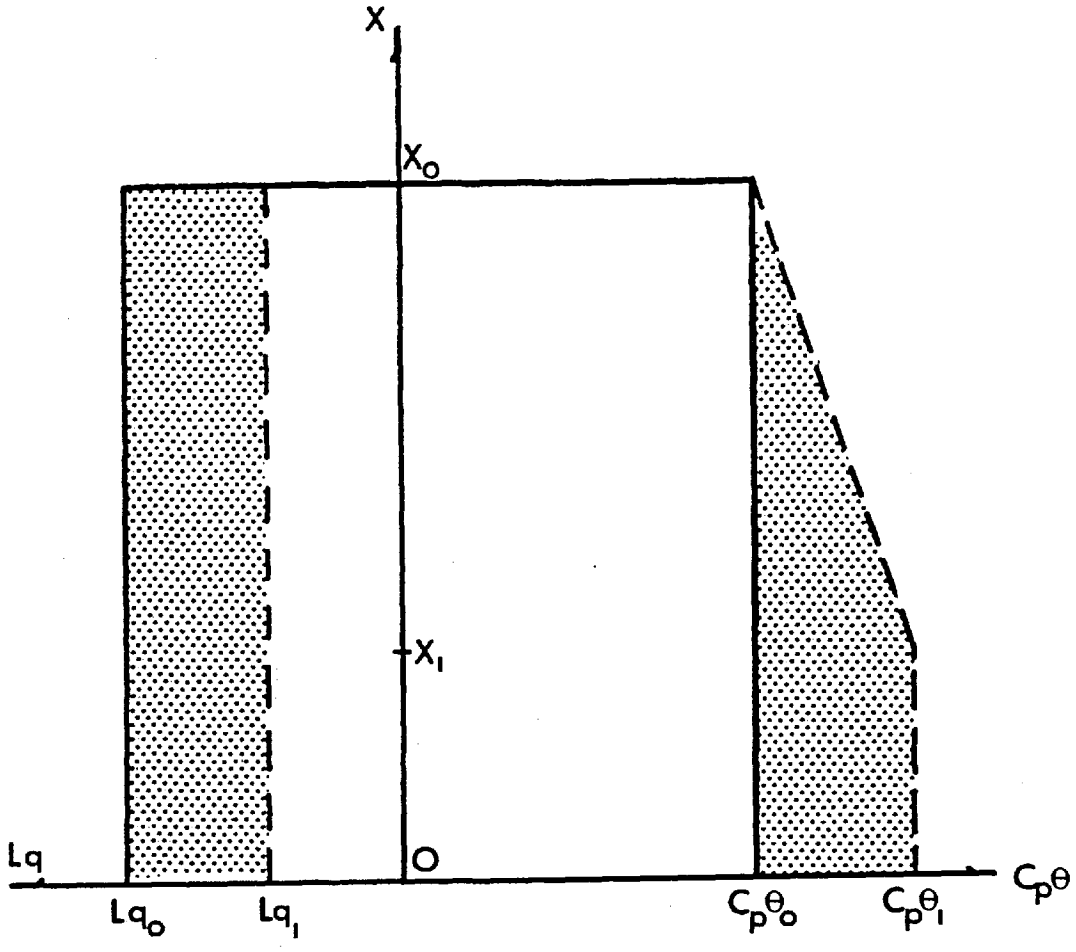

Fig. a1 The E-X Diagram

axes, the ordinate is the pressure axis X, the abscissa is divided into two parts: the dry static energy part in the normal positive direction, and a liquid energy content on the left side the ordinate.

The initial pressure weighted moist static energy (pwmse) H_o is represented by the area enclosed by the continuous line. If the potential temperature is increased at a constant rate, as the parcel ascends to a new level X_1, the pwmse is proportional to the area enclosed by the dashed boundary. It is made up of two parts -- the pwmse of the parcel at X_1, and the integral $\int C_p \Delta\theta \; dX$.

The transfer of potential energy contained in the moisture to the potential energy of the parcel is proportional to one of the dotted areas. The area on the left is the change of pwmse due to condensation processes; the right dotted area represents the change in pwmse owing to warming. The two areas are equal. Thus it can be seen that, the change in dry static energy is not equal to the energy released when moisture condenses.

$$(C_p \Delta\theta) \neq \Delta(Lr)$$

In the case illustrated in the diagram

$$(C_p \Delta\theta) = 2\,\Delta(Lr)$$

The example quoted is an unrealistic larse rate, most of the latent heat is released in the lower half of the troposphere, thus making the magnitude of $C_p \Delta\theta$ similar to $\Delta(Lr)$.

Rewrite equation (a.6)

$$H_o - H_e = C_p X_1 (\theta_1 - \theta_e) + L X_o (r_1 - r_e) - \int_o^1 C_p \theta_1 \, dX \qquad (a.7)$$

Where H_e is the pwmse of the environment at the same height as H_1. The difference between X_1 and X_e is small, the value of θ in the last term can be regarded as a constant over the interval X_1 to X_e, thus

$$H_o - H_e = C_p X_e (\theta_1 - \theta_e) + L X_o (r_1 - r_e) - \int_o^e C_p \theta_1 \, dX \qquad (a.8)$$

Since r is the saturated moisture content of the parcel and that of the environment, they are functions of the two temperatures. From the Clausius-Clapeyron relation

$$\frac{\Delta r}{r} = \left[1 + \frac{r}{.622} \right] \frac{LM}{RT} \frac{\Delta T}{T} \qquad (a.9)$$

Where $\Delta T/T$ can be expressed in terms of $\delta\phi$ and $\Delta P/P$ the pressure difference between the parcel and the surrounding is due to the dynamics of the updraught as well as the temperature difference, let

$$\frac{\Delta P}{P} = e \frac{\Delta T}{T} \qquad (a.10)$$

Where e is a constant to be determined empirically. From the numerical data of Miller (1978), there is a consistent relationship between the height perturbation of constant pressure surface and the temperature perturbation inside the updraught. For a temperature perturbation of 3 deg.C, there is a height perturbation of 10 metres. Thus

$$e \approx 3g/R \qquad (a.11)$$

Let $S_e = C_p X_e \theta_e$, equation (a.8) can be written as

$$\frac{H_e - H_e}{S_e} = \Delta\phi + \left(\frac{H_e - S_e}{S_e}\right)\left(1 + \frac{r}{.622}\right)\frac{LM}{RT}\left(1 + \frac{Re}{C_p}\right)\Delta\phi - \frac{1}{X_e\theta}\int_0^e \theta_i\, dX_i \qquad \text{(a.12)}$$

The environmental lapse rate is not a smooth function of height, thus, the equation is best solved by numerical means, where the environmental profile can be inputed as data points. If the depth is divided into N levels, and n denote the current point to be considered. Then

$$\Delta\phi_n = \frac{H_o - H_e + \sum_{i=1}^{n} C_p\theta_i\left(1 + \Delta\phi_i\right)\Delta X_i + \frac{\Delta X_n}{X_{e_n}} S_{e_n}}{\left(1 - \frac{\Delta X_n}{X_{e_n}}\right)S_{e_n} + \left(H_{e_n} - S_{e_n}\right)\left(1 + \frac{r}{.622}\right)\frac{LM}{RT}\left(1 - \frac{Re}{C_p}\right)^{-1}} \qquad \text{(a.13)}$$

and the value of convective potential energy is

$$CAPE = \sum_{n=1}^{N} g\,\Delta\phi_n\,\Delta z_n \qquad \text{(a.14)}$$

ACKNOWLEDGEMENT

The author would like to thank his supervisor, Dr. M.W. Moncrieff, for his continual guidance, encouragement and constructive criticism given throughout the period of this work. Thanks are also conveyed to Dr. J.A.S. Green, Dr. A.J. Thorpe, Dr. G. Shutts and Dr. M.J. Miller for their constructive criticism, to Dr. M.J. Miller for permission to use the results of his storm simulations and to reproduce figure 3.4.1, and to Mr. A.G. Seaton for programming assistance.

The receipt of a N.E.R.C. Research Studentship is gratefully acknowledged.

REFERENCES

Asai, T	1964	Cumulus Convection in the Atmosphere with Vertical Wind Shear: Numerical Experiment. J.Met.Soc.of Jap.,vol.42, pp.245-259.
Betts, A.K.	1976	Structure and Motion Of Tropical Squall-lines Over Venezuela. Quart.J.Roy.Met.Soc., 102, pp.395-404.
Betts, A.K. Grover, R.W. And Moncrieff, M.W.	1976	The Dynamics and Simulaion Of Tropical Squall Lines. Quart.J.Roy.Met.Soc.,102,pp.317-394.
Bolton, D	1979	Theoretical Studies of Cumulonimbus Convection. Ph.D. Thesis. U. Of London. (to be submitted).
Brook, H.B.	1946	A Summary of Some Radar Thunderstorm Observations. Bull. Of Amer.Met.Soc., 27, pp 557-563.
Browning, K.A.	1962	Air Motion and Precipitation Development In Severe Convective Storms. Ph.D Thesis, Imperial College, London.
Browning, K.A. And Ludlam, F.H.	1962	Airflow In Convective Storms. Quart.J.Roy.Met.Soc., 89, pp.117.
Browning, K.A.	1964	Airflow and Precipitation Trajectories Within Severe Local Storms Which Travels To The Right. J.Atmos.Sci., 21, pp.634-639.
Browning, K.A.	1965	A Family Outbreak of Severe Storms --- A Comprehensive Study of the Storms in Oklahoma on the 26th May 1963. Air Force Cambridge Research Lab. Sp.Report, No.32. 346pp.
Byers, H.R.	1942	Nonfrontal Thunderstorms, Dept. Of Met., U.of Chicago, Misc.Rep.No.3,26pp.
Byers, H.R. And Braham, R.R.	1949	The Thunderstorm. Washington D.C., U.S. Government Printing Office.
Chisholm, A.J.	1973	Alberta Hailstorms: Radar Case Studies and Airflow Model. Met. Monograph, 14.
Fujita, T. And Grandoso, H.	1968	Split of A Thunderstorm Into Anti- And Cyclonic Storms and Their Motion As Determined From Numerical Model Experiment. J.Atmos.Sci., 25, pp.416-444
Fawbush, E.J.	1951	An Empirical Method of forecasting

Miller, R.C. And Starrett, L.G. — Tornado Development. Bull.Amer.Met.Soc., 32,pp.1-9.

Green, J.A.S. And Pearce, R.P. 1962 — Cumulonimbus Convection In Shear. Tech. Note 12, Dept. Met.,imperial College, London.

Hall, G. And Watt, J.M. 1976 — Modern Numerical Methods for Ordinary Diferential Equations. Clarendon Press, Oxford.

Haman, K.E. 1978 — On The Motion of A 3-D Quasi steady Convective Storm In Shear. Mon.Wea.Rev., 106, pp.1622-1627.

Hammond, G.R. 1967 — Study of A Left Moving Thunderstorm Of 23rd April 1964. N.S.S.L. Technical Memorandum Iertum-nssl 31.

Hane, C.E. 1973 — The Squall Line Thunderstorm: Numerical Experimentation. J.Atmos.Sci., 30, pp.1672-1670.

Heymsfields, G.M. 1978 — Kinematic and Dynamic Aspects of The Harrah Tornadic Storm Analysed From Dual Doppler Radar Data. Mon.Wea.Rev., 106, pp.233-254.

Hill, G.E. 1974 — Factors Controlling The Size of Cumulus Clouds As Revealed By Numerical Experiments. J.Atmos.Sci., 31, pp646-673.

Houze, R.A.,Jr. 1973 — A Climatological Study of Vertical transports By Cumulus-scale Convection. J.Atmos.Sci., 30, pp.1112-1123.

Johnson, M. 1978 — The Structure of Vorticity In Cumulonimbus Convection: A Numerical Study. Ph.D. Thesis, U. Of London.

Humphrey, W.J. 1928 — Physics of The Air. McGraw Hill, New York.

Klemp, J.B. And Wihelmson, R.B. 1978(a) — The Simulations of 3-d Convective Storm Dynamics. J.Atmos.Sci., 35, pp.1070-1096.

Klemp, J.B. And Wihelmson, R.B. 1978(b) — Simulations of Right and Left Moving Storms Produced Through Storm Splitting. J.Atmos.Sci., 35, pp.1097-1110.

Kuo, H.L. 1963 — Perturbations of Plane Couette Flow In Stratified Fluid and Origin of Cloud

		Streets. The Phys of Fluids, 6,pp.195-211.
Lamb, H	1895	Hydrodynamics. Dover Pub. New York.
Ligda, M.G.H. And Mayhew, W.A.	1954	On The Relationship Between The Velocities of Small Precipitation Areas and The Geostrophic Winds. J.Met., 11,pp.421-423.
Lindzen, R.S.	1974	Wave-CISK In The Tropics. J.Atmos.Sci., 31, pp.156-179
Liu, J.V. And Orville, H.D.	1969	Numerical Modelling of Precipit-Ation and Cloud Shadow Effect On Mountain-induced Cumuli. J.Atmos.Sci.,26, pp.1283-1298.
Mansfield, D.A.	1977	Squall Line Observed In GATE. Quat.J.Roy.Met.Soc.,103,pp.569-574
Marwitz, J.D.	1972	The Structure and Motion of Severe Hailstorms, Pt.1:multicell Storm, J.App.Met.,11,pp.180-188.
Miller, R.C.	1959	Tornado-producing Synoptic Patterns. Bull. Of Amer.Met.Soc., 40, pp.465-472
Miller, M.J. And Pearce, R.P.	1974	A Three-dimensional Primitive Equation Model of Cumulonimbus Convection. Quart.J.Roy.Met.Soc.,100, pp.133-154
Miller, M.J. And Betts, A.K.	1977	Travelling Convective Storms over Venezuela. Mon.Wea.Rev., 105,no.7,pp.833-848.
Miller, M.J.	1978	The Hampstead Storm: A Numerical Simulation of A Quasi-stationary Cumulonimbus System. Quart.J.Roy.Met.Soc., 104, pp.413-427
Moncrieff, M.W. And Green, J.A.S.	1972	The Propagation and Transfer Properties of Steady Convective Overturning In Shear. Quart.J.Roy.Met.Soc., 98, pp.336-352
Moncrieff, M.W.	1978	Convection In Constant Vertical Shear. Quart.J.Roy.Met.Soc., 104, pp.543-567.
Moncrieff, M.W. And Miller, M.J.	1976	The Dynamics and Simulation Of Tropical Cumulonimbus and Squall Lines. Quart.J.Roy.Met.Soc., 102, pp.373-394
Murray, F.W.	1970	Numerical Models of A Tropical Cumulus Cloud With Bilateral and Axial Symmetry.

Mon.Wea.Rew. 98, pp.14-28

Murray, F.W. And Koenig, L.R. 1972 Numerical Experiments on The Relation Between Microphysics and Dynamics In Cumulus Convesction. Mon.Wea.Rev., 100, pp.717-732.

Newton, C.W. And Fankhauser, J.C. 1964 On The Movements Of Convective Storms, Emphasis on Size Discrimination In Relation To Water Budget Requirements. J. App.Met. 3,pp.651-668.

Newton, C.W. And Katz, S. 1958 Movement of Large Convective Rainstorms In Relation To Winds Aloft. Bull.Amer.Met.Soc., 39, pp.129-136.

Newton, C.W. And Newton, H.B. 1959 Dynamical Interactions Between Large Convective Clouds and Environment With Vertical Shear. J.Meteorol., 16, pp.483-496.

Orgura, Y. And Charney, J. 1960 A Numerical Model of Thermal Con-Vection In The Atmosphere. Pre.of Int.Sym.Num.Wea.Pred. Met.Soc.of Jap., pp.431-452.

Orgura, Y. 1963 The Evaluation of A Moist Convection Element In A Shallow, Conditionally Unstable Atmosphere, A Numerical Calculation. J.Atmos.Sci., 20,pp.407-424.

Orville, H.D. 1965 A Numerical Study of The Initiation of Cumulus Cloud Over Mountain Terrain, J.Atm.Sci., 22,pp.684-699.

Orville, H.D. 1968 Ambient Wind Effects on The Initiation and Development of Cumulus Clouds Over Mountains, J.Atms.Sci., 25,pp385-403.

Orville, H.D. And Sloan, L.J. 1970 A Numerical Simulation of The Life History of A Rainstorm. J.Atmos.Sci., 8, pp.1148-1159.

Palmen, E. And Newton, C.W. 1969 Atmospheric Circulation Systems. Academic, New York. P.421.

Ramaswany, C. 1956 On the Sub-tropical Jet Stream and Its Role In the Development of Large Scale Convection. Tellus, 8,pp.26-60

Ray, P.S. 1976 Vorticity and Divergence Fields Within Tornadic Storms From Dual Doppler Observations. J.App.Met., 15,pp.879-890.

Raymond, D.J. 1975 A Model for Predicting the Movement of

Continuously Propagating Convective Storm. J.Atmos.Sci.,32, pp.1308-1317.

Sasaki, Y. 1959 A Numerical Experiment for Squall Line formation. J.Meteorol.,16,pp.347-352.

Schlesinger, R.E. 1973 A Numerical Model of Deep Moist Convection, I. Comparative Experiments for Variable Ambient Moisture and Wind Shear. J.Atmos.Sci.,30,pp.835-856.

Schlesinger, R.E. 1975 A Three-dimensional Numerical Model of An Isolated Deep Convective Cloud: Preliminary Results. J.Atmos.Sci., 32, pp.934-957.

Takeda, T. 1965 The Downdraught In Convective Shower-cloud Under the Vertical Wind Shear and Its Significance for The the Maintenance for Convective System. J.Met.Soc.of Jap.,43, pp.302-309.

Takeda, T. 1966 Effects of the Prevailing Wind With Vertical Shear on the Convective Accompanied With Heavy Rainfall. J.Met.Soc.of Jap.,44,pp.129-144.

Takeda, T. 1971 Numerical Simulation of A Precipitating Convective Cloud: the formation of A Long Lasting Cloud. J.Atmos.Sci., 28, pp.350-376.

Thorpe, A.J. And Miller, M.J. 1978 Numerical Simulations Showing The Role of the Downdraught In Cumulonimbus Motion and Splitting. Quart.J.Roy.Met.Soc., 104, pp.873-893.

Wilhelmson, 1974 The Life-cycle of A Thunderstorm In Three Dimensions. J.Atmos.Sci., 31,pp.1629-1651.

Wiggert, V. 1972 Cumulus Simulations By A Modified Axi-symmetric Model, With Comparisons To Four Observed Tropical Clouds. Tech.Memo.ERL OD-12, 96,pp., Nat.Oceanic Atmos.Admin.